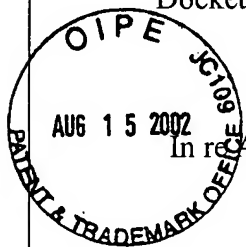


Docket No. 1413.02

PATENTS

IN THE UNITED STATES PATENT AND TRADEMARK OFFICE



In re Application of:

MOREJON ET AL.

Serial No.: 10/064,570

Filed: 07/26/2002

For: Symmetric Spherical QAM Constellation

Art Unit: 2631

Director: Unassigned

Asst. Commissioner for Patents
Washington, D.C. 20231

RECEIVED

AUG 19 2002

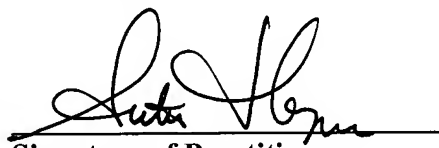
Technology Center 2600

TRANSMITTAL OF PETITION TO MAKE SPECIAL

1. Transmitted herewith is a Petition to Make Special for this application.

FEE DEFICIENCY

2. If any additional extension and/or fee is required, charge Deposit Account No. 500745.

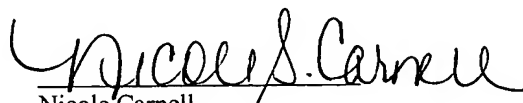

Signature of Practitioner

Reg. No. 41,849
Tel. No.: (727) 507-8558

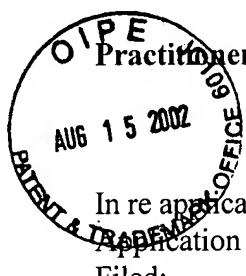
Anton J. Hopen
Smith & Hopen, P.A.
15950 Bay Vista Drive, Ste. 220
Clearwater, FL 33760

CERTIFICATE OF MAILING
(37 C.F.R. § 1.8)

I HEREBY CERTIFY that this correspondence is being deposited with the United States Postal Service by First Class Mail in an envelope addressed to: Assistant Commissioner for Patents, Washington, D.C. 20231 on August 12, 2002.


Nicole Carnell

#4/ald
10-30-02
PATENT



Practitioner's Docket No. 1413.02

IN THE UNITED STATES PATENT AND TRADEMARK OFFICE

In re application of: Morejon, et al.
Application No.: 10/064,570
Filed: 07/26/2002
For: Symmetric Spherical QAM
Constellation

Group No.: 2631
Examiner: Unassigned

RECEIVED

AUG 19 2002

Technology Center 2600

Assistant Commissioner for Patents
Washington, D.C. 20231

PETITION TO MAKE SPECIAL FOR NEW APPLICATION
UNDER M.P.E.P. section 708.02, VIII

1. Petition

Applicant hereby petitions to make this new application, which has not received any examination by the Examiner, special.

2. Claims

All the claims in this case are directed to a single invention. If the Office determines that all the claims presented are not obviously directed to a single invention, then applicant will make an election without traverse as a prerequisite to the grant of special status.

3. Search

Field of search: The following areas were searched:

Class 178, subclass 67;
Class 332, subclass 103;
Class 341, subclass 61; and
Class 375, subclass 39, 59, 261, 265 and 298;

08/16/2002 CNGUYEN 00000003 10064570

01 FC:122

130.00 DP

Patent References:

<u>Inventor</u>	<u>Patent Number</u>	<u>Year</u>
Forney, Jr. et al.	3,887,768	1975
Forney, Jr. et al.	4,894,844	1990
Betts	5,103,227	1992
Forney, Jr. et al.	5,150,381	1992
Arai	5,515,400	1996
O'Dea	5,606,578	1997
Heegard	5,621,761	1997
Betts	6,026,120	2000
Betts	6,101,223	2000
McCallister et al.	6,392,500	2002

Non-patent literature included:

"Efficient Modulation for Band-limited Channels", G.D. Forney Jr. et al.

"Multidimensional Constellations – Part I: Introduction, Figures of Merit, and Generalized Cross Constellations", G.D. Forney Jr. et al.

"A Coherent Digital Amplitude and Phase Modulation System", C.N. Campopiano and B.G. Glazer

"An Efficient Power-Reduction Technique on DSL Modems", H. Kwok and D.L. Jones

"PAR Reduction Via Constellation Shaping", H. Kwok and D.L. Jones

"Higher-Order Optimum Hexagonal Constellations", C.D. Murphy

4. Copy of references

There is submitted herewith a copy of the references deemed most closely related to the subject matter encompassed by the claims.

Also attached is Form PTO-1449. (PTO/SB/08A and 08B)

5. Detailed discussion of the references

There is submitted herewith a detailed discussion of the references, which discussion particularly points out how the claimed subject matter is distinguishable over the references.

Also attached is a copy of the Information Disclosure Statement previously filed with the application. Copies of references already filed and of record are not included herewith. MPEP §708.02(VIII)(D).

Applicant claims a quadrature amplitude modulation signal space, comprising a symmetric spherical quadrature amplitude modulation constellation in a multidimensional complex plane, the constellation bounded by a surface comprising all symbol points at a predetermined distance from a center point, coincident with an intersection of at least two axes, and corresponding in relative position to the symbol points on opposite sides of the axes. The following discussion of the references points out with the particularity required by 37 CFR §1.111(b) and (c), how the claimed subject matter is patentable over the references.

U.S. Patent No. 5,150,381 to Forney, Jr. et al. and assigned to Codex Corporation suggests constellations that are shaped to be as nearly spherical as possible. Forney further describes the implementation of a quasi-spherical constellation utilizing the Voronoi region of a lattice to define the constellation boundary. Referring to Fig. 3 of the Forney patent, the quasi-spherical constellation described by Forney does not anticipate, suggest or teach the symmetric spherical QAM constellation claimed in the present invention.

U.S. Patent No. 5,515,400 to Arai and assigned to Fujitsu Limited describes a signal point arranging method for use with a quadrature amplitude modulator/demodulator device. The constellation described by Arai comprises a plurality of concentric circles with their center at the coordinate origin of a rectangular plane, each of the concentric circles having a radius equal to

that of a previously established symmetric grid, the desired number of symbol points then being arranged on the concentric circles. Referring to Fig. 4 of the Arai patent, the constellation taught by Arai does not anticipate or suggestion the symmetric spherical constellation claimed in the present invention.

IEEE Journal Article, "Efficient Modulation for Band-Limited Channels", describes several QAM constellation schemes well known in the art, including rectangular constellations, cross constellation, circular constellations and hexagonal constellations. It can be see from Fig. 5 and Fig. 6 of the article, that these known constellations do not describe the symmetric spherical constellation claimed in the present invention.

IEEE Journal Article, "Multidimensional Constellations – Part I: Introduction, Figures of Merit, and Generalized Cross Constellations, describes the theoretical advantages of a spherical constellation, however a method for implementing a spherical constellation is not described.

The Henry K. Kwok and Douglas L. Jones articles, "An Efficient Power-Reduction Technique on DSL Modems" and "PAR Reduction via Constellation Shaping", describe a technique for shaping a constellation into a hypersphere in an effect to reduce the peak-to-average ratio. This shaping technique results in constellations with a spherical boundary, but it does not provide a symmetric spherical constellation.

Applicant believes the remaining references to be immaterial to the patentability of Applicant's invention. However, a brief discussion of each reference is provided to illustrate the field of search. U.S. Patent No. 3,887,768 to Forney, Jr. et al. and assigned to Codex Corporation describes a quadrature amplitude modulation constellation comprising signal points mapped on the complex plane which are drawn from an alphabet consisting of at least 8 points, and are set up in concentric rings each rotated by 45° with respect to adjacent rings. U.S. Patent No. 4,894,844 to Forney, Jr. et al. and assigned to Codex Corporation describes a Voronoi constellation. U.S. Patent No. 5,606,578 to O'Dea and assigned to Motorola, Inc. describes a modulation method utilizing known signal constellations. U.S. Patent No. 5,621,761 to Heegard and assigned to General Instrument Corporation of Delaware describes a rotationally invariant

trellis coder. U.S. Patent No. 6,026,120 to Betts and assigned to Paradyne Corporation describes a system and method for communicating information using circular multidimensional signal space constellations. U.S. Patent No. 6,101,223 to Betts and assigned to Paradyne Corporation describes a system and method for optimizing the uncoded transmission and reception of data using circular constellations. U.S. Patent No. 6,392,500 to McCallister et al. and assigned to Silcom, Inc. describes a rotationally invariant phase point constellation utilizing phase point voids. IRE Transactions of Communications Systems article, "A Coherent Digital Amplitude and Phase Modulation Scheme", describes a technique for a combination of amplitude and phase modulation. The article "High-Order Optimum Hexagonal Constellations" by Charles D. Murphy describes a method of constructing hexagonal constellations.

Section 102 of the United States Patent Laws provides in relevant part:

A person shall be entitled to a patent unless . . . the invention was known or used by others in this country, or patented or described in a written publication in this or a foreign country . . .

None of the references obtained in the prior art search disclose or describe Applicant's invention.

Section 103 of the United States Patent Laws provides in relevant part:

A patent may not be obtained . . . if the differences between the subject matter sought to be patented and the prior art are such that the subject matter as a whole would have been obvious at the time the invention was made to a person having ordinary skill in the art to which said subject matter pertains.

No combination of references obtained in the prior art search teach or suggest Applicant's invention.

Petition to Make Special
In re **Morejon et al.**

Ser. No. **10/064,570**
Filing Date: **July 26, 2002**

Examiner: **Unassigned**
Group Art: **2631**

6. Fee

The fee required by 37 C.F.R. 1.17(i) is to be paid by the attached check for \$130.00



Anton Hopen
Registration No. 41,849
Smith & Hopen, PA
15950 Bay Vista Drive
Suite 220
Clearwater, FL 33760
727-507-8558

Efficient Modulation for Band-Limited Channels

G. DAVID FORNEY, JR., FELLOW, IEEE, ROBERT G. GALLAGER, FELLOW, IEEE, GORDON R. LANG, FRED M. LONGSTAFF, AND SHAHID U. QURESHI, SENIOR MEMBER, IEEE

BEST AVAILABLE COPY

Abstract—This paper attempts to present a comprehensive tutorial survey of the development of efficient modulation techniques for band-limited channels, such as telephone channels. After a history of advances in commercial high-speed modems and a discussion of theoretical limits, it reviews efforts to optimize two-dimensional signal constellations and presents further elaborations of uncoded modulation. Its principal emphasis, however, is on coded modulation techniques, in which there is an explosion of current interest, both for research and for practical application. Both block-coded and trellis-coded modulation are covered, in a common framework. A few new techniques are presented.

I. HISTORICAL INTRODUCTION

BAND-LIMITED channels (as opposed to power-limited) are those on which the signal-to-noise ratio is high enough so that the channel can support a number of bits/Hz of bandwidth. The telephone channel (particularly the dedicated private line) has historically been the scene of the earliest application of the most efficient modulation techniques for band-limited channels. The reasons have to do both with the commercial importance of such channels and with the fact that they can be modeled to first order as linear time-invariant channels, sharply band-limited between typically 300–3000 Hz, with high signal-to-noise ratios, typically 28 dB or greater. Their relatively low bandwidth permits a great deal of signal processing per transmission element, and therefore early application of the most advanced techniques, which have often then been applied several years later to broader-band channels (e.g., radio).

The earliest commercially important telephone-line modems appeared in the 1950's and used frequency shift keying to achieve speeds of 300 bits/s (Bell 103), or 1200 bits/s on private lines (Bell 202). The earliest commercially important synchronous modem was the Bell 201, introduced in about 1962, which used 4-phase modulation in a nominal 1200 Hz bandwidth to achieve 2400 bits/s on private lines. This remained the state of the art for most of the

decade. (It was not unknown in this period to encounter users who thought that Nyquist or Shannon or someone else had proved that 2400 bits/s was about the maximum rate theoretically possible on phone lines.)

The first commercially important 4800 bit/s modem was the Milgo 4400/48, introduced in about 1967, which included a manually adjustable equalizer to allow use of a nominal 1600 Hz bandwidth in conjunction with 8-phase modulation to send 3 bits/Hz. The development of digital adaptive equalization soon allowed expansion of the nominal bandwidth to 2400 Hz, essentially the full telephone line bandwidth. Following a first generation of single-sideband 9600 bit/s modems in the late 1960's, which were only marginally successful, broad success was achieved by the Codex 9600C, introduced in 1971, which used quadrature amplitude modulation (QAM) with a 16-point signal constellation to send 4 bits/Hz in a nominal 2400 Hz bandwidth. (16-point QAM had been used at 4800 bits/s by ESE and ADS about 1970.) Modems with these characteristics remained the state of the art for another decade and it was thought by many (including some of the present authors, who should have known better) that higher-speed modems would never be widely used commercially.

In 1980, a first generation of 14 400 bit/s modems were introduced by Paradyne (MP 14400), followed in 1981 by the Codex/ESE SP14.4 and by others. These modems simply extended 2400 Hz QAM modulation to 6 bits/Hz by using 64-point signal constellations, and by using advanced implementation techniques and exploiting the gradual upgrading of the telephone network, proved to operate successfully over a high percentage of circuits. In a second generation of 14.4 kbit/s modems that will begin appearing in 1984, coded QAM modulation is being introduced to provide greater performance margins. The principal focus of this paper will be on these new coded modulation techniques.

This evolution of high-speed modems to ever higher rates using successively more complicated modulation schemes is summarized in Table I, along with the designation and year of final adoption of CCITT international standards embodying these schemes. How far can the evolution go? History would suggest caution in stipulating any ultimate ceiling. However, without any dramatic general upgrading of the telephone network, we venture that 19.2 kbits/s is the maximum conceivable rate for

Manuscript received February 14, 1984; revised May 3, 1984.

G. D. Forney, Jr. is with the Motorola Information Systems Group, Mansfield, MA 02048.

R. G. Gallager is with the Department of Electrical Engineering and Computer Science, Massachusetts Institute of Technology, Cambridge, MA 02139.

G. R. Lang and F. M. Longstaff are with Motorola Information Systems Ltd., (ESE) Rexdale, Ont., Canada M9V 1C1.

S. U. Qureshi is with the Codex Corporation, Canton, MA 02021.

TABLE I
MODEM MILESTONES

YEAR	MODEL	SPEED	BANDWIDTH	n	CONSTELLATION	COMMENTS	CCITT STANDARD
1962	Bell 201	2400	1200 Hz	2	4-phase	fixed eq.	V.29 (1968)
1967	Milgo 4400/48	4800	1600 Hz	3	8-phase	manual eq.	V.27 (1972)
1971	Codex 9600 C	9600	2400 Hz	4	16-QAM	adaptive eq.	V.29 (1976)
1980	Paradyne MP14400	14,400	2400 Hz	6	64-QAM	rectangular	
1981	Codex/ESE SP14.4	14,400	2400 Hz	6	64-QAM	hexagonal	
1984		14,400	2400 Hz	6	128-QAM	8-state trellis	

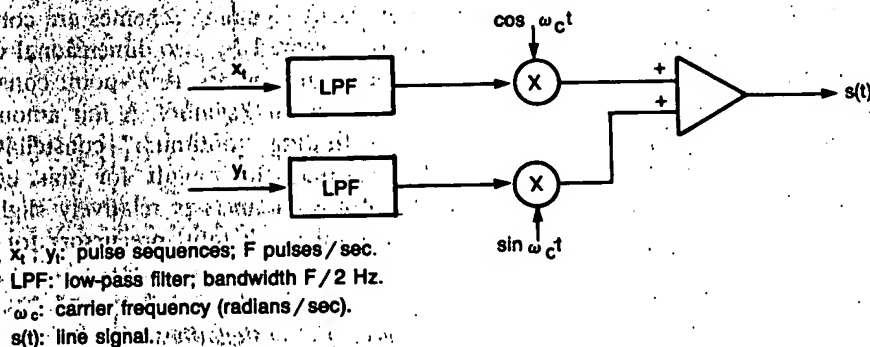


Fig. 1. Canonical QAM modulator.

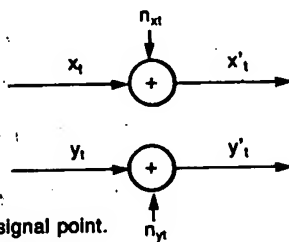


Fig. 2. QAM channel model.

telephone-line modem for general use, even with all-out use of the most powerful coded modulation. We shall see.

II. CHANNEL MODEL AND BASIC LIMITS

An quadrature amplitude modulator can be used to generate any standard linear double-sideband modulated carrier signal (including forms of phase modulation and phase/amplitude modulation), which includes all types of modulation in general use in synchronous modems. A canonical QAM modulator is shown in Fig. 1.

Assuming that the only channel impairment is Gaussian noise, and that the receiver achieves perfect carrier phase tracking, the simple model of Fig. 2 applies. Signals are sent in pairs (x_i, y_i) ; the channel is essentially two-dimensional. We shall call such a pair a "signal point," imagined to lie on a two-dimensional plane. Signal points are sent at

a regular rate of F points/s where F Hz is the nominal (Nyquist) bandwidth of the channel. A signal point is also called a "symbol," and the symbol interval is $1/Fs$. The model indicates that the two signal point coordinates (x_i, y_i) are independently transmitted over decoupled parallel channels and perturbed by Gaussian noise variables (n_{xi}, n_{yi}) , each with zero mean and variance N . Alternatively, we could regard the two-dimensional signal point as being perturbed by a two-dimensional Gaussian noise variable. If the average energy (the mean squared value) of each signal coordinate is S , then the signal-to-noise ratio is S/N .

The simplest method of digital signaling through such a system is to use one-dimensional pulse amplitude modulation (PAM) independently for each signal coordinate. (This is sometimes called narrow-sense QAM.) In PAM, to send m bits/dimension, each signal point coordinate takes on

one of 2^m equally likely equispaced levels, conventionally $\pm 1, \pm 3, \pm 5, \dots, \pm(2^m - 1)$. The average energy of each coordinate is then

$$S_m = (4^m - 1)/3,$$

and it follows that

$$S_{m+1} = 4S_m + 1.$$

That is, it takes approximately (asymptotically, exactly) 4 times as much energy (or 6 dB) to send an additional 1 bit/dimension or 2 bits/symbol. The probability $P(E)$ that either x_i or y_i is in error is upperbounded and closely approximated by the probability that the two-dimensional Gaussian noise vector (n_{xi}, n_{yi}) lies outside a circle of radius 1, which is easily calculated to be $P(E) = \exp(-1/2N)$. A noise variance N of about $1/24$ therefore yields an error probability per symbol in the range of about 6×10^{-6} .

The channel capacity of the Gaussian channel was calculated in Shannon's original papers [1]. Subject to an energy constraint $x_i^2 \leq S$, the capacity is

$$C = (1/2) \log_2(1 + S/N) \text{ bits/dimension},$$

achieved when x_i is a zero-mean Gaussian variable with variance S . Note that when S becomes large with N constant, it takes approximately (asymptotically, exactly) 4 times as much power to increase the capacity by an additional 1 bit/dimension. Therefore the ratio of bits/dimension achieved by PAM to channel capacity approaches 1 as S becomes large. This fact was used in [2] to argue that coding has little to offer on highly band-limited channels.

We can make a more quantitative estimate of the potential gains from coding as follows. Using narrow-sense QAM (two-dimensional PAM) to send m bits/dimension or $n = 2m$ bits/symbol at an acceptable error rate (of the order of 10^{-5} – 10^{-6}) requires an average energy in each dimension of

$$S = (2^n - 1)/3$$

when $N = 1/24$, or $S/N = 8 \times 2^n$ for n moderately large. If channel capacity could be achieved, we could send about $n' = \log_2(S/N)$ bits/symbol, or about $n + 3$ bits/symbol at the same signal-to-noise ratio. Thus, the potential gain is about 3 bits/symbol or, alternatively, about a factor of 8 (9 dB) of power savings.

Many authors (see, e.g., [3], [4]) regard the parameter R_o as a better estimate than C of the maximum rate that is practically achievable using coding. On the Gaussian channel, R_o is [5]

$$R_o = (1/2) \log_2(1 + S/2N) \text{ bits/dimension}.$$

It thus takes a factor of 2 (3 dB) more power to signal at R_o than to signal at C . The maximum practical improvement obtainable by coding might therefore be estimated as of the order of 6 dB, or 2 bits/symbol (although the R_o estimate is not universally accepted).

In what follows we shall show that simple coding techniques gain about 3 dB or 1 bit/symbol, while the most elaborate techniques described have theoretical gains of the order of 6 dB or about 2 bits/symbol. This is entirely consistent with the R_o estimate given above, and suggests that little can be gained by seeking still more elaborate schemes. (In [6] the capacity of the telephone channel was estimated as of the order of 23 500 bits/s, roughly consistent with what we are saying here.)

III. UNCODED MODULATION SYSTEMS

Digital QAM signaling schemes are conventionally and usefully represented by two-dimensional constellations of all possible signal points. A 2^n -point constellation can be used to send n bits/symbol. A fair amount of effort has gone into finding "optimum" constellations. We shall shortly see that the payoff for this effort on pure Gaussian-noise channels is relatively slight, although the schemes found are helpful precursors for more elaborate schemes.

A. Rectangular Constellations

A brief flurry of theoretical papers in the early 1960s [7]–[10] developed two-dimensional signal constellations from various viewpoints. The most interesting for our present purposes are the family of constellations developed by Campopiano and Glazer [9], reproduced in Fig. 3. (We have taken the liberty of substituting a "cross constellation" for theirs at $n = 7$; the two are equally good.) For even integer numbers of bits/symbol, the constellations are simply representations of two independent PAM channels; so the constellations are square and have points drawn from the rectangular lattice of points with odd integer coordinates. It takes about 6 dB more power to send more bits/symbol, as expected. For odd integer numbers of bits/symbol, the constellations lie within an envelope the form of a cross (and have hence come to be called "cross constellations") and the points are drawn from the same rectangular lattice (except for the 8-point constellation, where the outer points are put on the axes for symmetry and energy savings). With the figures scaled so that the minimum distance between any two points is equal to 2, the average signal energy in absolute terms and in dB is as given in Table II. We see that the "cross constellations" require about 3 dB more or less than the next lower or higher square constellation, respectively, as we would expect.

The Campopiano–Glazer construction can be generalized as follows: from an infinite array of points closely packed in a regular array or lattice, select a closely packed subset of 2^n points as a signal constellation. This important principle is at the root of much recent work. We shall explore applications of this principle, working up from the simpler to the more sophisticated.

When constellations are drawn from a regular lattice within some enclosing boundary, the following asymptotic

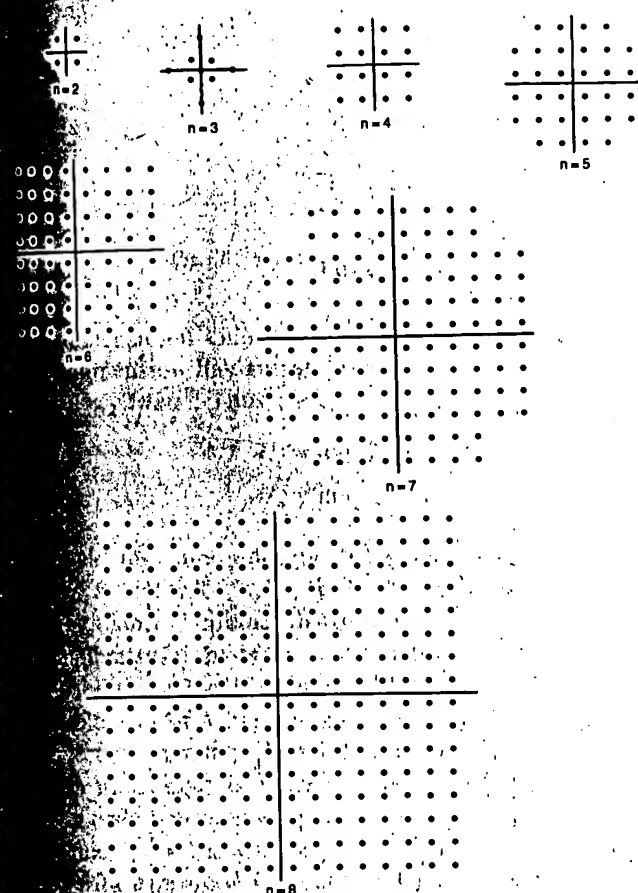


Fig. 3. Rectangular signal constellations (after Campopiano and Glazer [9]).

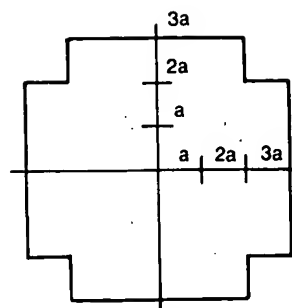
TABLE II
CAMPOPIANO-GLAZER CONSTELLATIONS

No. Points	S	(dB)	\hat{S}	(dB)
4	2	3.0	2.7	4.3
8	5	7.4	5.5	7.4
16	10	10.0	10.7	10.3
32	20	13.0	20.7	13.2
64	42	16.2	42.7	16.3
128	82	19.1	82.7	19.2
256	170	22.3	170.7	22.3

approximation is useful and remarkably accurate for constellations of even moderate size (16 points and up). Let A be the area of the region consisting of points that are closer to a given lattice point than to any other (i.e., the decision region belonging to that point, or the Voronoi (or Dirichlet) region [11]). If we take some boundary that encloses a region in space of area B , then the number of lattice points in that region will be approximately B/A , and the average energy of these lattice points will be approximately equal to the average energy ($x^2 + y^2$) of all points within the boundary.

For example, the Campopiano-Glazer constellations are drawn from a rectangular lattice with $A = 4$, and are bounded by a square of side $2 \times 2^{n/2}$ and area $B_s = 4 \times 2^n$ for n even and by a cross of area $B_c = 4 \times 2^n$ for n odd, with dimensions as shown in Fig. 4. The energy calculated by the integral approximation is

$$\begin{aligned} \hat{S} &= (2/3)2^n \text{ (square)} \\ &= (31/48)2^n \text{ (cross)}. \end{aligned}$$



$$a = 2^{(n-1)/2} \text{ for Campopiano/Glazer constellations, } n \text{ odd}.$$

Fig. 4. Cross constellation boundary.

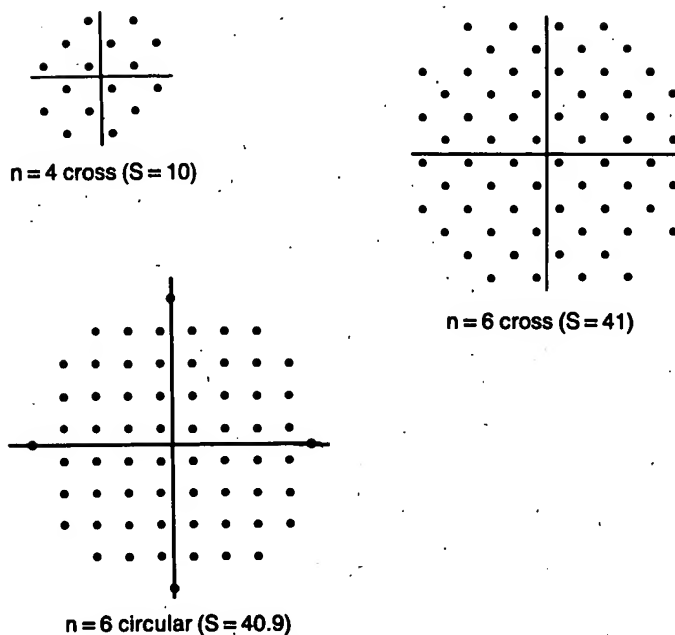


Fig. 5. Improved rectangular constellations.

Comparisons between S and \hat{S} are given in Table II; the approximations are good ones. Furthermore, note that the cross is slightly more efficient than the square, by a factor of 31/32 or 0.14 dB (because it is more like a circle); this suggests that the cross would be the better shape even for n even, and indeed this is the case and can be easily achieved by taking alternate points from the next higher cross constellation, as shown in Fig. 5 for $n = 4$ and $n = 6$. The $n = 4$ cross constellation is as good as the conventional 4×4 square constellation, and the $n = 6$ cross constellation is 0.1 dB better than the 8×8 square constellation, about as predicted.

Of course, the best enclosing boundary would be a circle, the geometrical figure of least average energy for a given area. A circle with radius R has area πR^2 and average energy equal to $R^2/2$; setting $R^2 = 4 \times 2^n$, we find that the average energy for a 2^n -point circular constellation ought to be about

$$\hat{S} = (2/\pi)2^n \text{ (circle)}$$

which would be only about $\pi/3$ or 0.20 dB better than the square, or 0.06 dB better than the cross. Fig. 5 also shows a

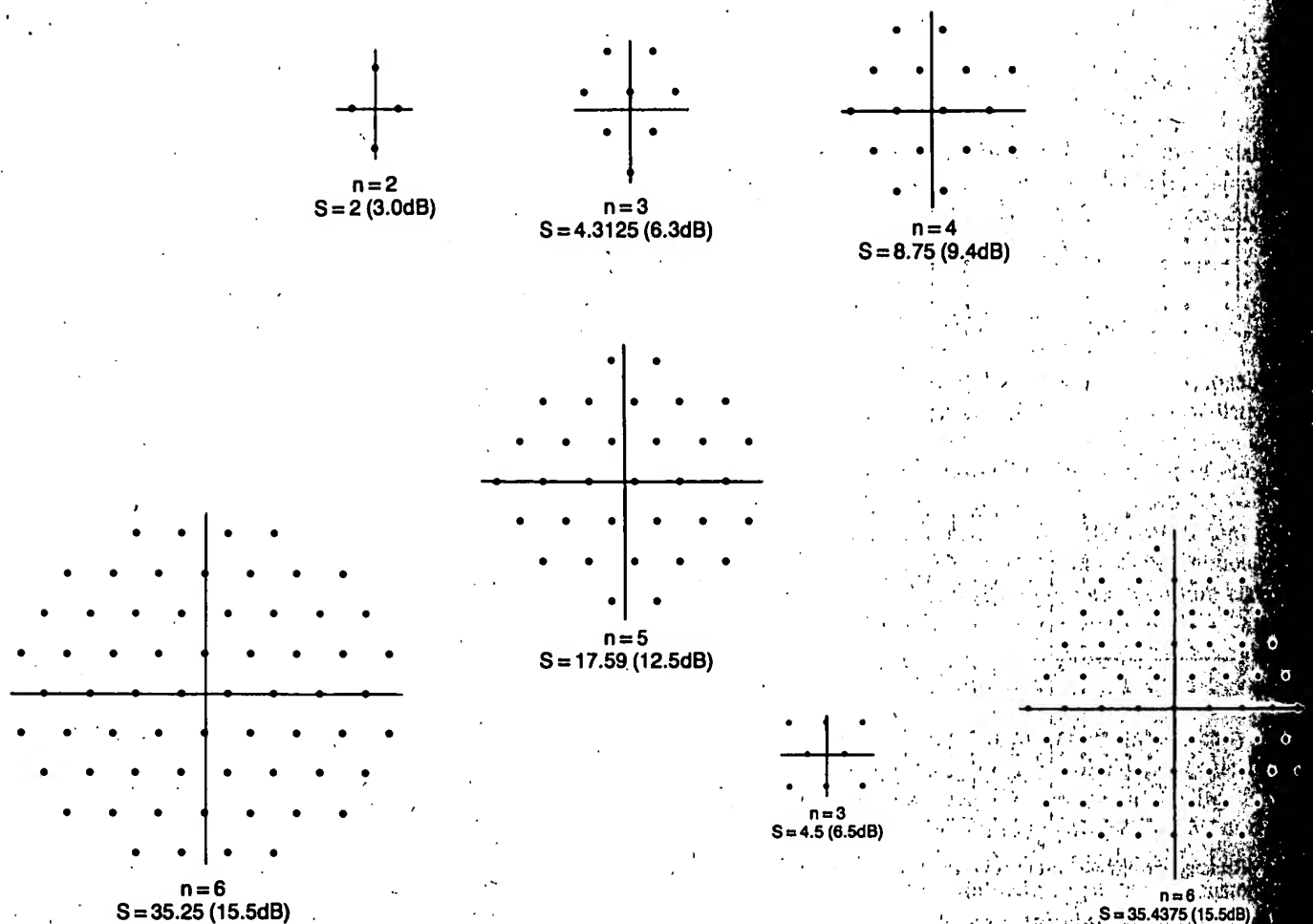


Fig. 6. Optimum hexagonal constellations.

more circular constellation for $n=6$, with the outer points moved to the axes as in Campopiano-Glazer's 8-point constellation; this constellation has been used in the Paradyne 14.4 kbit/s modem and, like the $n=6$ cross, is about 0.1 dB better than the $n=6$ square.

B. Hexagonal Constellations

As the densest lattice in two dimensions is the hexagonal lattice (try penny packing), constellations using points from a hexagonal lattice ought to be the most efficient. Indeed, the area of the hexagonal Voronoi region for a hexagonal lattice with minimum distance 2 is $2\sqrt{3} = 3.464$, or 0.866 the size of the square region, which according to our approximation principle should translate to a 0.6 dB gain for a hexagonal constellation over a rectangular one with the same boundary. (A hexagonal boundary, as suggested in [12], has an energy efficiency within 0.03 dB of the circular boundary, or 0.03 dB better than the cross.)

Fig. 6 shows the best hexagonal packings for $n=2$ through 6. For $n \geq 4$, the predicted 0.6 dB gain is effectively obtained over the best rectangular packings. (Historical notes: suggestions that the hexagonal lattice would asymptotically be the best were made very early; see, e.g., [13]. The suboptimal $n=3$ "double diamond" structure

was actually used in a 4800 bit/s Hycom modem in the mid-1970's. There was a great deal of attention to $n=6$ structures in the early 1970's because of their importance in 9600 bit/s modems; the rather strange-looking one shown here was apparently first discovered by Foschini *et al.* [14], and is still the best 16-point constellation known. The $n=6$ suboptimal structure is used in the Codex/ESF SP14.4 modem.)

IV. ELABORATIONS OF UNCODED MODULATION

In this section we shall discuss further variants of uncoded modulation: constellations with nonuniform probabilities, higher-dimensional uncoded constellations, and constellations for nonintegral numbers of bits/symbol.

A. Nonuniform Probabilities

Attainment of the channel capacity bound requires that the signal points have a Gaussian probability distribution; whereas with all the constellations of the previous section it is implicit that points are to be used with equal probabilities. A uniform circular distribution of radius R has average energy $S_c = R^2/2$ and entropy $H_c = \log_2 \pi R^2$.

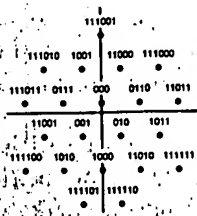


Fig. 7. Source-coded constellation.

two-dimensional Gaussian distribution of variance σ^2 in each dimension has average energy $S_g = 2\sigma^2$ and entropy $H_g = \log_2 2\pi e\sigma^2$. Thus,

$$H_c = \log_2 2\pi S_c$$

$$H_g = \log_2 \pi e S_g$$

To yield the same entropy, the Gaussian distribution requires a factor of $e/2 = 1.36$ (or 1.33 dB) less average energy than the circular distribution.

Implementation of a constellation with nonuniform probabilities presents a number of practical problems. One possible way of achieving some of the potential gain is to divide the incoming data bits into words of nonuniform length according to a prefix code, and then to map the prefix code words into signal points drawn as before from a regular two-dimensional lattice. The probability associated with a prefix code word of length t bits is then 2^{-t} . For example, Fig. 7 gives a set of prefix code words and a mapping onto the hexagonal lattice that yields an average energy of $S = 7.02$ while transmitting an average of 4 bits/symbol, an improvement of close to 1 dB over the best $n = 4$ uniform code known. Of course, the fact that the number of data bits transmitted per unit time is a random variable leads to system problems (e.g., buffering, delay) that may outweigh any possible improvement in signal-to-noise margin.

B. Higher-Dimensional Constellations

It is possible to achieve the same gain in another way by coding blocks of data into higher-dimensional constellations without going to the true block coding to be described in later sections. (By "true coding," we refer to schemes in which the distance between sequences in a higher number of dimensions is greater than that between points in two dimensions.) We have already seen in Section III-A that a small (0.2 dB) gain is possible by going from one-dimensional PAM to two-dimensional QAM and choosing points on a two-dimensional rectangular lattice from within a circular rather than a square boundary. In the same way, by going to a higher number N of dimensions and choosing points on an N -dimensional rectangular lattice from within an N -sphere rather than an N -cube, further modest savings are possible. Table III gives the energy savings possible in N dimensions, based on the difference between average energy of an N -sphere versus an N -cube of the same volume. Note that as N goes to infinity, the gain goes to $\pi e/6$ (by the Stirling approxima-

TABLE III
ENERGY SAVINGS FROM N -SPHERE MAPPING

N	Gain	dB
2	1.05	.20
4	1.11	.45
8	1.18	.73
16	1.25	.98
24	1.29	1.10
32	1.31	1.17
48	1.34	1.26
64	1.35	1.31

$$\text{Gain} = \frac{\pi(N+2)}{12} [(N/2)] - 2/N \text{ (for } N \text{ even)}$$

tion, $(n!)^{-1/n}$ goes to e/n), or 1.53 dB; the improvement over $N = 2$ goes to $e/2$ or 1.33 dB, as computed above. This is because for large N , the probabilities of points in any two dimensions become nonuniform and ultimately Gaussian. (It seems remarkable that a purely geometric fact like the asymptotic ratio of the second moment of an N -sphere to that of an N -cube can be derived from an information-theoretic entropy calculation in 2-space, but so it can.)

Implementation of such a scheme also involves added complexity that may outweigh the performance gain. To send n bits/symbol in N dimensions (assuming N even), incoming bits must be grouped in blocks of $Nn/2$. Some sort of mapping must then be made into the $2^{Nn/2}$ N -dimensional vectors with odd-integer coordinates (assuming a rectangular lattice) which have least energy among all such vectors. This can rapidly become a huge task; and a corresponding inverse mapping must be made at the receiver. Compromises can be made to simplify the mapping, at the cost of some suboptimality in energy efficiency; e.g., the cross is an effective compromise between the square and the circle in two dimensions.

C. Nonintegral Number of Bits/Symbol

It is sometimes desirable (as we shall see in Section VI) to transmit a nonintegral number of bits/symbol. Since in general an additional 1 bit/symbol costs about an additional 3 dB, it ought to be possible to send an additional 1/2 bit/symbol for about 1.5 dB. In this section we give a simple method that effectively achieves such performance. The method can be generalized to other simple binary fractions at the expected costs, but we shall omit the generalization here.

To send $n + 1/2$ bits/symbol, we proceed as follows. Use a signal constellation comprising 2^n "inner points" drawn from a regular grid, such as any of those of Section III, and an additional 2^{n-1} "outer points" drawn from the same grid and of as little average energy as possible, subject to whatever symmetry constraints may be imposed. Incoming bits are then grouped into blocks of $2n + 1$ bits and sent in two successive symbol intervals as follows. One bit in the block determines whether any outer point is to be used. If not, the remaining $2n$ bits are used, n at a time, to select two inner points. If so, then one additional bit selects which of the two signals is to be an outer point, $n - 1$ bits select which outer point, and the remaining n bits select which inner point for the other signal. (That is, at most one outer point is sent.) With random data, the average

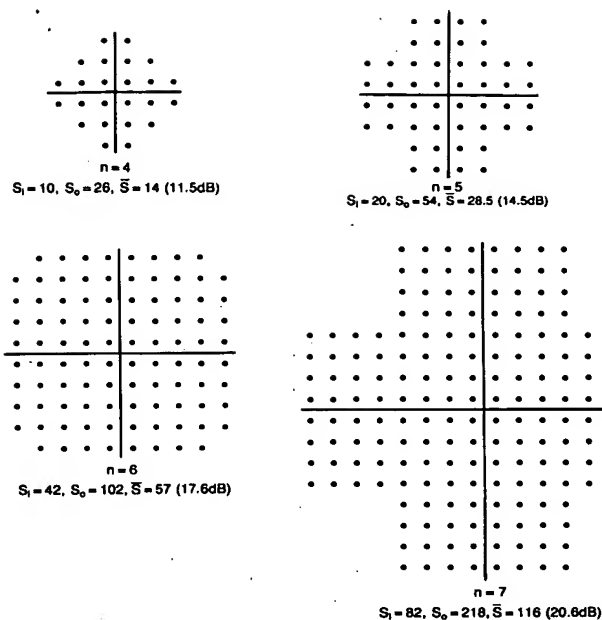


Fig. 8. Constellations to send $(n + \frac{1}{2})$ bits/symbol.

energy is $3/4$ the average energy of inner points plus $1/4$ the average energy of outer points. Fig. 8 shows constellations of 24, 48, 96, and 192 points that can be used in such schemes for $4 \leq n \leq 7$; the average energy in all cases for $n + 1/2$ bits/symbol is approximately halfway between that needed for n and that for $n + 1$ bits/symbol. Thus, these constellations are intermediate between the Campiano/Glazer constellations in the same way that the cross constellations are intermediate between the squares. (In fact, it can be shown that the 2-dimensional cross constellations can be derived from 1-dimensional PAM constellations with "inner" and "outer" points in an analogous way.)

V. CODING FUNDAMENTALS

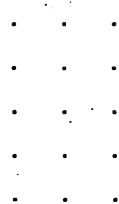
Heretofore we have been concerned with methods of mapping input bits to signal point constellations in two or more dimensions, where in higher dimensions the bits simply lie on the lattice that is the Cartesian product of two-dimensional rectangular lattices, so that the distance between points in N -space is no different from that in two dimensions. Now we shall begin to discuss methods of coding of sequences of signal points, where for the purposes of this paper we mean by coding (or "channel coding") the introduction of interdependencies between sequences of signal points such that not all sequences are possible; as a consequence, perhaps surprisingly, the minimum distance d_{\min} in N -space between two possible sequences is greater than the minimum distance d_o in 2-space between two signal points in the constellation from which signal points are drawn. Use of maximum likelihood sequence detection at the receiver yields a "coding gain" of a factor of d_{\min}^2/d_o^2 in energy efficiency, less whatever

additional energy is needed for signaling. (In practice, some of the "coding gain" may be lost due to there being a large number of sequences at distance d_{\min} from the correct sequence and therefore a large number of possibilities for error, called the "error coefficient" effect. We shall not be able to discuss the "error coefficient" much in this paper, but offer some general remarks at the end of Section VIII.)

Conventional coding techniques cannot be directly applied in conjunction with band-limited modulation techniques, at least with significant gain. (In 1970-1971, at least four companies prototyped conventional coding schemes for use in high-speed modems; two of the companies failed, and two shortly withdrew their products from the market.) In recent years, however, a number of effective coding techniques have been developed for such applications. The most important point to be made in this paper is that all of these coding schemes can be developed from a common conceptual principle. This principle was set forth clearly by Ungerboeck [15], who called it "mapping by set partitioning," although its roots may perhaps be found elsewhere as well. We describe it in this section, and in succeeding sections then use it to develop all known and some new coding schemes, both block and trellis.

We shall consider only 2-dimensional constellations with points drawn from a 2-dimensional rectangular grid. (From research to date, we cannot find any advantage to starting with hexagonal grids when higher orders of coding are to be used.)

Such a constellation can be divided into two subsets by assigning alternate points to each subset; i.e., according to the pattern



The resulting two subsets (A and B), have the following properties.

- The points in each subset lie on a rectangular grid (rotated 45° with respect to the original grid).
- The minimum squared distance between points within a subset is twice the minimum squared distance $[d_o^2]$ between points in the original constellation.

Furthermore, because of the first property, the partitioning can be repeated to yield 4, 8, 16, ... subsets with similar properties, and in particular within-subset squared distances of 4, 8, 16, ... times d_o^2 . Fig. 9 shows the 64-point square constellation divided into two subsets of 32 points, 4 subsets of 16 points, 8 subsets of 8 points, and

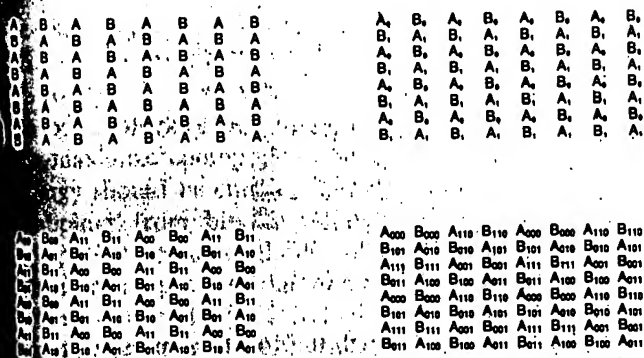
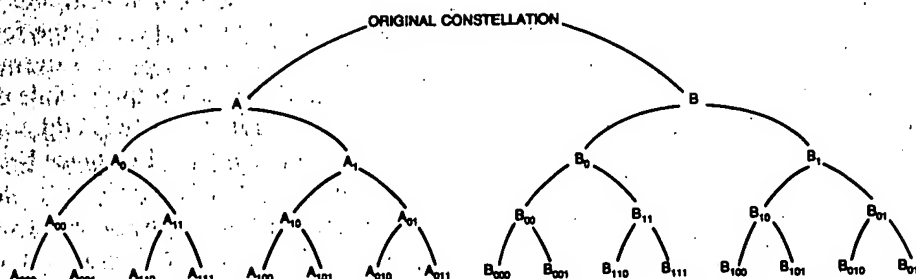


Fig. 9. A 64-point constellation partitioned four times.

16 subsets of 4 points. The subset nomenclature is according to the following binary tree:



This nomenclature is different from that of Ungerboeck [5], who uses a more natural subscript notation that reflects the successive binary partitions; our nomenclature will be useful in the next section, where we shall use the fact (evident by inspection) that at both the 4-subset and 16-subset levels, the minimum squared distance between two A -subsets, say, is $2d_0^2$ times the Hamming distance between their subscripts: e.g., $d^2(A_{00}, A_{11}) = 2d_0^2$; $d^2(A_{00}, A_{01}) = 2d_0^2$; $d^2(A_{00}, A_{10}) = 4d_0^2$; and so forth.

These subsets may then be used to implement relatively simple but effective coding schemes, illustrated in general in Fig. 10. Certain incoming data bits are encoded in a binary encoder, resulting in a larger number of coded bits. The coded bits are then used to select which subsets are to be used for each symbol. The remaining incoming bits are not coded, but merely select points from the selected subsets, with the signal constellation chosen large enough to accommodate all incoming bits. The coding scheme is thus more or less decoupled from the choice of constellation, as long as it is of the rectangular grid type. The coding gain is effectively determined by the distance properties of the subsets combined with those of the binary code, regardless of the size of the constellation. On the other hand, the constellation size, boundary, symmetries, and other "uncoded" properties such as were investigated in earlier sections are more or less independent of the coded bits and are determined by the mapping of the remaining bits. This may be regarded as effectively decou-

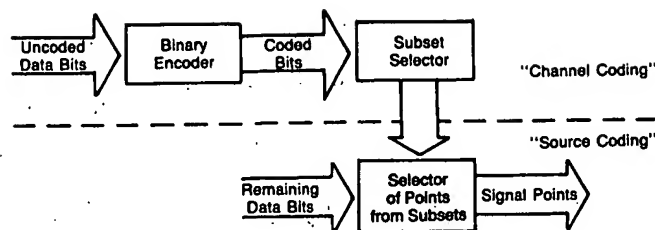


Fig. 10. General coding scheme.

pling "source coding" from "channel coding" and is important both conceptually and in implementation.

We now show how this general scheme can be applied to both block and trellis codes, with performance approaching the R_0 estimate.

VI. BLOCK CODES

In Section IV-B we saw what could be achieved by using points from an N -dimensional rectangular lattice and using an N -sphere, rather than an N -cube, as a boundary.

The rectangular lattice comprising all N -dimensional vectors with odd-integer coordinates is not the most densely packed for any N greater than 1; for example, for $N = 2$, the hexagonal lattice is 0.6 dB denser, as we have seen. Finding the densest lattice in N dimensions is an old and well-studied problem in the mathematical literature. Table IV gives the densest packings currently known for all N up to 24 and selected larger N , with the improvement in packing density over the rectangular lattice given in absolute and in dB terms [16]. The dimensions $N = 4, 8, 16$, and 24 are locally particularly good and are known to be optimum in the sense of being the densest possible lattice packing in these dimensions.

A body of recent work [11], [12], [18]–[21] generalizes the Campopiano–Glazer construction to N dimensions by taking all points on the densest lattice in N -space that lie within an N -sphere, where the radius of the sphere is chosen just large enough to enclose 2^m points, to send m bits per dimension. These codes obtain a "coding gain" over PAM which is a combination of both the lattice packing density gain of Table IV ("channel coding") and the N -sphere/ N -cube boundary gain of Table III ("source coding"). The resulting coding gains achievable for $N = 2$,

TABLE IV
ENERGY SAVINGS FROM DENSE LATTICES

N	Density	Gain	dB
1	.500	1.00	.00
2	.289	1.15	.62
3	.177	1.26	1.00
4	.125	1.41	1.51
5	.088	1.52	1.81
6	.072	1.67	2.21
7	.063	1.81	2.58
8	.063	2.00	3.01
9	.044	2.00	3.01
10	.037	2.07	3.18
11	.035	2.18	3.38
12	.037	2.31	3.63
13	.035	2.39	3.78
14	.036	2.49	3.98
15	.044	2.64	4.21
16	.063	2.83	4.52
17	.063	2.89	4.60
18	.072	2.99	4.75
19	.068	3.10	4.91
20	.125	3.25	5.11
21	.177	3.39	5.30
22	.289	3.57	5.53
23	.500	3.77	5.78
24	1.000	4.00	6.02
32	1.000	4.00	6.02
36	2.000	4.18	6.19
40	18.000	4.59	6.82
48	19832.947	6.00	7.78
64	4194304.000	6.44	8.09

TABLE V
COMBINED ENERGY SAVINGS

N	Gain	dB
2	1.21	.82
4	1.57	1.96
8	2.36	3.74
16	3.54	5.50
24	5.18	7.12
32	5.24	7.19
48	8.04	9.04
64	8.69	9.40

4, 8, 16, 24, 32, 48 and 64 are shown in Table V. Because the number of near neighbors in these densely packed lattices becomes very large, the total number of error events ("error coefficient") becomes large, which reduces the coding gain realized in practice. Also, the mapping of all mN bit combinations to their corresponding signal points can be an enormous task, even if all possible symmetries and simplifications are cleverly exploited [20], [21].

We will now show that certain of these dense N -dimensional lattices can be constructed using 2-dimensional rectangular lattices, the subset partitioning idea, and simple binary block codes. In particular, we shall give constructions for $N=4, 8, 16$ and 24 that form a natural sequence both in complexity and in nominal coding gain (respectively 1.5, 3.0, 4.5, and 6.0 dB, using the simplest implementations). (Cusack [21a] has recently shown how to construct dense 2^n -dimensional lattices from 2-dimensional lattices using Reed-Muller codes, for any n ; for $N=4, 8$, and 16 , the lattices obtained are the same as those we obtain here.)

To generate the optimum N -dimensional lattices for $N=4, 8, 16$, and 24 , we shall use sequences of 2, 4, 8, and 12 points from the 2-dimensional rectangular lattice, partitioned as shown in Fig. 9, into 2, 4, 8, and 16 subsets, respectively.

The 4-dimensional lattice is generated by taking all sequences of two points in which both points come from the same subset, i.e., sequences of the form (A, A) or (B, B) .

The 8-dimensional lattice consists of all sequences of four points in which all points are either A points or B points and further in which the 4 subset subscripts satisfy an overall parity check, $i_1 + i_2 + i_3 + i_4 = 0$; e.g., sequences of the form (A_0, A_0, A_0, A_0) , (B_0, B_1, B_0, B_1) , and so forth. (In other words, the subscripts must be codewords in the $(4, 3)$ single-parity-check block code, whose minimum Hamming distance between codewords is 2.)

The 16-dimensional lattice consists of all sequences of eight points in which all points are either A points or B

points, and further, in which the 16 subset subscripts (each subset now having two subscripts) are codewords in the $(16, 11)$ extended Hamming code, whose minimum Hamming distance between codewords is 4.

The 24-dimensional lattice consists of all sequences of 12 points in which all points are either A points or B points; the 24 (i, j) subscripts are codewords in the $(24, 12)$ Golay code, known to have minimum Hamming distance 8, and further, in which the third subscripts k are constrained to satisfy an overall parity check in the following way: if the sequence is of all A points, then overall k parity is even (an even number are equal to 1), while if the sequence is of all B points, overall k parity is odd.

If the minimum squared distance between points in the 2-dimensional constellation is d_0^2 , then the minimum squared distance between points (sequences) in these higher-dimensional lattices can be shown to be $2d_0^2$, $4d_0^2$, $8d_0^2$, and $16d_0^2$, respectively, as follows.

a) A sequence of A points and a sequence of B points differ from each other by squared distance at least d_0^2 in every point and therefore by at least $2d_0^2$, $4d_0^2$, $8d_0^2$, and $12d_0^2$ in total. In fact, in the 24-dimensional case there is a distance of at least $5d_0^2$ in at least one symbol, so the minimum squared distance between A sequences and B sequences is at least $16d_0^2$. The proof depends on the properties of the Golay code as well as the particular partitioning shown in Fig. 9 and is in the Appendix.

b) Two different sequences with points all from the same sequence of subsets must differ in at least one point by the minimum within-subset squared distance, which is $2d_0^2$, $4d_0^2$, $8d_0^2$, or $16d_0^2$, respectively. This is all we need to establish $2d_0^2$ as the minimum squared distance between sequences in the 4-dimensional case.

c) For $N=8, 16$, and 24 , the i or (i, j) subset subscripts are drawn from $(4, 3)$, $(16, 11)$, or $(24, 12)$ codes with minimum Hamming distances 2, 4, and 8, respectively. By the relation between subscript Hamming distance d_H and subset squared distance $d_s^2 = 2d_H d_0^2$ given in Section V, two sequences with points drawn from subsets of the same type (A or B) but different i or (i, j) subscripts must differ by squared distance at least $4d_0^2$, $8d_0^2$, or $16d_0^2$, respectively. This is all we need for the 8- and 16-dimensional cases.

d) For $N=24$, two sequences of points from subsets of the same type and with the same (i, j) subscripts but different k subscripts must differ by at least $8d_0^2$ in at least two symbols because of the overall k parity check, and the fact that the minimum squared distance between points of

the same type and with the same (i, j) subscripts is $8d_o^2$. This concludes the 24-dimensional proof.

To send m bits/symbol using these lattices, we need to encode a block of mN bits into one of 2^{mN} lattice points. To maximize coding gain, the 2^{mN} lattice points of least energy should be chosen; however, implementation of the mappings from bits to points and vice versa becomes complex. Simpler methods will now be given, using the binary codes used to construct the lattices, and the constellations either of Fig. 3 (for $N=8$ and 24) or of Fig. 8, along with the method of sending half-integral numbers of bits/symbol given in Section IV-C (for $N=4$ and 16). The loss in coding gain is relatively small, ranging from a few tenths of a decibel for $N=4$ or 8, up to about 1 dB for $N=24$; it is upperbounded by the N -sphere/ N -cube gain given in Table III.

Of the block of mN bits, we always use one bit to specify whether A or B points will be used. For $N=8, 16$, and 24, a further set of bits is used as input to a binary block coder, which produces appropriate codewords to be used as subset subscript designators: 3 bits to produce 4 for $N=8$, 11 bits to produce 16 for $N=16$, and $12+11=23$ bits to produce $24+12=36$ for $N=24$. Thus, a total of 1, 12, or 24 incoming bits are used as in Fig. 10 to select the subsets, or $\frac{1}{2}, 1, 1\frac{1}{2}$, or 2 bits/symbol, respectively.

The remaining bits are used to select points from the selected subsets. We use the rectangular constellations of Figs. 3 and 8 as follows: for $N=4$, constellations of 1.5×2^m points, as in Fig. 8, divided into two $1.5 \times 2^{m-1}$ point subsets, A and B ; for $N=8$, constellations of 2^{m+1} points as in Fig. 3, divided into four 2^{m-1} point subsets; for $N=16$, constellations of $1.5 \times 2^{m+1}$ points as in Fig. 8, divided into eight $1.5 \times 2^{m-2}$ point subsets; and for $N=24$, constellations of 2^{m+2} points as in Fig. 3, divided into 16 2^{m-2} point subsets. (In all cases m must be large enough so that the subsets resulting from the partitioning have equal size and other desired properties, e.g., symmetries.) These can be used to send $m - \frac{1}{2}, m - 1, m - 1\frac{1}{2}$, or $m - 2$ bits/symbol, where for $N=4$ and 16, the method of sending half-integral bits/symbol of Section IV-C may be used.

Since the minimum squared distance in N -space is 2, 4, or 16, times the minimum squared distance for an uncoded 2^m -point constellation, there is a distance gain of 6, 9, or 12 dB, respectively. However, the expanded constellations required with coded modulation cost 1.5, 3, 5, and 6 dB, respectively, yielding a net coding gain of 5, 3, 4.5, and 6 dB for $N=4, 8, 16$, and 24. The family relationship of this progression of codes is apparent.

Maximum likelihood sequence detection of the lattice point closest to a sequence of received points is easy for $N=4$ and 8. General methods are given in [22]. For $N=8$, given four received points, assume first that A points were sent. Find the closest A point to each received point, and check subscript parity of the four subsets tentatively decided. If the parity check fails, change the least reliable decision to the next closest A point (which must be in the other A subset). This gives the best A sequence satisfying

the parity-check constraint. Repeat, assuming that B points were sent, to get the best B sequence. Compare the best A and B sequences, and choose the better as the final decision.

Detection for $N=16$ or 24 is harder, involving either generalization of soft-decision decoding of the (16,11) or (24,12) block codes to perform error correction on tentative decision subscripts (as above; the method of changing the least reliable decision if an overall parity check fails was used in the 1950's as a soft-decision error-correction method for single-parity-check codes by Wagner), or exhaustive search of a neighborhood of the received sequence in N -space. Note that as its first step the decoder can always choose the closest point in each subset to each received point as representative of that subset, there being no reason to prefer any more distant point, and then proceed to determine the best sequence of subsets using those points (with their distances from the received point) as proxies for the corresponding subsets; the decoding task may thus be partitioned in the same way as coding is partitioned in Fig. 10.

VII. TRELLIS CODES

On power-limited channels (such as the satellite channel), convolutional coding techniques have more or less become the standard (although there are some who continue to champion block codes [23]). Generally, anything that can be achieved with a block code can be achieved with somewhat greater simplicity with a convolutional code. We have just seen that relatively simple ($N=8$) block codes can achieve of the order of 3 dB coding gain on band-limited channels, and relatively complex ($N=24$) block codes can achieve of the order of 6 dB. We shall now see that trellis codes can do the same, perhaps a bit more simply.

A. Ungerboeck Codes

For band-limited channels, the trellis codes came first, in the work of Ungerboeck [15]. In Ungerboeck's paper, to send n bits/symbol with two-dimensional modulation, a constellation of 2^{n+1} points is used, partitioned into 4 or 8 subsets. 1 or 2 incoming bits/symbol enter a rate- $\frac{1}{2}$ or rate- $\frac{2}{3}$ binary convolutional encoder, and the resulting 2 or 3 coded bits/symbol specify which subset is to be used. The remaining incoming bits specify which point from the selected subset is to be used.

The coding gain obtainable increases with the number M of states in the convolutional encoder. Ungerboeck's simplest scheme uses a 4-state encoder and achieves a nominal 3 dB coding gain (a factor of 4, or 6 dB, in increased sequence distance, less 3 dB due to use of the larger 2^{n+1} -point constellation). His most complex scheme uses a 128-state encoder and gains 6 dB (the limit with 8 subsets and a 2^{n+1} -point constellation since the within-subset distance is $8d_o^2$ for a 9 dB gain, less the 3 dB due to the larger constellation). Table VI gives the coding gains obtained by

TABLE VI
CODING GAINS FOR UNGERBOECK CODES

States	Gain	dB
4	2.0	3.0
8	2.5	4.0
16	3.0	4.8
32	3.0	4.8
64	3.5	5.4
128	4.0	6.0

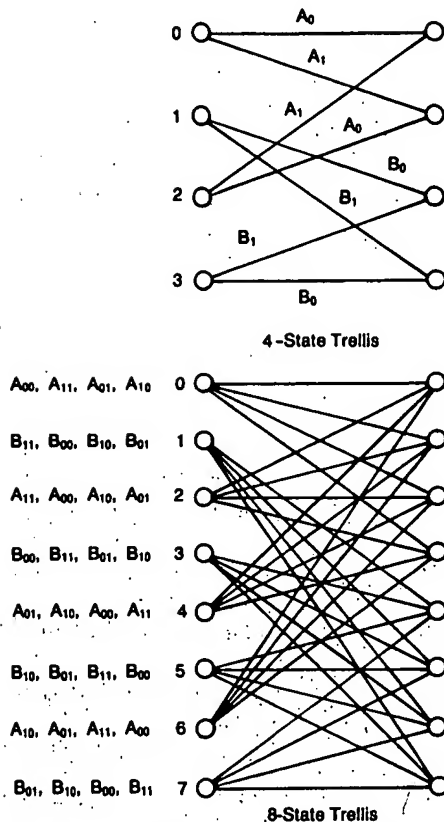


Fig. 11. Ungerboeck 4- and 8-state trellis codes.

Ungerboeck for these and intermediate numbers of states.

Decoding is assumed to be by the Viterbi algorithm [24], a maximum likelihood sequence estimation procedure for any trellis code. The complexity of such a decoder is roughly proportional to the number of encoder states. With these codes, each branch in the trellis corresponds to a subset rather than to an individual signal point; but if the first step in decoding is to determine the best signal point within each subset (the one closest to the received point), then that point and its metric (squared distance from the received point) can be used thereafter for that branch, and Viterbi decoding can proceed in a conventional manner. Fig. 11 gives trellises with branches labeled by subset for Ungerboeck's 4-state and 8-state codes.

(Note: the block codes of the previous section can be represented as trellises; Fig. 12 shows the trellises corresponding to the $N=4$ and $N=8$ codes. Viterbi decoding could therefore be used for them as well. It is interesting that the block code with 3 dB coding gain is also associated with a 4-state trellis, albeit decomposable into two parallel

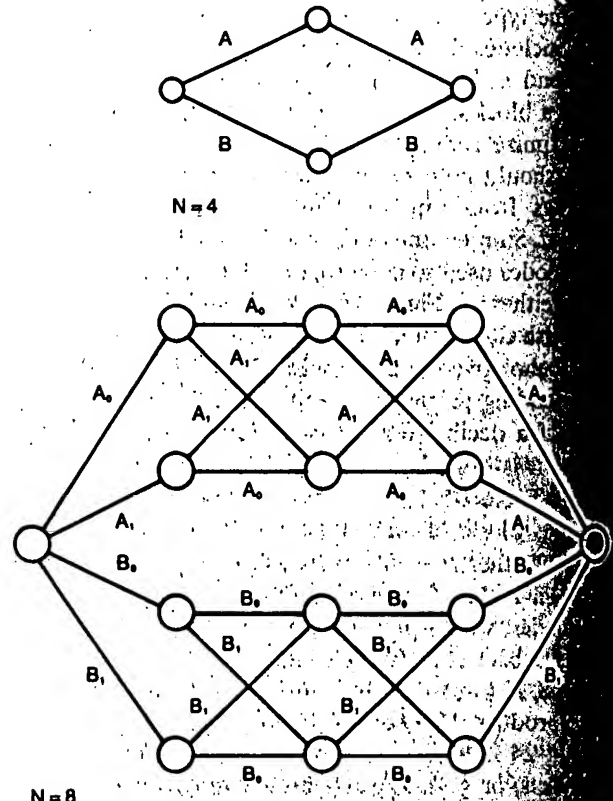


Fig. 12. Trellises corresponding to $N=4$ and $N=8$ block codes.

2-state trellises. The $N=16$ block code can similarly be associated with a 64-state trellis decomposable into two parallel 32-state trellises, and the $N=24$ block code can be associated with a 2×4096 -state trellis.)

8-state trellis codes with nominal 4 dB coding gain are the process of being adopted as international CCITT standards for 9600 bit/s transmission over the switched (dial) telephone network [25] and potentially for 14.4 kbit/s transmission over private lines as well [26]. A slight variant [27] of the Ungerboeck scheme involving a nonlinear convolutional encoder is being used in these standards; with this variant, whose trellis is shown in Fig. 13, a 90° rotation of a coded sequence is another coded sequence, so that differential coding techniques may be used. The distance properties and therefore coding gain of the variant are apparently identical to those of Ungerboeck's 8-state scheme.

B. Other Trellis Codes

The Ungerboeck codes seem to cover the range of possible coding gains with complexity of the order of what one might expect, and may therefore be taken as a benchmark of how much complexity is needed to achieve different coding gains in the 3–6 dB range. Can they be improved upon? From our research, the answer seems to be: yes, but not very much. In this section we shall describe two schemes that exhibit modest improvements and some new ideas: a 2-state code that has a nominal coding gain of almost 3 dB, and an 8-state trellis code with a coding gain

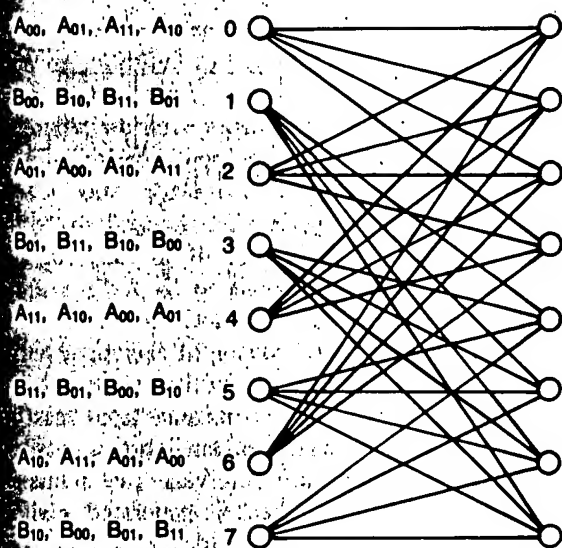


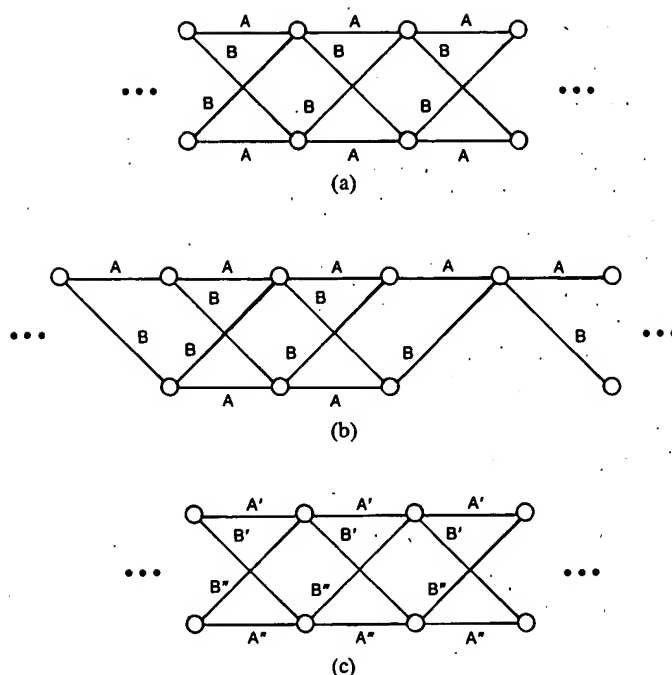
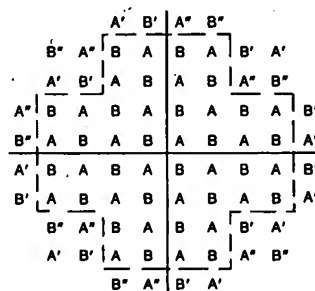
Fig. 13. Nonlinear 8-state trellis code with 90° symmetry.

(4.5 dB). The new idea in the 2-state scheme is to use subsets that are partially overlapping and partially distinct. The new idea in the 8-state scheme is to use a 4-dimensional constellation rather than 2-dimensional as the basic constellation. (4-dimensional trellis codes have also been studied by Wilson [28] and Fang *et al.* [28a].)

1) 2-state Trellis Code: If a 2^n -point signal constellation is partitioned into two subsets of A points and B points, and channel coding is done using the (infinite) 2-state trellis shown at the top of Fig. 14, it would appear at first glance that a 3 dB gain is obtained at no cost. This scheme sends n bits/symbol with no signal constellation expansion; further, any two sequences that start at one common node and end at another differ by a squared distance of at least $2d_o^2$, because the paths differ by at least d_o^2 when they diverge and another d_o^2 when they merge, so the nominal coding gain is apparently a factor of 2 or 3 dB.

Of course, we cannot get something for nothing, and the fallacy in this scheme (called "catastrophic error propagation" in the convolutional coding literature) is that there are paths of infinite length starting from a common node that never remerge and have squared distance only d_o^2 , namely any two paths of the form $AXYZ \dots$ and $BXYZ \dots$. (The "error coefficient" is infinite.)

One way of curing this problem is to terminate the trellis every b symbols by forcing it to a single node, illustrated in Fig. 14(b). In other words, at the b th symbol, the subset is constrained to be A or B , as necessary to reach the designated node. Only $n-1$ bits can be used to determine the b th symbol, so there is a cost of 1 bit per b symbols of transmission capacity, but now a legitimate coding gain of 3 dB is obtained minus $(1/b) \times 3$ dB for the rate loss. The space block code would operate in just this way if it used only A points, partitioned into A_0 and A_1 (see the top half of this trellis in Fig. 12); happily it is possible to insert a similar code made up of B points into the interstices of the code lattice without compromising distance, and the additional bit involved in specifying A or B compensates


 Fig. 14. 2-state trellises. (a) Infinite nonredundant 2-state trellis. (b) 2-state trellis terminated every 4 symbols. (c) Time-invariant 2-state trellis with $A' \neq A''$, $B' \neq B''$.

 Fig. 15. 80-point signal constellation. 32-point subsets A' , A'' , B' , B'' have 24 common points, 8 unique points; e.g., $A' = 24$ A inner points plus 8 A' outer points. $S_i = 31.3$; $S_o = 80$; $S = 43.5$ (16.4 dB).

for the bit lost at the fourth symbol, and allows a full 3 dB gain. This terminated trellis code may be regarded as a generalization of a single-parity-check block code.

Another way of gaining almost 3 dB while using a time-invariant trellis code is as follows. The signal constellation is modestly expanded to include $(1+p)2^n$ points, arranged on a rectangular grid and divided as usual into A and B subsets of $(1+p)2^{n-1}$ points each. The A and B subsets are further divided into $(1-p)2^{n-1}$ "inner" points and $2p$ "outer" points. Finally, sets A' , A'' , B' , and B'' , each of 2^{n-1} points, are created as follows: A' and A'' both include the $(1-p)2^{n-1}$ inner A points, but each includes a different half of the $2p$ outer points; and similarly with B' and B'' . Thus A' and A'' are partially overlapping and partially disjoint, and so are B' and B'' . The probability that a random choice from A' will not be a member of A'' is p . Such a construction is illustrated for $n=6$ and $p=0.25$ in Fig. 15.

Now the sets A' , A'' , B' , and B'' may be used in a 2-state trellis as illustrated in the last part of Fig. 14. The

squared distance between two paths beginning and ending at common nodes remains $2d_0^2$ since the basic distance properties between A subsets and B subsets remain. But now, although there are still pairs of infinite sequences comprising only inner points that start from a common node and never accumulate distance of more than d_0^2 , their probability is zero. The squared distance between any branch that uses an outer point and its counterpart branch must be at least $2d_0^2$ since the counterpart branch cannot use the same outer point and the distance between different points in the same subset is at least $2d_0^2$. For practical purposes, this means that a sequence containing such a branch cannot be confused with a sequence containing the counterpart branch, their squared distance being at least $3d_0^2$, so that in effect, whenever an outer point is sent, reconvergence to a common node is forced, as in the trellis termination method. Here, however, the reconvergence is probabilistic and happens on average every $1/p$ symbols, e.g., every 4 symbols if $p = 0.25$.

There is a slight reduction in power due to the increased constellation size; e.g., the average power using the constellation of Fig. 15 is 43.5 or 16.4 dB, versus 42 or 16.2 dB for the 8×8 constellation, or 41 (16.1 dB) for the Fig. 5 $n = 6$ cross constellation. Use of an integral approximation gives an estimate of additional power required of a factor of $1 + p^2$, or 1.0625 (0.26 dB) for $p = 0.25$. This can be made as small as desired by reducing p ; the cost, however, is a greater average time to converge and a greater average number of near-neighbor sequences ("error coefficient") increasing inversely proportional to p ; for this code the "error coefficient" is rather large and must be taken into account. Any p greater than zero in principle avoids catastrophic error propagation; a p of about 0.25 seems a good choice in practice.

2) *8-State Trellis Code*: For the 8-state four-dimensional scheme, we shall use a two-dimensional rectangular grid divided into four subsets as before. The binary convolutional encoder for this scheme, however, operates on pairs of symbols rather than single symbols. An appropriate encoder is shown in Fig. 16. During each pair of symbol intervals, three bits enter the encoder and four coded bits are produced. The first two coded bits select the subset for the first symbol and the second two bits select the subset for the second symbol.

If the Hamming distance between two encoded sequences is K , then the squared distance between the mappings onto grid points is at least Kd_0^2 . We now show that the minimum free Hamming distance of this convolutional code is 4. First note that the response of the encoder to a single 1 on any input line is a sequence with even weight, from which it follows that all encoded sequences have even weight and the minimum free distance is even. By inspection, it is easy to verify that there is no encoded sequence of weight 2, and a simultaneous 1 on all inputs yields an encoded sequence of weight 4. Thus, the squared distance between any two sequences corresponding to different encoded outputs is at least $4d_0^2$. If the encoded outputs are the same, but different elements are chosen from the same

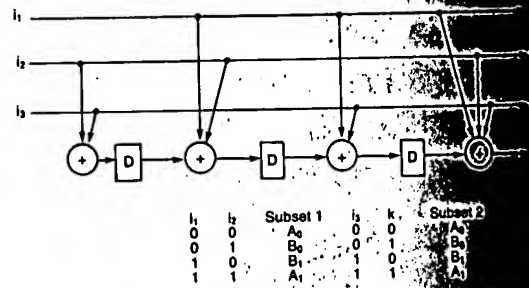


Fig. 16. Encoder for 8-state four-dimensional

subsets, then again the squared distance is at least $2d_0^2$. Suppose now that the signal constellation consists of $2n$ points. Then, over two symbol intervals, $2n$ bits enter the modem and one parity check is generated. Since $n = 3$ bits enter the modem, there is a loss of 1.5 dB due to the signal constellation and a gain of 6 dB in distance, for a nominal coding gain of 4.5 dB.

Section IV discussed encoding for a half-integer number of bits/symbol, and that method can be applied as an alternative which is somewhat more attractive. For an integer number n of bits/symbol, enter the modem $2n - 3$ bits entering the convolutional encoder and $2n - 3$ bits entering a prefix encoder as described in Section IV. This both maintains an integer number of bits/symbol and also gains an additional possible 1.33 dB for nonuniform probabilities.

VIII. CONCLUDING REMARKS

It has not been possible in this paper to cover all of the topics that are of importance in practice.

The only channel disturbance considered has been Gaussian noise. Other disturbances are usually encountered on telephone channels. There is some evidence that the coded modulation schemes are more robust relative to uncoded schemes than would be predicted by Gaussian noise calculations against important disturbances, such as nonlinear distortion, phase jitter, perhaps due to the memory inherent in modulation and sequence estimation over multiple symbols.

Because of the symmetries of attractive constellations, e.g., the 90° symmetry of most of our rectangular constellations, there may be an ambiguity in phase at the receiver. In general, there are two ways to handle this with coded modulation. If the code is such that the sequence basis, every 90° rotation of a code sequence is another legitimate code sequence, then it will be possible by differential quadrantal coding to make the transmission transparent to 90° rotations. Alternatively, if 90° rotations do not give valid code sequences, then it will be possible eventually to detect the force receiver phase to a valid setting. The latter technique is generally preferred. Of the codes we have discussed, the block codes generally are differentially

and the trellis codes are generally not, although they can often be modified to be; e.g., the modification of Fig. 11 shown in Fig. 13.

Finally, we have mostly used nominal coding gain as a figure of merit of coding schemes. In fact, error probabilities for coded systems on Gaussian channels are typically [24] of the form $P(E) = K \exp(-E)$, where the exponent E is governed by the nominal coding gain and the "error coefficient" K is of the order of the number of coded sequences at minimum distance from an average transmitted sequence. In general, the error coefficient

- a) increases with the complexity of coding;
- b) can cost a significant fraction of a dB for coding schemes with moderate (3–4 dB) gain, for error probabilities in the 10^{-5} – 10^{-6} range;
- c) can become very large for schemes with large (6+ dB) gain, such as the block codes with $N = 24$, or the most complex trellis codes; and
- d) is generally significantly larger for block codes than for trellis codes with comparable nominal coding gain.

Thus, the error coefficient cannot be ignored in a more detailed assessment of coded systems.

VIII. SUMMARY

On the band-limited channel, dense packing of 2-dimensional constellations with optimal (circular) boundaries yields less than 1 dB improvement over simple pulse amplitude modulation. Uncoded schemes in higher dimensions or, alternatively, source coding can gain somewhat more than 1 dB by using signal points with nonuniform probabilities. These gains pale by comparison with what can be obtained with (channel) coding, where relatively simple block or trellis codes easily yield coding gains of the order of 3 dB, or 1 bit/symbol. Relatively complex block and trellis codes have been constructed that yield of the order of 6 dB, or 2 bits/symbol. Because this is as much gain as would be predicted using the R_0 estimate and is only 3 dB below the capacity limit, it seems unlikely that further major improvements are possible. However, within the spectrum of performance of already known schemes, there will likely be some further embellishments that will reduce implementation complexity or have other desirable properties, such as the differentially coded variant of Ungerboeck's 8-state trellis code that is likely to become an international standard.

APPENDIX

PROOF THAT 24-SPACE LATTICE HAS $d_{\min}^2 = 16d_0^2$

If the grid of triple-subscripted signal points illustrated in Fig. 9 is rotated 45° with a point A_{000} at the origin, and scaled so that the coordinates (x, y) of all points are integers, then the following hold true.

- a) For A points, both x and y are even; for B points, both x and y are odd.

b) For A points, $i = 0$ iff $y = 0 \bmod 4$, and $j = 0$ iff $x = 0 \bmod 4$; for B points, $i = 0$ iff $y = 1 \bmod 4$, and $j = 0$ iff $x = 1 \bmod 4$.

c) For A points, $x + y = 2i + 2j + 4k \bmod 8$; for B points, $x + y = 2i + 2j + 4k + 2 \bmod 8$.

Two sequences with points from different groups differ by at least 1 in every one of the 24 (x, y) coordinates. They cannot all differ only by 1, however, because of the following. The sum S of all coordinates satisfies

$$\begin{aligned} S &= 2w_{ij} + 4w_k \bmod 8, & \text{for } A \text{ sequences;} \\ 2w_{ij} + 4w_k &\bmod 8, & \text{for } B \text{ sequences} \end{aligned}$$

where w_{ij} is the number of (i, j) subscripts equal to 1, and w_k the number of k subscripts equal to 1. But since the (i, j) subscripts form a Golay code word and all such words have weights equal to integer multiples of 4, and since w_k is even for A sequences and odd for B sequences by construction,

$$\begin{aligned} S &= 0 \bmod 8, & \text{for } A \text{ sequences;} \\ 4 &\bmod 8, & \text{for } B \text{ sequences.} \end{aligned}$$

Now suppose that there were a B sequence that differed from an A sequence by +1 in every coordinate, and let m be the number of coordinates in which the difference was +1. Since the sum S_A of the A coordinates is $0 \bmod 8$ and the sum S_B of the B coordinates is $4 \bmod 8$, and $S_A - S_B = m - (24 - m) = 2m \bmod 8$, it follows that $2m = 4 \bmod 8$, or $m = 2 \bmod 4$. Now, the construction of the array is such that if a B point has an x coordinate 1 larger than the x coordinate of an A point, then the j subscript is the same, whereas if it is 1 smaller, then the j subscript is different; similarly a difference of +1 in y gives the same i subscript, while a difference of -1 gives the opposite one. Thus, $m = w_{ij}$. But, $w_{ij} = 0 \bmod 4$, so $m = 0 \bmod 4$; contradiction. Hence, any B sequence must differ from every A sequence by at least +3 in one coordinate, Q.E.D.

This lattice and its distance properties were originally discovered by Leech [29].

REFERENCES

- [1] C. E. Shannon and W. Weaver, *A Mathematical Theory of Communication*. Urbana, IL: Univ. Illinois Press, 1949.
- [2] G. D. Forney, Jr., "Coding and its application in space communications," *IEEE Spectrum*, vol. 7, pp. 47–58, 1970.
- [3] J. M. Wozencraft and R. S. Kennedy, "Modulation and demodulation for probabilistic coding," *IEEE Trans. Inform. Theory*, vol. IT-12, pp. 291–297, 1966.
- [4] J. L. Massey, "Coding and modulation in digital communications," in *Proc. 1974 Int. Zurich Seminar Digital Commun.*, Zurich, Switzerland, pp. E2(1)–E2(4), 1974.
- [5] J. M. Wozencraft and I. M. Jacobs, *Principles of Communication Engineering*. New York: Wiley, 1965.
- [6] R. W. Lucky, J. Salz, and E. J. Weldon, Jr., *Principles of Data Communications*. New York: McGraw-Hill, 1968, ch. 3.
- [7] C. R. Cahn, "Combined digital phase and amplitude modulation communication systems," *IRE Trans. Commun. Syst.*, vol. CS-8, pp. 150–154, 1960.
- [8] J. C. Hancock and R. W. Lucky, "Performance of combined amplitude and phase-modulated communication systems," *IRE Trans. Commun. Syst.*, vol. CS-8, pp. 232–237, 1960.
- [9] C. N. Campopiano and B. G. Glazer, "A coherent digital amplitude and phase modulation scheme," *IRE Trans. Commun. Syst.*, vol. CS-10, pp. 90–95, 1962.

- [10] R. W. Lucky and J. C. Hancock, "On the optimum performance of N-ary systems having two degrees of freedom," *IRE Trans. Commun. Syst.*, vol. CS-10, pp. 185-192, 1962.
- [11] J. H. Conway and N. J. A. Sloane, "Voronoi regions of lattices, second moments of polytopes, and quantization," *IEEE Trans. Inform. Theory*, vol. IT-28, pp. 211-226, 1982.
- [12] J. H. Conway and N. J. A. Sloane, "A fast encoding method for lattice codes and quantizers," *IEEE Trans. Inform. Theory*, vol. IT-29, pp. 820-824, 1983.
- [13] R. W. Lucky, "Digital phase and amplitude modulated communication systems," Ph.D. dissertation, Purdue Univ., Lafayette, IN, 1961 p. 89 (attributed to Cahn).
- [14] G. J. Foschini, R. D. Gitlin, and S. B. Weinstein, "Optimization of two-dimensional signal constellations in the presence of Gaussian noise," *IEEE Trans. Commun.*, vol. COM-22, pp. 28-38, 1974.
- [15] G. Ungerboeck, "Channel coding with multilevel/phase signals," *IEEE Trans. Inform. Theory*, vol. IT-28, pp. 55-67, 1982.
- [16] J. Leech and N. J. A. Sloane, "Sphere packings and error-correcting codes," *Can. J. Math.*, vol. 23, pp. 718-745, 1971.
- [17] G. R. W. W. Lee and J. S. Lee, "Digital transmission with coherent four-dimensional modulation," *IEEE Trans. Inform. Theory*, vol. IT-20, pp. 497-502, 1974.
- [18] Canada, "An aspect of future modem development," CCITT Contrib. COM-Sp.A No. 142, 1974.
- [19] N. J. A. Sloane, "Tables of sphere packings and spherical codes," *IEEE Trans. Inform. Theory*, vol. IT-27, pp. 327-338, 1981.
- [20] P. deBuda, "Encoding and decoding algorithms for an optimal lattice-based code," in *ICC Conv. Rec.*, pp. 65.3.1-65.3.5, 1981.
- [21] Canada, "Block coding for improved modem performance," CCITT Contrib. COM-XVII No. 112, 1983.
- [21a] E. L. Cusack, "Error control codes for QAM signalling," *Electron. Lett.*, vol. 20, pp. 62-63, 1984.
- [22] J. H. Conway and N. J. A. Sloane, "Fast quantizing and decoding algorithms for lattice quantizers and codes," *IEEE Trans. Inform. Theory*, vol. IT-28, pp. 227-232, 1982.
- [23] E. R. Berlekamp, "The technology of error-correcting codes," *Proc. IEEE*, vol. 68, pp. 564-593, 1980.
- [24] G. D. Forney, Jr., "The Viterbi algorithm," *Proc. IEEE*, vol. 61, pp. 268-278, 1973.
- [25] Rapporteur on 9600 bit/s duplex family modem, "Draft recommendation V.32 for a family of 2-wire, duplex modems operating at data signalling rates of up to 9600 bit/s for use on the general switched telephone network and on leased telephone-type circuits," CCITT Contrib. COM-XVII No. T30, Geneva, Switzerland, Mar. 1984; also see J. D. Brownlie and E. L. Cusack, "Duplex transmission at 4800 and 9600 bit/s on the general switched telephone network and the use of channel coding with a partitioned signal constellation," in *Proc. Zurich Int. Sem. Digital Commun.*, 1984.
- [26] Rapporteur on 14 400 bit/s modem, "Working draft recommendation V.32 for a 14 400 bit/s modem standardized for use on point-to-point 4-wire leased telephone-type circuits," CCITT Study Group XVII, 1984.
- [27] L. F. Wei, "Rotationally invariant convolutional channel coding with expanded signal space—Part II: Nonlinear codes," *IEEE J. Select. Areas Commun.*, vol. SAC-2, pp. xxx-xxx, Sept. 1984.
- [28] S. G. Wilson and H. A. Sleeper, "Four-dimensional modulation and coding: an alternate to frequency reuse," Univ. Virginia, Rep. UVA/528200/EE83/107, Sept. 1983.
- [28a] R. Fang and W. Lee, "Four-dimensionally coded PSK systems for combating effects of severe ISI and CCI," in *Proc. 1983 IEEE Globecom Conv. Rec.*, pp. 30.4.1-30.4.7, 1983.
- [29] J. Leech, "Notes on sphere packings," *Can. J. Math.*, vol. 19, pp. 251-267, 1967.



G. David Forney, Jr. (S'58-M'61-F'73) was born in New York, NY, on March 6, 1940. He received the B.S.E. degree in electrical engineering from Princeton University, Princeton, NJ, in 1961, and the M.S. and Sc.D. degrees in electrical engineering from the Massachusetts Institute of Technology, Cambridge, MA, in 1963 and 1965, respectively.

In 1965, he joined the Codex Corporation, and became a Vice President and Director in 1970. Since 1982 he has been Vice President and Direc-

tor of Technology and Planning of the Motorola Information Systems Group, Mansfield, MA. During the 1971-1972 academic year he was a Visiting Scientist at Stanford University, Stanford, CA, and he has also served as an Adjunct Professor at the Massachusetts Institute of Technology.

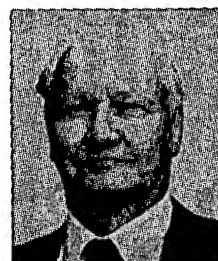
Dr. Forney was Editor of the IEEE TRANSACTIONS ON INFORMATION THEORY from 1970 to 1973 and has held numerous other IEEE positions. He was winner of the 1970 Information Theory Group Prize Paper Award and the 1972 Browder J. Thompson Memorial Prize Paper Award. He was elected to membership in the National Academy of Engineering in 1983.



Robert G. Gallager (S'58-M'61-F'68) received the S.B. degree in electrical engineering from the University of Pennsylvania, Philadelphia, PA, in 1953, and the S.M. and Sc.D. degrees in electrical engineering from the Massachusetts Institute of Technology, Cambridge, MA, in 1957 and 1960, respectively.

From 1953 to 1954 he was a Member of the Technical Staff at Bell Telephone Laboratories, and from 1954 to 1956 was in the Signal Corps of the U.S. Army. He has been with the Massachusetts Institute of Technology since 1956 and was Associate Chairman of the faculty from 1973 to 1975. He is currently a Professor in the Department of Electrical Engineering and Computer Science, Associate Director of the Laboratory for Information and Decision Systems, and Co-chairman of the Department Area I (Control, Communication, and Operations Research). He is a consultant to Codex Corporation, Western Union, and CNR. He is the author of the textbook *Information Theory and Reliable Communication* (New York: Wiley, 1968). His major research interests are data communication networks, information theory, and communication engineering.

Dr. Gallager was awarded the IEEE Baker Prize Paper Award in 1966 for the paper "A simple derivation of the coding theorem and some applications." He has been a member of the Administrative Committee of the IEEE Group on Information Theory, from 1965 to 1970 and from 1979 to the present, was Chairman of the Group in 1971, and was elected a member of the National Academy of Engineering in 1979.



Gordon R. Lang was born on September 7, 1922, in London, Ont., Canada. He received the B.Sc. degree (Hons.) in mathematics and physics, radio physics option, from the University of Western Ontario, London, in 1949.

He was with Ferranti Electric Ltd. from 1949 to 1965. He was a founding member of ESE Limited (now Motorola Information Systems Ltd.) in January 1965 and became a director of the company. He was appointed Associate Professor with the Department of Electrical Engineering, University of Toronto, Canada, in January 1965. He increased activity at ESE Limited as Director of Research in 1969 and became an Adjunct Professor with the Department of Electrical Engineering, University of Toronto. He is author or co-author of over 60 published papers plus a variety of conference papers. He has obtained approximately 16 patents. Presently, he is Vice-President of Research and Development at Motorola Information Systems Ltd.

Dr. Lang is a member of the Association of Professional Engineers of Ontario.



Fred M. Longstaff was born March 3, 1926, in Thornloe, Ont., Canada. He received the M.A.Sc. degree in engineering physics from the University of Toronto, Canada, in 1951.

He was with Ferranti Electric Ltd. from 1949 to 1965. He was a founding member of ESE Limited in January 1965 and became a Director of the company. He has had extensive experience since the early 1950's in the architecture of computer systems and in computer software, leading to the position since 1965 of Vice-President of

Systems and Software Development with ESE Limited (now Motorola Information Systems Ltd.), Rexdale, Ont.

Dr. Longstaff is a member of the Association of Professional Engineers of Ontario and the Association for Computing Machinery.



Shahid V. Qureshi (S'68-M'73-SM'81) was born in Peshawar, Pakistan, on September 22, 1945. He received the B.Sc. degree from the University of Engineering and Technology, Lahore, Pakistan, in 1967, the M.Sc. degree from the University of Alberta, Edmonton, Canada, in 1970 and the Ph.D. degree from the University of Toronto, Toronto, Canada, in 1973, all in electrical engineering.

From 1967 to 1968 he was a Lecturer with the Department of Electrical Engineering, University of Engineering and Technology, Lahore, Pakistan. He held the Canadian Commonwealth Scholarship from 1968 to 1972.

Since 1973 he has been with Codex Corporation, where he is currently Senior Director of Modulation Products Research. His interests include data communication, computer architecture for signal processing and the application of digital signal processing to communication.

Multidimensional Constellations—Part I: Introduction, Figures of Merit, and Generalized Cross Constellations

G. DAVID FORNEY, JR., FELLOW, IEEE, AND LEE-FANG WEI

Multidimensional constellations are desirable for representing fractional numbers of bits per two dimensions, useful for increasing SNR efficiency, and natural for use with multidimensional modulation. Desirable characteristics of such a constellation include SNR efficiency, low implementation complexity, compatibility with coded modulation and with QAM modems, including small peak-to-average power ratio (PAR) of its constituent 2D constellation, phase symmetry, scalability, and capability of supporting an "opportunistic secondary channel." The gain in SNR efficiency of an N -dimensional constellation (lattice code) consisting of the points of a lattice Λ within a region \mathcal{R} compared to a cubic constellation is to be approximately separable into the coding gain of the lattice and the "shape gain" of the region \mathcal{R} , for large constellations. Similarly, the expansion of the associated constituent 2D constellation is to be approximately separable into a coding component $CER_c(\Lambda)$ and a shaping component $CER_s(\mathcal{R})$. The N sphere is the region with the best shape gain; but also has large constellation expansion bounds for the best possible shape gain versus $CER_s(\mathcal{R})$ or PAR. Finally, generalized cross constellations are discussed; these constellations yield a modest shape gain with very low $CER_s(\mathcal{R})$ or PAR, are easily implemented, are well suited for use with coded QAM modems, and can be readily adapted to support an opportunistic secondary channel.

1. INTRODUCTION

An N -dimensional constellation C is a finite set of N tuples, or points, in N dimensional space. The size $|C|$ of a constellation is the number of its points.

There is a fairly long history of constellation designs, particularly for two-dimensional constellations with $|C| = 2^b$ points for b not too large, e.g., $2 \leq b \leq 8$. Much of this history is recounted in [1] and will not be repeated here.

In recent years, there has been increased attention to higher dimensional constellations. Some of this attention has been due to systems considerations, e.g., the need to send fractional numbers β of bits per two dimensions. Some has been due to the recognition that higher SNR efficiency is theoretically attainable in higher dimensions. However, the major impetus, in our view, has been the development of multidimensional coded modulation schemes that naturally lead to consideration of multidimensional constellations.

In this paper, we shall first discuss the major attributes desired in constellations, such as SNR efficiency, simplicity of mapping bits to points and vice versa, compatibility with coded modulation schemes, and compatibility with QAM modulation. The size and peak-to-average power ratio of the constituent 2D constellation are important considerations. We discuss one feature that has received more attention in practice than in the literature, namely, the capability of supporting an "opportunistic secondary channel," often used for internal control signalling.

A general method for constellation design is to choose a finite set of $|C|$ points from an N dimensional lattice Λ (or a translate of Λ) that lie within a finite region \mathcal{R} . Such a constellation has also been called a *lattice code*. This method not only results in a regular array of points in N space, but also yields constellations suitable for use with coded modulation.

If C is a lattice code of reasonably large size, then the distribution of its points in N space is well approximated by a uniform continuous distribution over the region \mathcal{R} . This is called the *continuous approximation*. We review a standard figure of merit for constellations that determines SNR efficiency, and show that under the continuous approximation it is separable into two parts: one which depends on the density of Λ , which is measured by the *coding gain* $\gamma_c(\Lambda)$ of the lattice Λ , and the other which depends on the sphericity of the region \mathcal{R} , which is measured by the *shape gain* $\gamma_s(\mathcal{R})$ of the region \mathcal{R} .

Similarly, the same approximation shows that for lattice codes there are two more or less independent factors that influence the size of the constituent 2D constellation: the *coding constellation expansion ratio* $CER_c(\Lambda)$ of the lattice Λ , and the *shaping constellation expansion ratio* $CER_s(\mathcal{R})$ of the region \mathcal{R} . The former is the price paid for the lattice gain $\gamma_c(\Lambda)$, and the latter is the price paid for the shape gain $\gamma_s(\mathcal{R})$. The peak-to-average power ratio (PAR) in two dimensions is also primarily a function of the shaping constellation expansion ratio.

The coding gain of a lattice (or, more generally, of a coset code \mathcal{C}) and the coding constellation expansion ratio are addressed in the coded modulation literature (e.g., [4] and the references therein). This paper is primarily concerned with the shape gain $\gamma_s(\mathcal{R})$, the shaping constella-

Manuscript received April 18, 1988; revised October 24, 1988.

G. D. Forney, Jr., is with Codex Corporation, Mansfield, MA 02048.

L. F. Wei is with AT&T Bell Laboratories, Holmdel, NJ 07733.

IEEE Log Number 8928305.

tion expansion ratio $\text{CER}_s(\mathbb{R})$, and other aspects of shaping with a region \mathbb{R} .

As discussed in [1], it is relatively easy to get coding gains of the order of 3 to 4 dB, using either dense lattices Λ (lattice codes) or more general coset codes \mathbb{C} (e.g., trellis codes), and there are more complex lattices and codes that achieve coding gains up to 6 dB, or more. However, as shown in [4], when we consider the effective coding gain (the coding gain decreased by an "error coefficient" factor), and take decoding complexity into account, we find that after the initial 3–4 dB it takes of the order of a doubling of complexity to achieve each 0.4 dB further increase in effective coding gain, for the best codes known. Consequently, even though the shape gain $\gamma_s(\mathbb{R})$ is limited to 1.53 dB, as we shall see below, it may become more attractive to invest complexity in shaping rather than in more complex codes when we seek to achieve the best possible performance for a given amount of computational complexity.

When \mathbb{R} is an N cube, there is neither shape gain nor constellation expansion due to shaping. When \mathbb{R} is an N sphere, shape gain is optimized (for N dimensions), but $\text{CER}_s(\mathbb{R})$ and the PAR in two dimensions increase rapidly with N . By limiting the peak energy of the constituent 2D constellation, $\text{CER}_s(\mathbb{R})$ and PAR can be significantly reduced, without much reduction of shape gain. We develop bounds on the best possible tradeoff between the shape gain $\gamma_s(\mathbb{R})$ and $\text{CER}_s(\mathbb{R})$ or PAR, which are in principle achievable as $N \rightarrow \infty$.

The final section covers generalized cross constellations, which generalize some of the constructions that were presented in an uncoded context in [1], and that were independently developed for use in coded modulation systems by Wei [2]. We show that they have many desirable practical attributes; in particular, they are simple to implement in coded QAM modems, have very low constellation expansion, and do achieve a modest shape gain. We indicate how they may be adapted to support an opportunistic secondary channel.

A companion paper [Part II] discusses Voronoi constellations, which represent another approach to multidimensional constellation design based on a lattice-theoretic choice of \mathbb{R} . In general, Voronoi constellations also have most of these desirable attributes, and can achieve significantly higher shape gains, but at the cost of somewhat larger $\text{CER}_s(\mathbb{R})$ or PAR.

II. DESIRABLE CONSTELLATION CHARACTERISTICS

In this section we discuss various considerations that influence constellation design, with emphasis on attributes that are desirable for constellations to be used in coded QAM modems. Throughout this section, we use simple square (two-dimensional) or N cube (N dimensional) constellations as a baseline.

A. SNR Efficiency: Constellation Figure of Merit

Naturally, the first characteristic that we require of an N dimensional constellation C is that it be able to repre-

sent a desired number b of bits in N dimensions, which means that its size $|C|$ must be (at least) 2^b . (We implicitly assume that data words are binary b tuples, and that all data words are equally likely.) It is convenient to normalize to two dimensions; a constellation that can represent b bits per N dimensions can represent a *normalized bit rate* of $\beta = 2b/N$ bits per two dimensions (β "bits per baud," or, loosely speaking, β bits/Hz).

For a given size $|C|$ or normalized bit rate β , the key parameters that determine the SNR efficiency of a constellation C are the *minimum squared distance* $d_{\min}^2(C)$ between its points, and its *average power* $P(C)$. In this paper the average power $P(C)$ will be taken as the average energy of C per two dimensions where the energy of an N -dimensional constellation point x is its Euclidean norm $\|x\|^2$, and the average energy of C is the average $E[\|x\|^2]$ when all $|C|$ points are equiprobable, so $P(C) = 2E[\|x\|^2]/N$.

For a given normalized bit rate β , we generally wish to maximize $d_{\min}^2(C)$ for a given $P(C)$, or to minimize $P(C)$ for a given $d_{\min}^2(C)$. Therefore it is customary to take the ratio

$$\text{CFM}(C) \triangleq d_{\min}^2(C)/P(C)$$

as what we shall call the *constellation figure of merit*. When C is used for signaling over a white Gaussian noise channel, the required signal-to-noise ratio (SNR) is inversely proportional to $\text{CFM}(C)$. Since scaling all points in a constellation by a scale factor α multiplies both $d_{\min}^2(C)$ and $P(C)$ by α^2 , $\text{CFM}(C)$ is a dimensionless quantity that is unaffected by scaling. We therefore often evaluate the $\text{CFM}(C)$ by evaluating the average power $P(C)$ of a constellation C for which $d_{\min}^2(C)$ has been normalized to 1.

For example, in one dimension, a *PAM constellation* is a set of $M = 2^b$ equally spaced points on the real line centered at the origin, e.g., the M half-integers within range from $-M/2$ to $M/2$, for which $d_{\min}^2(C) = 1$, $E[\|x\|^2] = (M^2 - 1)/12$, so the average power per dimension is $P(C) = (M^2 - 1)/6$. The figure of merit of a PAM constellation is thus $\text{CFM}(C) = 6/(M^2 - 1) = 6/(2^\beta - 1)$ where $\beta = 2b$ is the normalized bit rate per two dimensions. Thus asymptotically $\text{CFM}(C) \approx 6/2^\beta$.

We therefore define the *baseline constellation figure of merit* for a normalized bit rate of β as $\text{CFM}_\oplus(\beta) \triangleq 6/2^\beta$. This represents the asymptotic SNR efficiency that is achievable with simple, conventional PAM constellations, and will be our reference; any more complex constellation with the same β had better achieve a figure of merit $\text{CFM}(C)$ that is greater than $\text{CFM}_\oplus(\beta)$. A *gain* obtained by a constellation C with normalized rate β over the baseline is defined as

$$\text{CFM}(C)/\text{CFM}_\oplus(\beta) = 2^\beta \cdot d_{\min}^2(C)/[6P(C)]$$

In N dimensions, a *cubic constellation* is the Cartesian product of a PAM constellation with itself N times.

ple, in two dimensions, a "cubic constellation" is a (or "strict-sense QAM") $M \times M$ constellation. A N -dimensional cubic constellation has size $|C| = M^N$, normalized bit rate $\beta = 2 \log_2 M$, and average power $P(C) = (M^2 - 1)/6$, if $d_{\min}^2(C) = 1$; for any N and M , the figure of merit of a cubic constellation is $\text{CFM}(C) = 6/(M^2 - 1) \approx 6/2^\beta = 6/\beta$, and there is no asymptotic constellation gain.

Implementation Complexity

The next desirable characteristic is that the mappings of b bit data words to N -dimensional signal points and vice versa be reasonably simple to implement. The complexity of implementation is not much of an issue for two-dimensional constellations, since table lookups with 2^b entries are quite feasible for numbers like $b = 7$, or some more. However, when we wish to send, say, $\beta \geq 7$ bits per two dimensions using constellations in $N = 4$ or more dimensions, then tables with $2^b = 2^{8N/2}$ entries tend to be impractical, and we must specify algorithms for mappings in both directions whose complexity is reasonable. We do not consider here the receiver's first task, to estimate the sequence of signal points actually received from the noisy received sequence; this task is "decoding" and is considered in the coded modulation literature.)

The implementation complexity of a cubic constellation is low since we can specify each coordinate (or pair of coordinates) independently. In general, if an N -dimensional constellation is the M -fold Cartesian product of an $N/2$ -dimensional constellation with itself, then the implementation complexity is that of the constituent $N/2$ -dimensional constellation; but then the constellation figure of merit, the normalized bit rate, and all other parameters are also no different from those of the constituent (N/M) -dimensional constellation.

Compatibility with QAM Modems I: Constituent 2D

Constellations

When interested in implementing codes and constellations, we are often interested in QAM (quadrature amplitude modulation) modems. A QAM modem transmits a sequence of two-dimensional symbols. Therefore, we will want to choose the constellation dimension N as an even integer, and to represent an N -dimensional signal point as a sequence of $N/2$ two-dimensional symbols. For an N -dimensional constellation C , a constituent 2D constellation [2] is the set of all values that a given 2D symbol takes on as the N -dimensional signal point ranges through C , i.e., the projection of C onto two dimensions. If the constituent 2D constellation is the same for all pairs of coordinates, we say C is a 2D-symmetric constellation. Then we may define the constituent 2D constellation C_2 of C . (More precisely, the constituent 2D constellation C_2 may be defined as the union of the various constituent 2D constellations, if they differ.)

With this definition, C must be some subset of the points in the N -dimensional signal set $C_2^{N/2}$, the Cartesian product of C_2 with itself $N/2$ times, so $|C| \leq |C_2|^{N/2} = |C_2|^{N/2}$. It follows that the size $|C|$ of the constituent 2D constellation is lowerbounded by $|C|^{2/N} = 2^{2b/N} = 2^\beta$, whether or not the normalized bit rate β is an integer.

In general, it is desirable that the constituent 2D constellation be as small as possible, as is discussed in [2]. We define the constellation expansion ratio of a constellation C as $\text{CER}(C) \triangleq |C_2|/2^\beta = |C_2|/|C|^{2/N}$. We will want to keep $\text{CER}(C)$ as close to its lower bound of 1 as we can.

For an N -dimensional cubic constellation, the constituent 2D constellation is a square $M \times M$ constellation, so $|C_2| = M^2 = 2^\beta$, and the constellation expansion ratio is 1.

D. Compatibility with Coded Modulation

Calderbank and Sloane [5] introduced the terminology of constructing trellis codes based on partitions of lattices into cosets of sublattices. In [4], it is shown that essentially all of the codes with large normalized bit rates that have been used in coded modulation systems to date, including both lattice codes and lattice-type trellis codes, can be characterized as codes of this type, called coset codes.

The key ingredients of a coset code $\mathcal{C}(\Lambda/\Lambda'; E)$ are a lattice Λ , sublattice Λ' of Λ , and an encoder E .

An N -dimensional lattice Λ is an infinite set of N -tuples (lattice points), such that the sum or difference of any two lattice points is another lattice point. That is, algebraically, Λ is a group under ordinary N -tuple addition. Geometrically, a lattice is a regular array of points that cover N -space (assuming that the lattice points span N -space).

A sublattice Λ' of Λ is a subset of the points of Λ that is itself a lattice. Since Λ' is a subgroup of Λ , it induces a partition of Λ into $|\Lambda/\Lambda'|$ cosets (translates) of the sublattice Λ' where the integer $|\Lambda/\Lambda'|$ is called the order of the lattice partition Λ/Λ' (or the index of Λ' in Λ). More generally, any translate $\Lambda + a$ of Λ is the union of $|\Lambda/\Lambda'|$ cosets of Λ' .

In most practical coset codes, Λ and Λ' are taken to be binary lattices. A binary lattice Λ is a lattice of integer N -tuples (i.e., a sublattice of the integer lattice \mathbb{Z}^N) that has $2^n \mathbb{Z}^N$ (the lattice of all N -tuples of integer multiples of 2^n) as a sublattice for some integer n , so that $\mathbb{Z}^N/\Lambda/2^n \mathbb{Z}^N$ is a lattice partition chain. If Λ' is a binary lattice that is a sublattice of a binary lattice Λ , then $\mathbb{Z}^N/\Lambda/\Lambda'/2^n \mathbb{Z}^N$ is a lattice partition chain for some integer n . From this it follows that the order $|\Lambda/\Lambda'|$ of the partition Λ/Λ' is a power of two, say 2^{k+r} .

The encoder E may then be a rate- $k/(k+r)$ binary encoder, which takes in k bits per N dimensions and generates $k+r$ coded bits per N dimensions. The redundancy of the encoder E is r bits per N dimensions, and its normalized redundancy is $\rho(E) = 2r/N$ bits per two dimensions.

Fig. 1 then illustrates the general structure of a coset code \mathcal{C} based on a partition Λ/Λ' of binary lattices, when the code is used to send n information bits per N dimensions. Of the n bits, k are encoded in the rate- $k/(k+r)$ binary encoder E , which generates $k+r$ coded bits that select one of the $|\Lambda/\Lambda'| = 2^{k+r}$ cosets of Λ' whose union is some given translate $\Lambda + a$ of Λ . The remaining $n-k$ "uncoded bits" select one of 2^{n-k} signal points from the selected coset. The encoder E is normally arranged so that the 2^{k+r} cosets of Λ' in $\Lambda + a$ are equiprobable.

Such a code therefore requires a constellation C consisting of $|C| = 2^b = 2^{n+r}$ signal points from a coset $\Lambda + a$ of the lattice Λ , divided evenly into 2^{k+r} subsets, each subset consisting of 2^{n-k} points from one of the 2^{k+r} cosets of Λ' whose union is $\Lambda + a$. For the purposes of constellation design, the effective bit rate is the coded bit rate of $b = n+r$ bits per N dimensions, rather than the information bit rate of n bits per N dimensions. The size $|C|$ is therefore a factor of 2^r larger than would be necessary to represent n information bits per N dimensions with a lattice code based on Λ . Per two dimensions, the constellation expansion ratio due to the encoder E is therefore $2^{2r/N} = 2^{\rho(E)}$.

As an example, consider the four-state two-dimensional code of Ungerboeck [6], illustrated in Figs. 2 and 3 for the case $n = 4$. This code is based on the 4-way lattice partition $Z^2/2Z^2$ where Z^2 is the two-dimensional lattice consisting of all pairs of integers, and $2Z^2$ is the two-dimensional lattice consisting of all pairs of even integers. The encoder E is a rate-1/2 binary convolutional encoder whose two output bits select one of four cosets of $2Z^2$. The constellation expansion due to E is therefore a factor of 2, in two dimensions.

To send $n = 4$ bits per two dimensions with this code, we thus require a 32-point signal constellation (rather than 16 points), whose points lie in a coset of Z^2 and divide evenly into four subsets lying in four distinct cosets of $2Z^2$. Two such constellations are shown in Fig. 3. Fig. 3(a) is a "cross constellation" whose points lie in the coset $Z^2 + (1/2, 1/2)$ of Z^2 (the set of all pairs of half-integers), which is the union of the four cosets $2Z^2 + (1/2, 1/2)$, $2Z^2 + (-1/2, 1/2)$, $2Z^2 + (-1/2, -1/2)$, and $2Z^2 + (1/2, -1/2)$ of $2Z^2$, labeled A, B, C, D. Fig. 3(b) is a "square" constellation whose points lie in the coset $Z^2 + (1/2, 0)$ of Z^2 , which is the union of the four cosets $2Z^2 + (-1/2, 1)$, $2Z^2 + (1/2, 1)$, $2Z^2 + (1/2, 0)$, and $2Z^2 + (-1/2, 0)$ of $2Z^2$, labeled A, B, C, D.

In general, the Ungerboeck two-dimensional lattice-type codes are based on the two-dimensional chain $Z^2/RZ^2/R^2Z^2/R^3Z^2/\dots$ of two-way lattice partitions $R^jZ^2/R^{j+1}Z^2$ where R is the two-dimensional "rotation operator" defined by the 2×2 matrix $\begin{bmatrix} 1 & 1 \\ 1 & -1 \end{bmatrix}$. Geometrically (apart from an immaterial reflection), R is a rotation by 45° with a scaling by a factor of $2^{1/2}$. Note that $R^2Z^2 = 2Z^2$; thus the code above can be considered to be based on the chain $Z^2/RZ^2/R^2Z^2$.

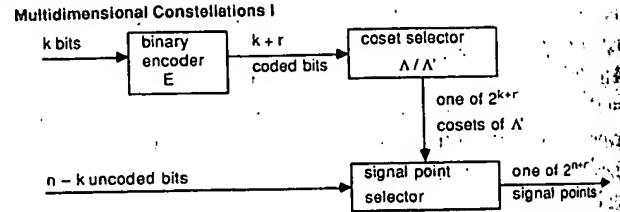


Fig. 1. General structure of a coset code \mathcal{C} based on a lattice partition Λ/Λ' , when used to send n information bits per N dimensions.

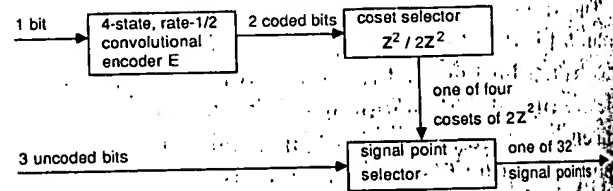


Fig. 2. Four-state two-dimensional Ungerboeck code ($n = 4$).

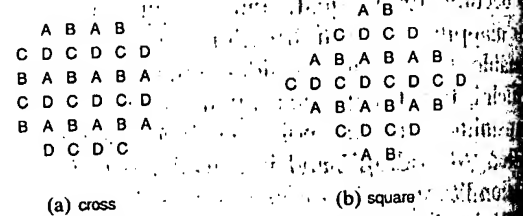


Fig. 3. Two 32-point signal constellations based on the 4-way partition $Z^2/2Z^2$: (a) cross; (b) square.

It is shown in [4] that, without loss of generality, a coset code $\mathcal{C}(\Lambda/\Lambda'; E)$ that is based on a partition Λ/Λ' of n -dimensional binary lattices may always be expressed as a code $\mathcal{C}(Z^N/R^\mu Z^N; E')$, i.e., as a code in which Λ is the cubic lattice Z^N , and Λ' is $R^\mu Z^N = (R^\mu Z^2)^{N/2}$, where R is called the *depth* of the partition Λ/Λ' , is the least integer such that $\Lambda/\Lambda'/R^\mu Z^N$ is a lattice partition chain. This representation involves an "augmented" encoder E' whose normalized redundancy $\rho(E')$ is equal to the normalized redundancy $\rho(\mathcal{C})$ of the code \mathcal{C} , as defined in [4]. The order of the partition $Z^N/R^\mu Z^N$ is $|Z^N/R^\mu Z^N| = 2^{\mu N/2}$, so that E' must put out $\mu N/2$ coded bits per two dimensions, or μ coded bits per two dimensions. It can be arranged to select a coset of $R^\mu Z^N$ in Z^N by selecting $N/2$ cosets of $R^\mu Z^2$ in a translate of Z^2 of two dimensions at a time. (In this representation, E' is arranged to select only those cosets of $R^\mu Z^N$ in Z^N that are actually in $\Lambda + a$, so the $2^{\mu N/2}$ cosets of $R^\mu Z^N$ are equiprobable.)

From this representation, we may draw the following consequences for multidimensional constellation design. First, the constituent 2D constellation C_2 must be drawn from some translate of Z^2 . Second, the points in C_2 divide evenly into 2^μ subsets, each corresponding to one of the 2^μ cosets of $R^\mu Z^2$ whose union is the given translate of Z^2 . For most good known codes, the depth μ lies in the range $2 \leq \mu \leq 4$, so that the partitioning of the constituent 2D constellation is 4-way, 8-way, or 16-way.

or example, the 16-state four-dimensional (4D) code [2] is based on the 8-way lattice partition Z^4/RD_4 where RD_4 is the four-dimensional lattice consisting of all 4-tuples that are either all even or all odd, and a $2/3$ encoder E whose three output bits select one of 8 cosets of RD_4 whose union is a translate of Z^4 , e.g., translate $Z^4 + (1/2, 1/2, 1/2, 1/2)$. To send n bits in 4 dimensions, the $n-2$ that are not inputs to the encoder select one of 2^{n-2} points in the selected coset of RD_4 . The four-dimensional constellation C therefore consists of 2^{n-1} points from a coset of Z^4 . The normalized redundancy of the encoder E is $\rho(E) = 1/2$ bit per two dimensions, and the corresponding constellation expansion ratio is $2^{1/2}$.

An alternative representation of this code is based on a 16-way lattice partition $Z^4/2Z^4$ and a rate-3/4 augmented encoder E' . The normalized redundancy remains $\rho(E') = 1/2$. Here E' selects two successive cosets of from a constituent 2D constellation that is partitioned into four equal subsets, each corresponding to a coset of $2Z^2$. Since the normalized redundancy of this code is only 1/2, the constellation expansion ratio is lowerbounded by $2^{1/2}$. To send 14 bits per four dimensions, for example, we need a constellation of only 2^{15} points from a coset of $2Z^4$, rather than the 2^{14} points required for an uncoded system. The minimum possible size of the constituent 2D constellation is thus only $2^{7.5} \approx 181$ points, compared to $= 128$ with no coding. Indeed, as was shown in [2], and as will be recapitulated below, there is a "generalized cross constellation" C that can be used with this code whose constituent 2D constellation has only $|C_2| = 192$ points, so that $CER(C) = |C_2|/2^{\beta} = 192/2^{7.5} = 1.06$.

Compatibility with QAM Modems II: Phase Symmetry

In QAM modems, a carrier phase offset of θ in the receiver rotates the received constellation by a phase angle θ . The receiver may, and generally does, track the carrier phase directly from the data signal, rather than from some carrier tone. This makes two additional characteristics desirable. First, there should be no point in the constituent 2D constellation at the origin, because such a point gives no information about carrier phase. (This consideration takes force for large constellations, where the probability of long runs of signal points at the origin becomes negligible.) Second, the constituent 2D constellation should be chosen to be invariant to as many phase rotations as possible, because the phase tracker may then quickly converge to steady state, and a differential coding technique may be applied to guarantee transparency to phase ambiguities, as shown, for example, in [7] and [2]. (In addition, such phase symmetry assures that the mean signal is zero and therefore that there will be no carrier component in the transmitted signal.)

For example, if the constituent 2D constellation is to be drawn from a coset of Z^2 , the only coset that has no point at the origin and has 4-way (quadrilateral) symmetry

is the half-integer grid $Z^2 + (1/2, 1/2)$, illustrated in Fig. 3(a). The grid $Z^2 + (1/2, 0)$ that is used in Fig. 3(b) has only 2-way (bilateral) symmetry.

Note that if the half-integer grid $Z^2 + (1/2, 1/2)$ is partitioned into four cosets of $2Z^2$ as in Fig. 3(a)—i.e., $A = 2Z^2 + (1/2, 1/2)$, $B = 2Z^2 + (-1/2, 1/2)$, $C = 2Z^2 + (-1/2, -1/2)$, and $D = 2Z^2 + (1/2, -1/2)$ —then a 90° rotation cycles A into B , B into C , C into D , and D into A . Therefore if the constituent 2D constellation is based on the half-integer grid and has 4-way symmetry, then it automatically divides equally into these four cosets of $2Z^2$; conversely, if C_2 is constructed from all of the 90° rotations of any set of points from any of these four cosets, it will automatically have 4-way symmetry.

In summary, for use in QAM modems with a code \mathcal{C} based on a partition Λ/Λ' of binary lattices, the constituent 2D constellation must be a set of points from a coset $Z^2 + a$ of Z^2 , preferably the half-integer grid $Z^2 + (1/2, 1/2)$, divided evenly as in Ungerboeck [6] into 2^μ subsets, where μ is the depth of the partition Λ/Λ' , and where the subsets consist of points from the 2^μ cosets of $R^\mu Z^2$ whose union is $Z^2 + a$. To send n information bits per N dimensions, the size $|C_2|$ of the constituent 2D constellation is lowerbounded by $2^{\nu + \rho(\mathcal{C})}$ where $\nu = 2n/N$, and $\rho(\mathcal{C})$ is the normalized redundancy of the code \mathcal{C} .

We may note that hexagonal constellations, with points from the hexagonal lattice A_2 , have also received some attention and have some modest advantages, although they have rarely been implemented in practice (but see [8]).

F. Scalability

Scalability is a property that is nice to have, although it is not necessary. Roughly speaking, a constellation C is said to be *scalable* if there is an infinite series of constellations C, C', C'', \dots of increasing normalized bit rate β such that the properties of all constellations in the series are essentially the same as those of C , when adjusted for β . In this section, we shall merely introduce this idea with a simple illustration.

Consider any two-dimensional constellation C based on the half-integer grid $Z^2 + (1/2, 1/2)$. We may consider each point in the grid to be surrounded by a square of side 1 centered on that point. This defines a region (template) \mathbb{R} that consists of $|C|$ such squares, and that has volume $V(\mathbb{R}) = |C|$. For example, the regions corresponding to a 4×4 square constellation and the 32-point cross constellation of Fig. 3(a) are shown in Fig. 4(a) and (b).

Suppose now that we subdivide each square into 4 squares. This defines a new constellation C' based on a scaled half-integer grid that, compared to the original constellation, has $|C'| = 4|C|$, $d_{\min}^2(C') = d_{\min}^2(C)/4$, and $P(C') \approx P(C)$. Thus, the constellation figure of merit is reduced by a factor of 4, as we expect when $|C| = 2^\beta$ increases by a factor of 4. If the original constellation has quadrilateral symmetry, then so does the new constellation.

By iterating this process, we can define a series of con-

Multidimensional Constellations

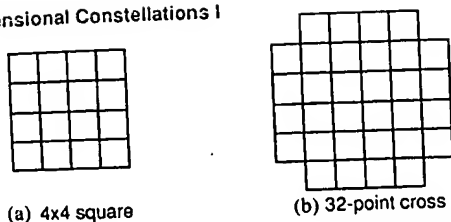


Fig. 4. Templates for 4×4 square and 32-point cross constellations: (a) 4×4 square, (b) 32-point cross.

stellations whose normalized bit rate increases by 2 bits per two dimensions at each step. The families of square and cross constellations can be generated in this way. (In the square case, we can start with the 2×2 square constellation.)

It is clear that as $|C|$ goes to infinity, the distribution of constellation points approaches a uniform distribution over \mathbb{R} . In this sense, the continuous approximation is asymptotically exact.

If we want to increase the normalized bit rate by 1 bit per two dimensions, we can put two points along a diagonal of each square, and thereby double $|C|$ while halving $d_{\min}^2(C)$ and thus approximately halving $\text{CFM}(C)$. For example, the 32-point "square" constellation of Fig. 3(b) can be obtained from the 4×4 square template in this way. The points so obtained are in general on a scaled translate of RZ^2 rather than of Z^2 , and have only bilateral symmetry, even if the template has quadrilateral symmetry. This is why different families (e.g., square and cross) are ordinarily used for even and odd normalized bit rates β .

G. Peak-to-Average Power Ratio

A measure of the sensitivity of a signal constellation to nonlinearities and other signal-dependent perturbations is the *peak-to-average power ratio* (PAR), defined as the ratio of the peak energy of any signal point to the average energy or power. With N dimensional constellations, there is some question as to whether to measure the PAR in N dimensions, or in some lower number of dimensions. With QAM modems, the PAR is usually defined in two dimensions, as the ratio of the peak energy of any signal point in the constituent 2D constellation C_2 to the average power (per two dimensions) $P(C)$. However, depending on the application, the value of the PAR in some other number of dimensions may be as or more significant. When necessary, we shall write PAR_2 or PAR_N to distinguish the PAR of C_2 in two dimensions from that of C in N dimensions.

N dimensional cubic constellations may be regarded as the $(N/2)$ fold Cartesian product of two-dimensional square constellations (for N even). The peak energy of an $M \times M$ square constellation based on the half-integer grid $Z^2 + (1/2, 1/2)$ is $(M-1)^2/2 \approx 2^\beta/2$ where β is the normalized bit rate per two dimensions. Thus the PAR in two dimensions goes asymptotically to 3. In fact, the PAR of cubic constellations is asymptotically equal to 3 in any number of dimensions.

H. Opportunistic Secondary Channels

The idea of an opportunistic secondary channel is as follows. Suppose that the primary data source generates a b bit data word for every N dimensional signal point to be transmitted. Choose an N dimensional signal constellation with size $|C|$ greater than 2^b , and let certain of the data words be associated with more than one point in the constellation. Whenever one of these words happens to be generated, there is an opportunity to transmit additional side information, by choosing one of the two or more signal points associated with the data word. For example, if $|C| = 2^b + w$, then we can associate a pair of signal points with w of the data words; with probability $w/2^b$, an additional "secondary channel bit" can then be transmitted along with the b bit primary data word by a single N dimensional signal point, by selection of one or the other of the pair of signal points associated with that data word.

Of course, increasing the size $|C|$ of the constellation will normally somewhat increase its average power and degrade its SNR efficiency. As we shall see in some of the examples below, the average data rate of the opportunistic secondary channel may be substantially higher than the increase in normalized bit rate that could ordinarily be obtained by the increase in average power. In other examples, the use of an opportunistic secondary channel allows an increase in normalized bit rate of a small fractional number of bits/Hz, such as might be needed for a low-speed control channel, with little or no increase in average power. These benefits are offset by the fact that the transmission of secondary channel data is probabilistic, so that secondary channel data must be queued in buffers for transmission. Also, there arises the possibility of insertions and deletions of secondary channel data above and beyond ordinary errors. However, for certain types of data, such as internal signaling and control, these are perfectly acceptable tradeoffs, and in fact, the ability of secondary channel data to "piggyback" on the primary data channel with little or no degradation in SNR efficiency is a highly desirable feature.

The expanded constellations used with opportunistic secondary channels must retain the desirable characteristics listed above. To minimize degradation of SNR efficiency, the points to be paired should come from the points of the constellation, and the additional points should have the smallest possible energy. The mapping of secondary channel bits to signal points should be easy to implement. With coded modulation, the two or more signal points associated with a given data word must belong to the same subset (coset of Λ). If quadrilateral symmetry is required, then the expanded constellation should be quadrilaterally symmetric, and generally the rotation of the set of signal points associated with one data word should be a set of points associated with another data word.

The opportunistic secondary channel idea seems to have been first embodied in the Codex/ESE SP14.4 mod-

[8], and subsequently to have been reinvented more recently [9], [10], [11]; see also [12].

III. SHAPING AND CODING

This section begins with a demonstration that for a large constellation C with normalized bit ratio β that consists of points from a translate $\Lambda + a$ of a lattice Λ that fall in a region R , the constellation figure of merit is given approximately by the product

$$\text{CFM}(C) \approx \text{CFM}_\oplus(\beta) \cdot \gamma_c(\Lambda) \cdot \gamma_s(R)$$

where $\text{CFM}_\oplus(\beta) = 6/2^\beta$ is the baseline figure of merit for a normalized bit ratio of $\beta = (2/N) \log_2 |C|$; $\gamma_c(\Lambda)$ is the coding gain of the lattice Λ ; and $\gamma_s(R)$ is the shape gain of the region R . Thus, the gain from shaping by the region R is almost completely decoupled from the coding gain due to Λ —or, more generally, the coding gain $\gamma_c(C)$ to use of a general coset code C . The shape gain $\gamma_s(R)$ is equal to $1/[12G(R)]$ where $G(R)$ is the so-called normalized second moment of the region R . The properties of the shape gain are analogous to those of the coding gain.

The constellation expansion ratio $\text{CER}(C)$ for such constellations also is approximately the product of two comparable terms, the coding constellation expansion ratio $\text{CER}_c(\Lambda)$ of the lattice Λ (or, more generally, of a code C), and the shaping expansion ratio $\text{CER}_s(R)$ of the region R . We derive an expression for the peak-to-average ratio of the constituent 2D constellation of C that is a function of R , and consists of the product of three terms: the peak-to-average ratio of the constituent 2D region R_2 of R , the ratio of the shape gain of R to that of R_2 , and the shaping constellation expansion ratio $\text{CER}_s(R)$, with the last usually being dominant.

A. Shape Gain and Coding Gain

A general method for constructing an N dimensional constellation C is to take the points of some N dimensional lattice Λ (or of a translate $\Lambda + a$ of Λ) that lie within some region R of N space, with the region chosen to be large enough to enclose the desired number $|C|$ of signal points. Such a constellation is also called a *lattice code*. We shall sometimes denote such a constellation by $C(\Lambda, R)$.

The principal geometric parameters of a lattice Λ are $d_{\min}^2(\Lambda)$, the minimum squared distance between its points, and its *fundamental volume* $V(\Lambda)$, which is the volume of N space corresponding to each lattice point. (In fact, if $R(\Lambda)$ is any *fundamental region* of Λ —i.e., a region containing one and only one point from each coset $\Lambda + a$ of Λ in real N space R^N —then the volume of $R(\Lambda)$ is $V(\Lambda)$, and N space is tessellated by the translates $R(\Lambda) + a$ of $R(\Lambda)$ as a ranges through all points in Λ .)

We can estimate the parameters $d_{\min}^2(C)$, $|C|$, and $\text{CFM}(C)$ of a constellation $C(\Lambda, R)$ as follows. First, the minimum squared distance of $C(\Lambda, R)$ is $d_{\min}^2(C) =$

$d_{\min}^2(\Lambda)$. If R is large relative to $V(\Lambda)$, then we have as a first approximation principle the following proposition.

Proposition 1: The size $|C|$ of any constellation $C(\Lambda, R)$ consisting of the points in any translate $\Lambda + a$ of any lattice Λ that lie within any region R of volume $V(R)$ is approximately $|C| \approx V(R)/V(\Lambda)$, if $V(R)$ is much larger than the fundamental volume $V(\Lambda)$ of Λ .

The normalized bit rate $\beta = (2/N) \log_2 |C|$ of $C(\Lambda, R)$ is therefore given approximately by $\beta \approx \log_2 [V(R)/V(\Lambda)]^{2/N}$. The baseline constellation figure of merit for this β is $\text{CFM}_\oplus(\beta) = 6/2^\beta \approx 6[V(\Lambda)/V(R)]^{2/N}$.

To estimate the average power $P(C)$, we may use the following old, convenient, and quite accurate approximation principle (called the “integral approximation” in [1], but perhaps better called the *continuous approximation*):

Proposition 2 (Continuous Approximation): The average power $P(C)$ of any constellation $C(\Lambda, R)$ consisting of the points in any translate $\Lambda + a$ of any lattice Λ that lie within any region R is approximately equal to the average power $P(R)$ of a continuous distribution that is uniform with R and zero elsewhere

$$P(C) \approx P(R) \triangleq \left[\int_R \|r\|^2 dV \right] / [NV(R)/2]$$

where $\|r\|^2$ is the energy of a point r in R and $V(R) = \int_R dV$ is the volume of R , so that $1/V(R)$ is the density of a uniform continuous probability distribution over R , and the division by $N/2$ normalizes to two dimensions.

For example, in one dimension, if R is a line segment of length R centered at the origin, the average energy is $R^2/12$ in one dimension, so the average power is $P(R) = R^2/6$ per two dimensions. In N dimensions, the average energy of a region R which is an N cube of side R is N times the average energy of one coordinate, so the average power per two dimensions remains $P(R) = R^2/6$. The volume of such a region is $V(R) = R^N$, so $P(R) = [V(R)]^{2/N}/6$.

The constellation figure of merit of any $C(\Lambda, R)$ is therefore approximated by $\text{CFM}(C) \approx d_{\min}^2(\Lambda)/P(R)$. The gain over the baseline figure of merit is

$$\begin{aligned} \text{CFM}(C)/\text{CFM}_\oplus(\beta) \\ = [d_{\min}^2(\Lambda)/V(\Lambda)^{2/N}] \cdot [V(R)^{2/N}/6P(R)]. \end{aligned}$$

Here we have grouped the gain into two terms, which depend only on Λ and on R , respectively. The first term is

$$\gamma_c(\Lambda) \triangleq d_{\min}^2(\Lambda)/V(\Lambda)^{2/N},$$

which we call the *coding gain* of the lattice Λ (i.e., the ‘fundamental coding gain’ [Forney, 1988] of the lattice Λ as a lattice code). Note that $\gamma_c(Z^N) = 1$. The second term is

$$\gamma_s(R) \triangleq V(R)^{2/N}/[6P(R)],$$

which we call the *shape gain* of the region R . Note that the shape gain of an N cube is 1.

The baseline figure of merit $\text{CFM}_{\oplus}(\beta)$ is approximately the figure of merit of a cubic constellation with a normalized bit rate of β , i.e., of a lattice code $C(\Lambda, \mathbb{R})$ in which Λ is the integer lattice \mathbb{Z}^N and \mathbb{R} is an N cube. We see that by drawing points from a lattice Λ that is denser than \mathbb{Z}^N , we can improve SNR efficiency by a factor of $\gamma_c(\Lambda)$, the coding gain of Λ . By choosing the constellation from a region \mathbb{R} that is more spherical than an N cube, we can improve SNR efficiency by a factor of $\gamma_s(\mathbb{R})$, the shape gain of \mathbb{R} . To the accuracy of our approximations, these two improvement factors are quite independent.

Similarly, if we use a coset code $\mathbb{C}(\Lambda/\Lambda'; E)$ with a constellation $C(\Lambda, \mathbb{R})$ consisting of the points from $\Lambda + a$ that lie within \mathbb{R} , then we can show that the gain over $\text{CFM}_{\oplus}(\beta)$ is given approximately by the product $\gamma_c(\mathbb{C}) \cdot \gamma_s(\mathbb{R})$, if the coding gain of \mathbb{C} is defined by

$$\gamma_c(\mathbb{C}) \triangleq d_{\min}^2(\mathbb{C})/V(\mathbb{C})^{2/N}$$

where $d_{\min}^2(\mathbb{C})$ is the minimum squared distance between sequences in \mathbb{C} , and $V(\mathbb{C})$ is the fundamental volume of \mathbb{C} . (In [4], it is shown that $V(\mathbb{C}) = 2^r V(\Lambda)$, where r is the redundancy of E , or $V(\mathbb{C})^{2/N} = 2^{\rho(\mathbb{C})}$ where $\rho(\mathbb{C})$ is the normalized redundancy of \mathbb{C} .) Thus, the separability of coding gain and shape gain extends to general coset codes, not just lattice codes.

B. Shape Gain and Normalized Second Moment

The "dimensionless second moment" [13] or *normalized second moment* [14] of a region \mathbb{R} is defined as

$$G(\mathbb{R}) \triangleq P(\mathbb{R})/[2V(\mathbb{R})^{2/N}] \\ = \left[\int_{\mathbb{R}} \|r\|^2 dV \right] / [NV(\mathbb{R})^{1+(2/N)}].$$

Thus the shape gain is simply $\gamma_s(\mathbb{R}) = 1/[12G(\mathbb{R})] = G_{\oplus}/G(\mathbb{R})$ where the baseline second moment $G_{\oplus} = 1/12$ is the normalized second moment of any N cube. Thus, the shape gain is a measure of the improvement in normalized second moment relative to an N cube, and numerically is simply a constant multiplied by the inverse of $G(\mathbb{R})$.

The shape gain $\gamma_s(\mathbb{R})$ [or equally the normalized second moment $G(\mathbb{R})$] has the following properties (compare the properties of the coding gain $\gamma_c(\Lambda)$ or of $\gamma_c(\mathbb{C})$ [4]).

- It is dimensionless; both $P(\mathbb{R})$ and $V(\mathbb{R})^{2/N}$ have the dimensions of a two-dimensional volume (area).
- It is invariant to scaling: $\gamma_s(\alpha\mathbb{R}) = \gamma_s(\mathbb{R})$ where α is any scale factor.
- It is invariant to orthogonal transformations of \mathbb{R} .
- It is invariant to the Cartesian product operation, $\gamma_s(\mathbb{R}^M) = \gamma_s(\mathbb{R})$ because $P(\mathbb{R}^M) = P(\mathbb{R})$ and $V(\mathbb{R}^M) = V(\mathbb{R})^M$.
- By definition, the shape gain $\gamma_s(\mathbb{R})$ is a power measure; it measures the reduction in the average power (per two dimensions) required by a constellation bounded by \mathbb{R} compared to what would be required by a constellation

bounded by an N cube of the same value. We shall often give its value in dB:

C. Shaping and Coding Constellation Expansion Ratio

If an N dimensional constellation $C(\Lambda, \mathbb{R})$ consists of the points of some N dimensional lattice Λ , or of a translate $\Lambda + a$ of Λ , that lie within some region \mathbb{R} of N space, then the constituent 2D constellation C_2 of $C(\Lambda, \mathbb{R})$ consists of the points of the two-dimensional projection Λ_2 of Λ , or a translate $\Lambda_2 + a$ of Λ_2 , that lie within the two-dimensional projection \mathbb{R}_2 of \mathbb{R} . If Λ_2 and \mathbb{R}_2 do not depend on which two dimensions we pick, then we call Λ and \mathbb{R} 2D-symmetric, and we may speak of Λ_2 as the constituent 2D lattice of Λ , and of \mathbb{R}_2 as the constituent 2D region of \mathbb{R} .

It is easy to verify that Λ_2 is in fact a two-dimensional lattice, since the sum and difference of any two points Λ_2 must be in Λ_2 . Also, Λ must be a sublattice of $(\Lambda_2)^{N/2}$. If Λ is a sublattice of \mathbb{Z}^N , then Λ_2 is a sublattice of \mathbb{Z}^2 . We usually use lattices Λ for which $\Lambda_2 = \mathbb{Z}^2$. The *normalized redundancy* of a binary lattice is defined as $\rho(\Lambda) \triangleq (2/N) \log_2 |(\Lambda_2)^{N/2}/\Lambda| = \log_2 [V(\Lambda)^{2/N}/V(\Lambda_2)]$ or, if $\Lambda_2 = \mathbb{Z}^2$, simply $\rho(\Lambda) = \log_2 V(\Lambda)^{2/N}$.

By Proposition 1, $|C| = V(\mathbb{R})/V(\Lambda)$. The size of constituent 2D constellation, by the same approximation is $|C_2| = V(\mathbb{R}_2)/V(\Lambda_2)$. Thus, the CER(C) is approximately

$$\text{CER}(C) = |C_2|/|C|^{2/N} \approx [V(\Lambda)^{2/N}/V(\Lambda_2)] \cdot [V(\mathbb{R}_2)/V(\mathbb{R})^{2/N}]$$

This is the product of two independent factors: the coding constellation expansion ratio of Λ , defined as

$$\text{CER}_c(\Lambda) \triangleq V(\Lambda)^{2/N}/V(\Lambda_2)$$

and the shaping constellation expansion ratio of \mathbb{R} , defined as

$$\text{CER}_s(\mathbb{R}) \triangleq V(\mathbb{R}_2)/V(\mathbb{R})^{2/N}$$

Note that $\text{CER}_c(\mathbb{Z}^N) = 1$, and $\text{CER}_s(\mathbb{R}) = 1$ if \mathbb{R} is an N cube. Again, as with the constellation figure of merit, the coding constellation expansion ratio $\text{CER}_c(\Lambda)$ due to the lattice Λ and the shaping constellation expansion ratio $\text{CER}_s(\mathbb{R})$ due to the region \mathbb{R} are completely decoupled to the accuracy of the approximation of Proposition 1.

The baseline size $|C|^{2/N} = 2^{\rho}$ is approximately the size of the constituent 2D constellation if we send per two dimensions using a constellation drawn from a translate of \mathbb{Z}^N and shaped like an N cube, in which $\Lambda_2 = \mathbb{Z}^2$. If we use a lattice Λ that is a strict sublattice $(\Lambda_2)^{N/2}$, we suffer a constellation expansion of a factor of $\text{CER}_c(\Lambda)$. By choosing the constellation from a region \mathbb{R} that is a strict subregion of $(\mathbb{R}_2)^{N/2}$, we suffer a shaping constellation expansion of a factor of $\text{CER}_s(\mathbb{R})$. The costs associated with achieving the lattice gain and shape gain $\gamma_s(\mathbb{R})$.

When Λ is a 2D symmetric binary lattice, $\text{CER}_c(\Lambda) = 2^{\rho(\Lambda)}$ where $\rho(\Lambda)$ is the normalized

of Λ . Similarly, for a coset code \mathbb{C} based on a pair of binary lattices, the coding constellation expansion is $\text{CER}_c(\mathbb{C}) = 2^{\rho(\mathbb{C})}$ where $\rho(\mathbb{C})$ is the normalized redundancy of \mathbb{C} [4]. It may be shown that if the constellation used with such a code is bounded by the region \mathbb{R} , then it remains true that

$$|\mathbb{C}_2| = 2^{\rho} \cdot \text{CER}_c(\mathbb{C}) \cdot \text{CER}_s(\mathbb{R})$$

where $\rho = 2n/N$ is the normalized information bit rate of the code.

Peak-to-Average Power Ratio

The peak-to-average power ratio of a constellation may be estimated by the continuous approximation, although with less accuracy when the points in Λ are at some distance from the maximum-energy points on the boundary of \mathbb{R} . In N dimensions, the peak energy $r_{\max}^2(\mathbb{C})$ is upperbounded and approximated by the peak energy $r_{\max}^2(\mathbb{R})$ of any point in the region \mathbb{R} . Similarly, in two dimensions, $r_{\max}^2(\mathbb{C}_2)$ is upperbounded and approximated by $r_{\max}^2(\mathbb{R}_2)$. The average power per two dimensions in the case is $P(\mathbb{C})$, which is approximated by $P(\mathbb{R})$. Therefore $\text{PAR}_2(\mathbb{C})$ is approximated by

$$\text{PAR}_2(\mathbb{C}) = r_{\max}^2(\mathbb{R}_2)/P(\mathbb{R}).$$

When taken by itself, the region \mathbb{R}_2 has a peak-to-average power ratio of

$$\text{PAR}(\mathbb{R}_2) = r_{\max}^2(\mathbb{R}_2)/P(\mathbb{R}_2).$$

where $P(\mathbb{R}_2)$ is the average power under a uniform distribution over \mathbb{R}_2 . But the shape gains of \mathbb{R} and \mathbb{R}_2 are given by

$$\gamma_s(\mathbb{R}) = V(\mathbb{R})^{2/N}/[6P(\mathbb{R})], \text{ and}$$

$$\gamma_s(\mathbb{R}_2) = V(\mathbb{R}_2)/[6P(\mathbb{R}_2)],$$

respectively. Therefore we have the useful relationship

$$\begin{aligned} \text{PAR}_2(\mathbb{C}) &= \text{PAR}(\mathbb{R}_2) \cdot [\gamma_s(\mathbb{R})/\gamma_s(\mathbb{R}_2)] \cdot [V(\mathbb{R}_2)/V(\mathbb{R})^{2/N}] \\ &= \text{PAR}(\mathbb{R}_2) \cdot [\gamma_s(\mathbb{R})/\gamma_s(\mathbb{R}_2)] \cdot \text{CER}_s(\mathbb{R}). \quad (*) \end{aligned}$$

In words, the peak-to-average power ratio in two dimensions is the product of three factors: the peak-to-average power ratio of the constituent 2D region \mathbb{R}_2 , the improvement in shape gain of the N dimensional region \mathbb{R} over that of \mathbb{R}_2 , and the constellation expansion ratio $\text{CER}_s(\mathbb{R})$ of the region \mathbb{R} . Since an improvement in shape gain is one of the purposes of going to N dimensions, this formula encourages the use of regions \mathbb{R} which have small constellation expansion ratios and which have constituent regions which themselves have a good PAR.

IV. BOUNDS ON SHAPE GAIN

In this section we first compute the shape gain of the N sphere, which is the largest possible shape gain of an N dimensional region \mathbb{R} . We note, however, that the shaping constellation expansion ratio and thus PAR become

large as N increases. The best tradeoff between shape gain $\gamma_s(\mathbb{R})$ and $\text{CER}_s(\mathbb{R})$ or $\text{PAR}(\mathbb{R})$ is obtained when we bound the peak energy of the constituent 2D constellation within a circle, and we evaluate this optimum tradeoff.

A. Spherical Constellations

For a given volume $V(\mathbb{R})$, the N dimensional region \mathbb{R} that has the minimum average power $P(\mathbb{R})$ and thus maximum shape gain $\gamma_s(\mathbb{R})$ is obviously an N sphere. The volume V_\otimes and average power P_\otimes of an N sphere of radius R are, for N even

$$V_\otimes = \pi^n R^{2n}/[n!];$$

$$P_\otimes = R^2/(n+1)$$

where (in this section only) we define $n \triangleq N/2$. Thus, the shape gain of the N sphere is

$$\gamma_\otimes = (V_\otimes)^{1/n}/[6P_\otimes] = \pi(n+1)/[6(n!)^{1/n}],$$

while the shaping constellation expansion ratio and peak-to-average power ratio are

$$\text{CER}_\otimes = (\pi R^2)/(V_\otimes)^{1/n} = (n!)^{1/n};$$

$$\text{PAR}_\otimes = R^2/P_\otimes = n+1$$

$$= (6/\pi)\gamma_\otimes \cdot \text{CER}_\otimes,$$

again with $n = N/2$. Table I gives $\gamma_\otimes(N)$, $\text{CER}_\otimes(N)$, and $\text{PAR}_\otimes(N)$ for reference.

As is noted in [1], using the Stirling approximation $n! \approx (n/e)^n$, we can see that the shape gain $\gamma_\otimes(N)$ approaches $\pi e/6$ (1.53 dB) as N goes to infinity.

The N sphere has the optimum shape gain in N dimensions and thus the optimum SNR efficiency. However, implementation complexity may be high. Also, as we see from Table I, the size and peak-to-average power ratio of the constituent 2D constellation become large as N increases. The main object of N dimensional constellation design is to obtain a shape gain as close to that of the N sphere as possible, while maintaining reasonable implementation complexity, constituent 2D constellation size, and other desirable constellation characteristics.

The peak-to-average power ratio (PAR) for the N sphere illustrates what may be expected in general for N dimensional constellations with good shape gains. The peak energy in N dimensions is R^2 , so the peak-to-average ratio $\text{PAR}_N = R^2/nP_\otimes$ in $N = 2n$ dimensions is $(n+1)/n$ and approaches 1 as N becomes large (as the volume of the sphere becomes concentrated near its boundary). However, the projection of an N sphere of radius R onto two dimensions (the boundary of the constituent 2D constellation) is a circle of radius R , so the peak energy in two dimensions is also R^2 ; the peak-to-average ratio $\text{PAR}_\otimes = R^2/P_\otimes$ in two dimensions is thus $n+1 = (N+2)/2$, and approaches infinity as N becomes large. As shown in Table I, for $N = 2$, PAR_\otimes is only 2, better than that of the square, but for $N = 4$, PAR_\otimes is already 3, equal to that of the 4-cube, and for larger N , PAR_\otimes quickly exceeds the PAR of cubic constellations.

TABLE 1
SHAPE GAINS AND CONSTELLATION EXPANSION RATIOS OF N SPHERES

N	$\gamma_{\otimes}(N)$	(dB)	$CER_{\otimes}(N)$	$PAR_{\otimes}(N)$
2	$\pi/3 = 1.047$	0.20	1	2
4	$\pi/2^{3/2} = 1.111$	0.46	1.414	3
8	1.183	0.73	2.213	5
12	1.224	0.88	2.994	7
16	1.252	0.98	3.764	9
24	1.287	1.10	5.289	13
32	1.309	1.17	6.800	17

The relation $PAR_{\otimes}(N) = (6/\pi)\gamma_{\otimes}(N)CER_{\otimes}(N)$ is an instance of the general relation (*), since $PAR_{\otimes}(2) = 2$ and $\gamma_{\otimes}(2) = \pi/3$, and shows that the main contribution to the increase in $PAR_{\otimes}(N)$ as a function of N is the increase in $CER_{\otimes}(N)$.

For example, to send $\beta = 7.5$ bits per two dimensions using a spherical constellation of 2^{15} points from Z^4 , the constituent 2D constellation contains about $2^{1/2} \cdot 2^{15/2} = 256$ points and has a PAR of about 3. To send $\beta = 7.25$ bits per two dimensions using a spherical constellation of 2^{29} points from Z^8 , the constituent 2D constellation contains about $(24)^{1/4} \cdot 2^{29/4} \approx 337$ points and has a PAR of about 5. As shown in [1] and [2] and recapitulated below, there are easily implemented "generalized cross constellations" for these two cases with 192 and 160 points, respectively (compared to the baseline sizes of 181 and 152 points, respectively), with PARs close to 2, and with shape gains of the order of 0.3 dB.

Note Sloane [15] calls the set of points of an N dimensional lattice that lie within an N sphere a "code of bounded energy," employs the continuous approximation, and gives a bound on the approximation error due to Walfisz. Calderbank and Sloane [5] generally use spherical constellations with their codes, and include the N sphere shape gain in their figures for total coding gain, with asymptotic bounds.

B. Bounds on Shape Gain Versus CER_{\otimes} and PAR

We implicitly assume throughout this paper that the probability distribution on the 2^b points in an N dimensional constellation C is uniform. However, the induced probability distribution on the points in the constituent 2D constellation will be nonuniform in general (unless C is the Cartesian product of constituent 2D constellations). Indeed, with spherical constellations, this probability distribution becomes Gaussian as N becomes large, as we shall shortly see, so that the frequency of occurrence of the outermost points in the constituent 2D constellation becomes small. This suggests that the peak energy R^2 of the constituent 2D constellation may be bounded to some extent without greatly affecting the sphericity or shape gain of the N dimensional constellation.

In this section, we develop bounds on shape gain for such constellations, which show that substantial shape gains can be achieved even when the peak-to-average power ratio (PAR) and shaping constellation expansion ratio (CER_{\otimes}) are kept within reasonable limits.

Let $p(x)$ be the probability distribution on the points x in the constituent 2D constellation C_2 induced by a uniform distribution on the 2^b points in C ; we assume for simplicity that $p(x)$ is identical for all 2D constituent constellations. Let

$$H(C_2) \triangleq -\sum p(x) \log_2 p(x)$$

be the entropy (in bits per two dimensions) of this two-dimensional distribution. By a basic information-theoretic inequality, $(N/2)H(C_2) \geq H(C) = b$, the entropy of the uniform N dimensional distribution over the 2^b points in C , with equality if and only if the N dimensional distribution is the Cartesian product of $N/2$ two-dimensional distributions $p(x)$. Thus, the entropy of the distribution $p(x)$ is lowerbounded by the normalized bit rate

$$H(C_2) \geq 2b/N = \beta$$

Under the same assumptions, the average energy of the N dimensional constellation C is $N/2$ times the average energy

$$P(C_2) \triangleq \sum p(x) \|x\|^2$$

of the constituent 2D constellation, and the average power $P(C)$ per two dimensions is equal to $P(C_2)$.

For large constellations, we may again resort to the continuous approximation. The continuous probability distribution $p(x)$ that maximizes the differential entropy $H(X)$ for a given average power $P(X)$, or that minimizes $P(X)$ for a given $H(X)$, is a two-dimensional Gaussian distribution

$$p(x) = (2\pi\sigma^2)^{-1} \exp^{-\|x\|^2/2\sigma^2}$$

The average energy $P(X)$ per two dimensions is twice the one-dimensional variance σ^2 , and the differential entropy $H(X)$ per two dimensions is $\log_2 2\pi e\sigma^2$. If discrete points are taken from a coset of the integer lattice Z^2 , then each point is associated with a unit volume of two-space ($V(Z^2) = 1$), and the entropy $H(C_2)$ of a discrete probability distribution on these points that approximates $p(x)$ is also approximately $\log_2 2\pi e\sigma^2$. Hence, it takes an average power of $2\sigma^2$ to send a number of bits β per two dimensions that can be as large as $H(X) = \log_2 2\pi e\sigma^2$. The baseline average power for this bit rate is $P_{\otimes}(H(X)) = 2^{H(X)}/6 = 2\pi e\sigma^2/6$, therefore the shape gain with Gaussian $p(x)$ is $\pi e/6 = 1.423$ (1.53 dB). This amounts to a proof that the maximum possible shape gain for an N dimensional constellation C is 1.53 dB, and equality holds when and only when the induced distribution $p(x)$ is Gaussian, and a spherical constellation achieves this shape gain as $N \rightarrow \infty$; this argument shows that the induced two-dimensional distribution of a spherical constellation becomes Gaussian as $N \rightarrow \infty$.

Suppose now that we require that $p(x)$ be zero outside a circle of radius R . By standard variational argument using a Lagrange multiplier λ , the probability distribution $p(x)$ (discrete or continuous) that maximizes the entropy $H(X)$ for a given average power $P(X)$, or that minimizes

or a given $H(X)$, given this constraint, is a two-dimensional truncated Gaussian distribution

$$p(x) = \begin{cases} K(\lambda) \exp -\lambda \|x\|^2 / R^2, & \|x\|^2 \leq R^2; \\ 0, & \|x\|^2 > R^2 \end{cases}$$

λ is a parameter that governs the tradeoff between average power $P(\lambda)$ and the entropy $H(\lambda)$, and $K(\lambda)$ is chosen to make $\int p(x) dx = 1$. For $\lambda = 0$, $p(x)$ is uniform within the circle of radius R ; as $\lambda \rightarrow \infty$, $p(x)$ approaches a Gaussian distribution with variance

using the continuous approximation, we can define $K(\lambda)$, $P(\lambda)$, and $H(\lambda)$ in closed form as follows:

$$\begin{aligned} K(\lambda) &= \lambda / \pi R^2 J_1(\lambda); \\ P(\lambda) &= R^2 J_2(\lambda) / \lambda J_1(\lambda); \\ H(\lambda) &= -\log_2 [\lambda / \pi R^2 J_1(\lambda)] + [J_2(\lambda) / J_1(\lambda)] \log_2 e \end{aligned}$$

$$J_1(\lambda) = 1 - e^{-\lambda/2} \sum_{k=0}^{\infty} \frac{(\lambda/2)^k}{k!} \frac{1}{2k+1}$$

$$J_2(\lambda) = J_1(\lambda) - \lambda e^{-\lambda/2} \sum_{k=0}^{\infty} \frac{(\lambda/2)^k}{k!} \frac{1}{2k+2}$$

peak-to-average power ratio of the constituent 2D constellation and the shape gain are then given parametrically by

$$\begin{aligned} \text{PAR}(\lambda) &= R^2 / P(\lambda) = \lambda J_1(\lambda) / J_2(\lambda); \\ \gamma_s(\lambda) &= P_{\oplus} [H(\lambda)] / E(\lambda) \\ &= [\pi J_1(\lambda) / 6 J_2(\lambda)] \exp J_2(\lambda) / J_1(\lambda). \end{aligned}$$

Of course, the size of the constituent 2D constellation is the constellation expansion ratio relative to the base constellation of $2^{H(\lambda)}$ is

$$\text{CER}_s(\lambda) = [\lambda / J_1(\lambda)] \exp -J_2(\lambda) / J_1(\lambda).$$

Again, the relation between these three quantities,

$$\text{PAR}(\lambda) = (6/\pi) \gamma_s(\lambda) \text{CER}_s(\lambda),$$

in particular case of the general relation (*), which can be interpreted as follows: The PAR is greater than its minimum value of $2 = \text{PAR}_{\oplus}(2) = (6/\pi) \gamma_{\oplus}(2)$ by the product of the (desirable) factor $\gamma_s(\lambda) / \gamma_{\oplus}(2)$ with the (desirable) factor $\text{CER}_s(\lambda)$.

For $\lambda = 0$, $p(x)$ becomes uniform over the circle of radius R , and $K(0) = 1/\pi R^2$, $P(0) = R^2/2$, $H(0) = \pi R^2$, $\text{PAR}(0) = 2$, $\gamma_s(0) = \pi/3 = 1.047$ (0.20 dB), and $\text{CER}_s(0) = 1$, as we have previously calculated for two-dimensional spherical constellations. As λ increases, $\text{PAR}(\lambda)$, $\text{CER}_s(\lambda)$, and $\gamma_s(\lambda)$ increase. The tradeoff between $\text{CER}_s(\lambda)$ and $\gamma_s(\lambda)$ is illustrated in Fig. 5. The tradeoff between $\text{PAR}(\lambda)$ and $\gamma_s(\lambda)$, in Fig. 6.

We see that the shape gain can be as large as 1.20 dB if we allow the two-dimensional peak-to-average power ratio to increase to 3 (the same as the PAR of a square constellation); this PAR is the product of the circular con-

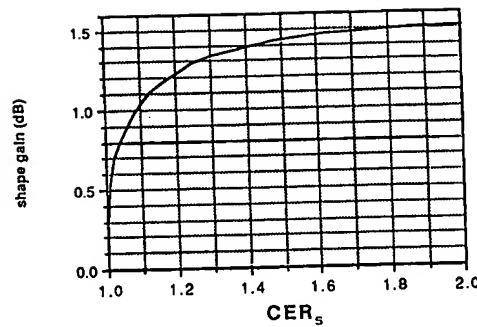


Fig. 5. Best possible tradeoff between shape gain γ_s (dB) and shaping constellation expansion ratio CER_s (dB).

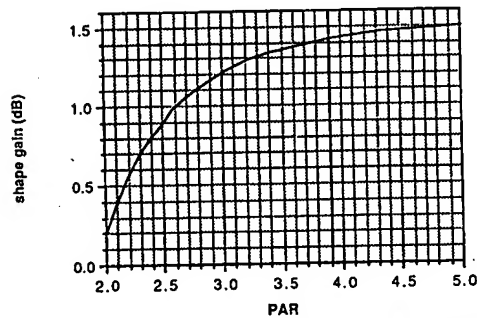


Fig. 6. Best possible tradeoff between shape gain γ_s (dB) and peak-to-average power ratio PAR (dB).

stellation PAR, namely 2, times a factor of about 1.25 due to an increase of 1 dB in shape gain, times the CER factor of about 1.2. The shape gain can be as large as 1.50 dB, effectively optimum, if we allow the two-dimensional peak-to-average power ratio to increase to 5; this PAR is 2, times a factor of about 1.35 due to an increase of 1.3 dB in shape gain, times the CER factor of about 1.85. As $\lambda \rightarrow \infty$, $J_1(\lambda) \rightarrow 1$, $J_2(\lambda) \rightarrow 1$, $\text{PAR}(\lambda) \rightarrow \infty$, $\text{CER}_s(\lambda) \rightarrow \infty$, and $\gamma_s(\lambda) \rightarrow \pi e / 6 = 1.423$ (1.53 dB), as we already know.

On the other hand, given a two-dimensional distribution $p(x)$ with average energy $P(X)$ and entropy $H(X)$, it follows from fundamental theorems of information theory that, for N large, the $(N/2)$ fold Cartesian product of $p(x)$ with itself is an N dimensional distribution, under which there are a set of approximately $2^{NH(X)/2}$ "typical sequences" (N tuples), each of probability approximately $2^{-NH(X)/2}$, that account for nearly all of the total probability measure on N tuples. Taking these "typical sequences" as the coordinates of N dimensional signal points, we arrive at a constellation C that represents nearly $H(X)$ bits per two dimensions with average energy $P(X)$. Thus, the tradeoffs shown in Figs. 5 and 6 are effectively achievable, if we are prepared to consider arbitrarily large numbers N of dimensions.

We conclude that it is possible in principle to achieve shape gains of more than 1 dB while keeping the peak-to-average power ratio of the constituent 2D constellation below 3, with the constellation size no more than 1.2 times the minimum possible (for such a shape gain), or, to achieve effectively optimum shape gains (1.5 dB) with PAR no greater than 5. In order to achieve these results,

the induced two-dimensional distribution $p(x)$ must approximate a Gaussian distribution, truncated within a circle.

V. GENERALIZED CROSS CONSTELLATIONS

Cross constellations are practical 2^b -point two-dimensional constellations based on the half-integer grid, and have been incorporated into international standards for 9.6 kbit/s dial modems (CCITT Recommendation V.32) and 14.4 kbit/s private-line modems (CCITT Recommendation V.33). Extensions of the cross constellation construction have been previously published in [1] and [2]. In this section we review previous constructions, describe a general construction for sending any integer number b of bits per $N = 2^{m+1}$ dimensions, and show that the resulting generalized cross constellations have moderate shape gains (of the order of 0.3 dB), very small shaping constellation expansion ratios, and other desirable practical attributes. Such constellations have in fact been used in Codex 19.2 kbit/s modems, in conjunction with multidimensional trellis codes [2].

A. Cross Constellations

A "cross constellation" is a simply constructed 2^b -point two-dimensional constellation that asymptotically achieves a shape gain of 32/31 (0.14 dB) relative to a square constellation with the same number of points [1].

To construct a 2^{5+2k} -point cross constellation, we use the 32-square template \mathbb{R} of Fig. 4(b), and scale (by partitioning each square into 4 squares) k times; the constellation is then the set of 2^{5+2k} half-integer grid points located in the middle of the resulting squares. (For a 2^{4+2k} point constellation, we simply take every other point from the 2^{5+2k} point cross constellation in checkerboard fashion; the resulting constellation has points from the grid $RZ^2 + (1/2, 1/2)$ and has only two-way rather than four-way symmetry.)

The template \mathbb{R} of Fig. 4(b), which has the shape of a cross, has $V(\mathbb{R}) = 32$ and $P(\mathbb{R}) = 31/6$, so $\gamma_s(\mathbb{R}) = V(\mathbb{R})/6P(\mathbb{R}) = 32/31$ (0.14 dB). Therefore, asymptotically, cross constellations achieve most of the 0.20 dB of shape gain that could be obtained by circular constellations in two-space. The 32-point cross constellation of Fig. 3(a) has average power $P(C) = 5$ (6.99 dB) [compare the continuous approximation $P(\mathbb{R}) = 31/6 = 5.1/6$ (7.13 dB)]; the 32-point square constellation of Fig. 3(b) has average power $P(C) = 63/12 = 5.25$ (7.20 dB), which is 0.21 dB worse. [The baseline average power is $P_\oplus(5) = 32/6 = 5.33$ (7.27 dB)].

To the accuracy of the continuous approximation (which is not too good until 2^b becomes quite large), the peak energy of \mathbb{R} is 13, so the peak-to-average power ratio is asymptotically $13/(31/6) = 78/31 = 2.52$, about halfway between the square and the circle. (The constellation expansion ratio is of course 1 because a cross constellation C is two dimensional.) Implementation complexity for cross constellations is trivial. Cross constellations of 32 or more points divide evenly into 4

or 8 subsets corresponding to cosets of $2Z^2$ or $2RZ^2$, and those of 128 points or more divide evenly into 16 subsets corresponding to cosets of $4Z^2$. Thus, cross constellations are well suited for QAM modems, and for coded modulation.

"Reverse scaling" of the cross template of Fig. 4(b) suggests a constellation that gives us a first chance to illustrate an opportunistic secondary channel. Fig. 7(a) is a template consisting of 8 "squares" where the four outer "squares" are composed of two half-squares that wrap (modulo 3) around the boundaries. If we place a constellation point in the "middle" of each of these eight "squares," then four of the points lie on the boundary, and there are two possible positions where they could be placed. If we leave this ambiguity unresolved, then we arrive at the 12-point constellation of Fig. 7(b), with 4 inner points and 4 pairs of boundary points.

This constellation can be used to send 3 bits per two dimensions, and in addition to support an opportunistic secondary channel with average rate of 1/2 bit per two dimensions. The average power is now $P(C) = 1.5$ (1.76 dB), which is nearly 1 dB better than the baseline average power to send $\beta = 3.5$ bits per two dimensions of $P_\oplus(3.5) = 2^{3.5}/6 = 1.89$ (2.75 dB). Also, Fig. 7(b) has quadrilateral symmetry and other desirable characteristics. However, the fact that the secondary channel is probabilistic leads to systems issues such as those discussed in Section II-H. Subject to this qualification, this example shows that opportunistic secondary channels can yield high SNR efficiency.

B. Generalized Cross Constellations

We now begin to generalize the cross constellation idea to higher dimensions where fractional normalized bit rate β can be obtained. Since it takes $2^{bN/2}$ -point N -dimensional constellations to represent β bits per two dimensions, it becomes increasingly desirable to maintain coding simplicity, even at some cost in shape gain.

Generalized cross constellations are built up from constituent 2D constellations C_2 whose points are drawn from a coset $Z^2 + a$ of the integer lattice Z^2 ; e.g., the half-integer grid $Z^2 + (1/2, 1/2)$. The $(N/2)$ -fold Cartesian product $C_2^{N/2}$ is then a set of $|C_2|^{N/2}$ points from the corresponding coset $(Z^2 + a)^{N/2} = Z^N + a^{N/2}$ of Z^N , as long as $|C_2|$ is greater than or equal to the baseline 2^b , it will be possible to find a subset C of $C_2^{N/2}$ with elements where $\beta = 2b/N$ is the normalized bit rate. If principal virtues of generalized cross constellations (that their constellation expansion ratio $|C|/2^b$ is close to 1, and that the subset C can be defined by a simple coding rule.

(Generalized cross constellations can also be used to construct constellations C with points from any binary lattice Λ . We start with a generalized cross constellation that we would use if Λ were Z^N . Since any translate Z^N is the union of $|Z^N/\Lambda|$ cosets (translates) of Λ , will be a union of $|Z^N/\Lambda|$ constellations each composed of points from a single coset of Λ , each with about (of

Multidimensional Constellations I



Template and "cross constellation" for sending $b = 3$ bits per two dimensions, plus a $1/2$ -bit (per 2D) opportunistic secondary channel, pairs of boundary points (shaded).

ly $|C|/|Z^N/\Lambda|$ points, and we may take any of as C . Note that the effective bit rate β is reduced by normalized redundancy $\rho(\Lambda) = (2/N) \log_2 |Z^N/\Lambda|$. we shall consider only the case $\Lambda = Z^N$.

send a half-integer number of bits per two dimensions, say $\beta = n + 1/2$ with n an integer, we may use a dimensional 2^{2n+1} -point constellation. One way of this is to generalize cross constellations as follows, to build up the 4D constellation from constituent 2D constellations. (This idea appears both in [1] and in [2].) two dimensions, construct a $3 \cdot 2^{n-1}$ -point constellation C_2 with 2^n "inner points" and 2^{n-1} "outer points." four-dimensional constellation C then consists of the Cartesian product C_2^2 of this constellation with itself, except that pairs of outer points are not allowed. Then there are 2^{2n} 4D points of the type (inner, inner), 2^{2n-1} of the type (inner, outer), and 2^{2n-1} of the type (outer, inner), 2^{2n+1} 4D points in all. The average power $P(C)$ (per two dimensions) is thus $3/4$ the average power of the inner points plus $1/4$ the average power of the outer points. The 2^{2n+2k} -point 2D cross constellation can be seen to be built up from constituent $3 \cdot 2^{k+1}$ -point 1D constellations exactly this way.)

Two specific scalable templates for appropriate 2D constellations are illustrated in Fig. 8(a) and (b). In Fig. 8(a), the inner points are the 2^n points in a 2D cross constellation, and the outer points are an additional 2^{n-1} points from the same grid in the shaded outer region. The average power of the inner region is then $31/6$; the average energy of the outer region can be computed to be $41/3$; therefore, to the accuracy of the continuous approximation, the average power of the 4D region \mathbb{R} that defines the generalized cross constellation, per two dimensions, is $P(\mathbb{R}) = 175/24$. The volume of this region is $V(\mathbb{R}) = 2^{11}$, so the shape gain $\gamma_s(\mathbb{R}) = V(\mathbb{R})^{1/2}/[6P(\mathbb{R})]$ is $2^{11}/175$ (0.15 dB), scarcely more than that of the 2D cross. Two such constellations are shown in [1, Fig. 8]; with $d_{\min}^2(C) = 1$, they actually have average power $P(C) = 7.125$ (8.53 dB) and 29 (14.62 dB) for $\beta = 5.5$ and 7.5 bits per two dimensions, respectively (compare the approximations $P(\mathbb{R}) = 175/24$ (8.63 dB) and $175/6$ (14.65 dB), respectively). Similarly, the template of Fig. 8(b) defines a square inner region with average power $32/3$ and an outer region with average power $11/3$, which generates a 4D region with $P(\mathbb{R}) = 173/12$ and $V(\mathbb{R}) = 2^{13}$, so $\gamma_s(\mathbb{R}) = 2^{13}/173$ (0.20 dB), a small

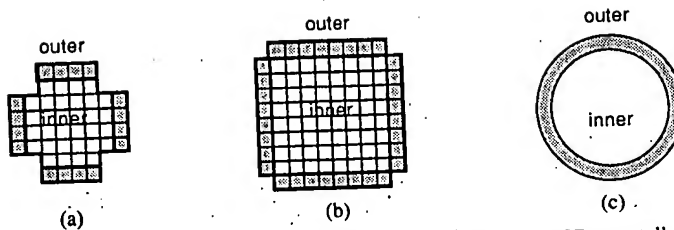


Fig. 8. Templates for inner and outer points of constituent 2D constellations for construction of 4D generalized cross constellations: (a) with inner points forming a cross constellation, (b) with inner points forming a square constellation, (c) circular constellation, with inner points forming a circular constellation.

improvement over Fig. 8(a). The corresponding constellation for $\beta = 6.5$ actually has $P(C) = 14.25$ (11.54 dB) [compare the approximation $P(\mathbb{R}) = 173/12$ (11.59 dB)].

If we wish to construct large 4D constellations, and do not care how complex the encoding of the constituent 2D constellation becomes, then the inner and outer points of the 2D constellation should be approximately delimited by circles of radius R_0 and R_1 , with $R_1^2 = (3/2)R_0^2$ so that the area of the inner circle is twice that of the surrounding annulus, as shown in Fig. 8(c). In this case, $V(\mathbb{R}) = 2(\pi R_0^2)^2$, and $P(\mathbb{R})$ can be calculated to be $(11/16)R_0^2$, so that the shape gain is $\gamma_s(\mathbb{R}) = V(\mathbb{R})^{1/2}/6P(\mathbb{R}) = \pi^{7/2}/33 = 1.08$ (0.32 dB). This is halfway between what is achieved with the templates of Fig. 8(a) or (b) and the 4-sphere limit of 0.46 dB.

As with cross constellations, these generalized cross constellations are very suitable for use with coded QAM modems. They are relatively simple to implement, since the mapping complexity is approximately that of a 2D constellation, with a very simple "inner/outer" coding rule to create the 4D constellation from its 2D constituents. The size of the constituent 2D constellation is $3 \cdot 2^{n-1}$, compared to the minimum possible size of $2^{n+1/2}$, so the shaping constellation expansion ratio $\text{CER}_s(C)$ is only $3/2^{3/2} = 1.06$. The peak-to-average power ratio is also well bounded; to the accuracy of the continuous approximation, it is $480/175 = 2.74$ for Fig. 8(a), $492/173 = 2.84$ for Fig. 8(b), and $24/11 = 2.18$ for Fig. 8(c).

The inner and outer regions of the three 2D templates of Fig. (8) all have four-way phase symmetry, so if points are chosen from the half-integer grid $Z^2 + (1/2, 1/2)$, the constituent 2D constellation will necessarily have 4-way symmetry. For use with a coset code of depth μ , the 2D points in each of these regions must be evenly divided among the 2^μ cosets of $R^\mu Z^2$ whose union is the half-integer grid. If μ is 2 (or less), then this requirement is automatically satisfied. For $\mu > 2$, minor modifications of the templates of Fig. 8 may be needed to satisfy this requirement. (See [2] for examples.)

We now give an example to show that an opportunistic secondary channel with a small fractional average bit rate may be added to generalized cross constellations, in such a way that all design constraints are respected.

Consider the 48-point constituent 2D constellation partitioned into 4 equal subsets that is shown in Fig. 9(a). Its

Multidimensional Constellations I

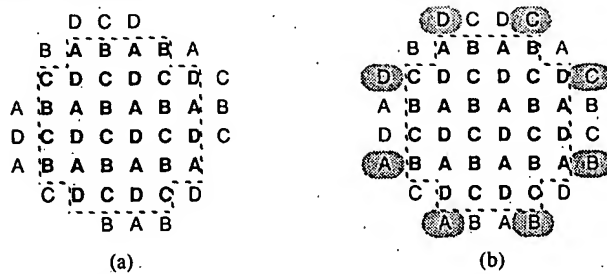


Fig. 9. Constituent 2D constellations for 4D generalized cross constellations with normalized bit rate $\beta = 5.5$ bits per two dimensions, evenly divided into 4 subsets, with inner points bold; (a) optimum 48-point constellation, (b) 52-point constellation with 4 paired outer points, to support an opportunistic secondary channel with average bit rate 1/16 bit/Hz.

inner points are the 32-point cross constellation of Fig. 3(a) [the 32 least-energy points from the half-integer grid], and its outer points have been chosen as the next 16 least-energy points, respecting quadrilateral symmetry. [This improves SNR efficiency very slightly over the 48-point constellation that would be obtained by using the template of Fig. 8(a)].

Fig. 9(b) is a more symmetrical 52-point constellation, which adds the next 4 least-energy points. We may take 4 pairs of outer points, each pair consisting of two points from the same subset, such as the pairs shown shaded in the figure, to create an opportunistic secondary channel whose average rate is $(1/4) \times (4/16) = 1/16$ bit per two dimensions (e.g., a bit rate of $2400/16 = 150$ bits/s if the baud rate is 2400) where $1/4$ is the probability of an outer point and $4/16$ is the fraction of outer points that are paired. The pairs are chosen to maintain 4-way symmetry. Since the paired points have the same energy, the average power using Fig. 9(b) is the same as that of Fig. 9(a), namely, $P(C) = 7$ (8.45 dB). (The baseline average power is $2^{5.5}/6 = 7.54$ (8.78 dB), so the shape gain is 1.08 (0.32 dB), as predicted for circular 4D generalized cross constellations.) Thus, in this example a low-rate opportunistic secondary channel costs nothing in SNR efficiency.

C. Generalization to Arbitrary Binary Fractions

We now give a further generalization that permits sending any number $\beta = n + d/2^m$ of bits per two dimensions, where n is an integer that is "large enough" (to be defined later) and d is any integer in the range $0 \leq d < 2^m$, using two-dimensional constituent constellations. This requires the construction of an N dimensional constellation with $2^{n(N/2)+d}$ points where $N = 2^{m+1}$. A construction of this type for fractions with $d = 1$ has been published in [2].

We first express the number d in the standard binary representation as $d = d_0 + 2d_1 + \dots + 2^{m-1}d_{m-1}$, e.g., if $d = 5$, then $d = 1 + 4$. Let $J(d)$ be the set of j for which d_j is nonzero: $J(d) = \{j: d_j = 1\}$. Each $j \in J(d)$ will correspond to a two-way partition of the constituent

2D constellation C_2 . We may take these partitions in any order, but let us take the $j \in J(d)$ in ascending order. If the smallest $j \in J(d)$ is j' , then the first partition divides C_2 into two subsets whose sizes are in the ratio $1:2^{-(m-j')}$, called " j' -inner" and " j' -outer." Each additional $j \in J(d)$ further partitions each of these subsets into two smaller subsets in the ratio $1:2^{-(m-j)}$. Consequently, we finally arrive at a partition of C_2 into 2^K subsets where $K = |J(d)|$ is the number of nonzero coefficients in the binary representation of d , consisting of all possible combinations of j -inner and j -outer points for the $|J(d)|$ different partitions. The ratio of the size of the largest subset to that of the smallest subset is the product of the constituent ratios.

As in Section V-B, the points of each subset should be chosen from the half-integer grid in such a way as to maintain four-way symmetry, and, for use with a code C , should be evenly divisible into 2^μ cosets of $R^\mu Z^2$, where μ is the depth of the code C , which may represent an additional constraint when $\mu > 2$.

The size of the largest subset is fixed as 2^n points. Since the smallest subset must have at least $\max[4, 2^n]$ points to meet the two requirements of the previous paragraph, this determines how large the integer n must be.

For example, let 2^m be 8, and let d range from 1 to 7. For $d = 4$, the sizes of the two subsets of C_2 are 2^n and 2^{n-1} , and this method will reduce to the generalized cross constellation construction for half-integer numbers β of bits per two dimensions given in the previous section. For $d = 1$ or 2, there are two subsets with sizes 2^n and 2^{n-1} or 2^n and 2^{n-2} , respectively. For $d = 3, 5$, or 6, C_2 divides into four subsets, with sizes $2^n, 2^{n-2}, 2^{n-3}$ and 2^{n-4} for $d = 3$, for example. The worst case is $d = 7$, which requires eight subsets with sizes $2^n, 2^{n-1}, 2^{n-2}, 2^{n-3}, 2^{n-4}, 2^{n-5}$, and 2^{n-6} . Thus, in this last case, the integer n must be at least 8 (if $\mu \leq 2$).

Fig. 10 is an example of a constellation that can be used to send $7 \frac{3}{8}$ bits per two dimensions. The constellation consists of four subsets of sizes 128, 32, 16, and 4 points. The points in the subsets have been selected in a greedy manner—i.e., as the lowest-energy points not yet selected. However, quadrilateral symmetry has been respected; since the constellation is drawn from the half-integer grid, this means that it will automatically divide evenly into 4 cosets of $2Z^2$. (Of course, the subsets cannot be divided evenly into 8 or more cosets, because the smallest subset has only 4 points.)

The shaping constellation expansion ratio $CER(C) = |C_2|/2^\beta$ is very close to the minimum possible. For $d = 4$, $CER(C) = (3 \cdot 2^{n-1})/(2^n + 1/2) = 3/2^{1.5} = 1.0$ as already noted. For $d = 1, 2$, and 3, it is 1.03, 1.0, and 1.08. The worst case is $d = 7$, where it is 1.15.

The following code maps $2^m n + d$ bits into a sequence of 2^m points from the constituent 2D constellation so defined. For each $j \in J(d)$, we divide the sequence into subsequences, each of length 2^{m-j} . For each subsequence, we let one "designator bit" determine whether any element of that subsequence will be j -outer. If so,

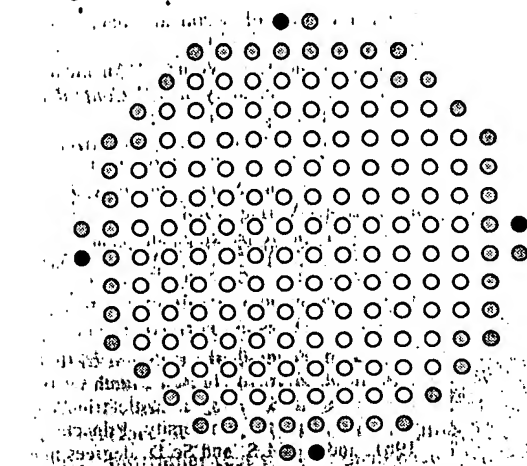


Fig. 10. 180-point constituent 2D constellation for sending $7\frac{3}{8}$ bits per dimension, divided into four subsets of 128, 32, 16, and 4 points.

a further $m - j$ bits determine which one of the 2^{m-j} elements will be j -outer. (Since that element will need $m - j$ fewer bits to be selected than will a j -inner point, we spare exactly the necessary number of bits.) When this process has been completed, every one of the 2^m elements of the sequence will have been designated as j -inner or j -outer for each of the $K = |J(d)|$ values of j . The number of designator bits used is 2^j for each $j \in J(d)$; in total, by the definition of d_j , is d . If all elements are inner for all $j \in J(d)$, then it takes n bits per element, $2^m n$ bits in all, to specify which of the 2^n points in the largest part of C_2 is to be used, so the total number of bits used is $2^m n + d$. For each element, for each $j \in J(d)$ for which the element is j -outer, $m - j$ fewer bits have to be used to select a point, so regardless of the values of the designator bits, the total number of bits used is $2^m n + d$. This code is simple to implement (if not to describe).

With this code, the probability that any given 2D point is j -outer is $2^{-(m-j)-1}$ for any $j \in J(d)$. For instance, for $j = m - 1$, the probability that a 2D point is j -outer is $1/4$, as determined earlier. The probability of selecting a point from a particular one of the 2^K subsets is the product of K constituent probabilities, where each constituent probability is a probability of being j -inner or j -outer, according to the composition of the subset. The probability that any particular point in a subset is selected is the probability of that subset (as determined above) divided by the number of points in that subset. The average power per two dimensions is the product of 2^K terms, one for each subset, each term being the product of the probability of that subset with the average energy of points in that subset. To minimize the average power, the constellation should be partitioned so that the points of larger energy are assigned so as to have lower probability.

For example, the probabilities of the four subsets of points in Fig. 10 are $(15/16) \times (7/8)$ for the 128 "inner-inner" points, $(15/16) \times (1/8)$ for the 32 "inner-outer" points, $(1/16) \times (7/8)$ for the 16 "outer-inner" points, and $(1/16) \times (1/8)$ for the 4 "outer-outer" points. Since the average powers of these four subsets are

TABLE II
AVERAGE POWER TO SEND β BITS PER TWO DIMENSIONS

β	$ C_2 $	CER_s	$P(C)$	(dB)	$P(R)$	(dB)	$\gamma_s(R)$	PAR
7	128	1.00	20.44	13.10	20.37	13.09	0.20	2.00
$7\frac{1}{8}$	$144 = 128 + 16$	1.03	21.85	13.39	21.81	13.39	0.28	2.10
$7\frac{1}{4}$	$160 = 128 + 32$	1.05	23.57	13.72	23.56	13.72	0.32	2.16
$7\frac{3}{8}$	$180 = 128 + 32 + 16 + 4$	1.08	25.49	14.06	25.45	14.06	0.36	2.25
$7\frac{1}{2}$	$192 = 128 + 64$	1.06	28.05	14.48	28.01	14.47	0.32	2.18
$7\frac{5}{8}$	$216 = 128 + 64 + 16 + 8$	1.09	30.30	14.81	30.30	14.81	0.36	2.27
$7\frac{3}{4}$	$240 = 128 + 64 + 32 + 16$	1.11	33.07	15.19	33.03	15.19	0.36	2.31
$7\frac{7}{8}$	$270 = 128 + 64 + 32 + 16 + 8 + 4 + 2$	1.15	35.96	15.56	35.93	15.55	0.37	2.39
8	256	1.00	40.69	16.09	40.74	16.10	0.20	2.00

20.44, 45.5, 54, and 56.5, respectively, the average power of the constellation is $P(C) = 25.49$ (14.06 dB).

Table II gives values of the smallest average power $P(C)$ that can be obtained by this construction for numbers β of bits per two dimensions equal to $\beta = 7 + d/8$ where d ranges from 0 to 7. The sets have been chosen as in Fig. 10, using the least-energy points available from the grid $Z^2 + (1/2, 1/2)$. Quadrilateral symmetry is attainable except for the case $\beta = 7\frac{7}{8}$. We also give for comparison an asymptotic average power $P(R)$, using sets bounded by circles of increasing radius as in Fig. 8(c), and the corresponding shape gain $\gamma_s(R)$. We see that the approximation is already accurate to within 0.01 dB. Finally, we give the shaping constellation expansion ratio $CER_s(R)$ and the asymptotic peak-to-average power ratio $PAR(R)$. (The asymptotic values of $CER_s(R)$, $\gamma_s(R)$, and $PAR(R)$ given in Table II are valid for $\beta = n + d/8$ for any integer n , not just $n = 7$.)

It seems that finer constellation partitioning leads to slightly greater shape gains, up to approximately 0.37 dB, but the difference beyond the half-integral method (0.32 dB) is small. The two-way (inner/outer) partitions used for $\beta = 7\frac{1}{4}$ and $7\frac{1}{8}$ yield about the same or slightly less gain. The more composite the constellation, the higher the CER_s and therefore PAR [by the relation (*)], but in general it is a virtue of this construction that the CER_s and PAR for the constituent 2D constellations are close to their minimum possible values, as noted in Wei [2] where other examples of such constellations satisfying various constraints are also given. The mapping complexity is also roughly that of a 2D constellation.

These methods can be generalized to construct N dimensional constellations with $2^{NM \cdot d}$ points from constituent partitioned (N/M) dimensional constellations. From the examples investigated so far, it appears that in general the resulting shape gains are limited to within about 0.1 to 0.2 dB more than the shape gains obtainable with (N/M) dimensional constellations, as we have already seen with $N/M = 2$.

VI. CONCLUSION

The principal purposes of this paper have been to provide an overview of multidimensional constellations, with a full discussion of characteristics that are desirable in practice; to develop figures of merit, principally the shape gain and shaping constellation expansion ratio, that de-

pend only on the shape of the constellation in N space, and that are more or less decoupled from the gain and expansion factors due to coding; to develop bounds on achievable shape gain as a function of dimension and of constellation expansion; and finally to present a class of constellations, namely generalized cross constellations, that are in fact good for practical applications.

Generalized cross constellations have most or all of the characteristics desired. They support fractional normalized bit rates with very small shaping constellation expansion ratios, usually less than 1.1, and with moderate shape gains, less than 0.4 dB. However, the bound plotted in Fig. 5 shows that in fact a shape gain of as much as 1.0 dB is achievable in principle with a shaping constellation expansion ratio of only 1.1. Thus there is room for considerable improvement in shape gain, perhaps with some sacrifice of other desirable constellation characteristics. The Voronoi constellations to be discussed in [Part II] can achieve considerably greater shape gains, but generally at the cost of greater constellation expansion and implementation complexity.

ACKNOWLEDGMENT

We are grateful to A. R. Calderbank and J. M. Cioffi for detailed comments on the first version of this paper.

REFERENCES

- [1] G. D. Forney, Jr., R. G. Gallager, G. R. Lang, F. M. Longstaff, and S. U. Qureshi, "Efficient modulation for band-limited channels," *IEEE J. Select. Areas Commun.*, vol. SAC-2, pp. 632-647, 1984.
- [2] L.-F. Wei, "Trellis-coded modulation with multidimensional constellations," *IEEE Trans. Inform. Theory*, vol. IT-33, pp. 483-501, 1987.
- [3] G. D. Forney, Jr., "Multidimensional constellations—Part II: Voronoi constellations," *IEEE J. Select. Areas Commun.*, see this issue.
- [4] —, "Coset codes—Part I: Introduction and geometrical classification," *IEEE Trans. Inform. Theory*, vol. 34, pp. 1123-1151, Sept. 1988.
- [5] A. R. Calderbank and N. J. A. Sloane, "New trellis codes based on lattices and cosets," *IEEE Trans. Inform. Theory*, vol. IT-33, pp. 177-195, 1987.
- [6] G. Ungerboeck, "Channel coding with multilevel/phase signals," *IEEE Trans. Inform. Theory*, vol. IT-28, pp. 55-67, 1982.
- [7] L.-F. Wei, "Rotationally invariant convolutional channel coding with expanded signal space—Parts I and II," *IEEE J. Select. Areas Commun.*, vol. SAC-2, pp. 659-686, 1984.
- [8] G. R. Lang, G. D. Forney, Jr., S. Qureshi, F. M. Longstaff, and C. H. Lee, "Signal structures with data encoding/decoding for QCM modulations," U.S. Pat. 4 538 284, Aug. 27, 1985.
- [9] T. Armstrong, "Secondary channel signaling in a QAM data point constellation," U.S. Pat. 4 630 287, Dec. 16, 1986.
- [10] R. D. Gitlin and J.-J. Werner, "Inband coding of secondary data," U.S. Pat. 4 644 537, Feb. 17, 1987.

- [11] H. K. Thapar, "Inband coding of secondary data," U.S. Pat. 4 651 320, Mar. 17, 1987.
- [12] R. D. Gitlin, H. K. Thapar and J.-J. Werner, "An inband coding method for the transmission of secondary data," *Conf. Record, Intern. Conf. Commun.*, June 1988, pp. 3.1.1-3.1.5.
- [13] A. Gersho, "Asymptotically optimum block quantizers," *IEEE Trans. Inform. Theory*, vol. IT-25, pp. 373-380, 1979.
- [14] J. H. Conway and N. J. A. Sloane, *Sphere Packings, Lattices and Groups*. New York: Springer-Verlag, 1988.
- [15] N. J. A. Sloane, "Tables of sphere packings and spherical codes," *IEEE Trans. Inform. Theory*, vol. IT-27, pp. 327-338, 1981.



G. David Forney, Jr. (S'58-M'61-F'73) was born in New York, NY, on March 6, 1940. He received the B.S.E. degree in electrical engineering from Princeton University, Princeton, NJ, in 1961, and the M.S. and Sc.D. degrees in electrical engineering from the Massachusetts Institute of Technology, Cambridge, MA, in 1963 and 1965, respectively.

In 1965, he joined Codex Corporation, and became a Vice President and Director in 1970. From 1982 to 1986, he was Vice President and Director of Technology and Planning of the Motorola Information Systems Group, Mansfield, MA. He is now once again a Vice President of Codex. He has been a Visiting Scientist at Stanford University, Stanford, CA, and an Adjunct Professor at M.I.T.

Dr. Forney was Editor of the *IEEE TRANSACTIONS ON INFORMATION THEORY* from 1970 to 1973. He has been a member of the Board of Governors of the Information Theory Group from 1970-1976 and again from 1986 to date. He was the winner of the 1970 Information Theory Group Prize Paper Award and of the 1972 Browder J. Thompson Memorial Paper Award. He was elected to membership in the National Academy of Engineering in 1983.



Lee-Fang Wei was born in Taipei, Taiwan, Republic of China, in 1951. He received the B.S. degree from the National Taiwan University, Taipei, in 1973, the M.S. degree from the University of New York, Stony Brook, in 1974, and the Ph.D. degree from the University of California, Berkeley, in 1980, all in electrical engineering.

From 1980 to 1982 he was with Bell Laboratories, Holmdel, NJ, and from 1983 to 1984 he was with AT&T Information Systems, Nepton, NJ, where he did research on voiceband data transmission and digital signal processing. His work on rotationally invariant trellis-coded modulation was adopted in the CCITT Recommendations V.32 and V.33 for high speed voiceband modems. In 1984, he joined Codex Corporation, Mansfield, MA, as a principal engineer, where he did research and development on 19.2 kbit/s voiceband modems and digital subscriber loops for ISDN. In 1985, he rejoined AT&T Bell Laboratories. His current interests are optical communications, mobile radio communications, and local area networks. He holds four patents in the field of trellis-coded modulation.

Dr. Wei received the IEEE Communications Society 1984 Stephen Rice Prize Paper Award in Communications Theory. He was also recipient of the J. Karp Prize Paper Award at Interface 1984.

A Coherent Digital Amplitude and Phase Modulation Scheme*

C. N. CAMPOPIANO†, MEMBER, IRE, AND B. G. GLAZER†, MEMBER, IRE

Summary—In this paper, we present a technique for a combination of amplitude and phase modulation for digital communication. This technique assumes phase coherence between transmitter and receiver. For purposes of analysis, we also assume baud synchronization. The technique involves the simultaneous and independent amplitude modulation of two carriers of the same frequency which are in quadrature with each other. The demodulation process consists of the separation of the in-phase and quadrature components followed by amplitude detection. This scheme appears to be easier to implement than either the system studied by C. R. Cahn or the system investigated by J. C. Hancock and R. W. Lucky. Furthermore this system is comparable in reliability to the latter scheme.

I. INTRODUCTION

THIS PAPER is concerned with digital communication over channels perturbed by additive, narrow-band, zero-mean Gaussian noise. For such channels, binary communication schemes make inefficient use of the channel capacity when the signal to noise ratio is high. For this reason, there is today considerable interest in nonbinary communication techniques. The results of Shannon [1] and of Blachman [2] suggest that a combination of amplitude modulation (AM) and phase modulation (PM) is especially to be considered in the design of systems for such channels when the SNR is high.

Combinations of digital amplitude and phase modulation (AM-PM) have recently been studied by Cahn [3] and by Hancock and Lucky [4]. Cahn has examined digital phase modulation alone [5] as well as AM-PM. Following the terminology of Hancock and Lucky we shall call the AM-PM system studied by Cahn the Type I system. In the Type I system, the same number of phase positions is used with each amplitude level. The possibility of improving efficiency by using more phase positions with the larger amplitude levels was suggested by Taber (see [3], p. 151). Hancock and Lucky [4] investigated the latter possibility in detail. For fixed average signal power they determined that number of phase positions for each amplitude level which would yield a minimum probability of error. A similar optimization process was carried out for fixed peak power. We shall use the terminology of Hancock and Lucky in referring to the AM-PM scheme which they investigated as the Type II system.

In the present paper we present an AM-PM system which we call the Type III system. The Type III system is comparable in reliability to the Type II system. In addition, it may be fairly readily implemented. In fact,

although the initial motivation for the Type III system was the problem of modulation and demodulation with large signaling alphabets, it appears that it may be recommended even for signaling alphabets of moderate size. The Type III system amounts essentially to the amplitude modulation and demodulation of two carriers that have the same frequency but are in quadrature with each other. The simplicity of mechanization of this scheme lies in its reliance upon amplitude modulation and demodulation. It must be emphasized, however, that the Type III system requires phase coherence whereas the Type I and Type II systems can function in a differentially coherent mode.

In the present paper, we describe the Type III system, give analytical expressions for the probability of error for this system, and compare the Type III system with the systems of Type I and Type II. It is convenient, in the following exposition, to begin by describing a general modulation and demodulation process that includes, as special cases, the three systems considered in this paper. This is done in Section II. In Section III the results of Section II are specialized to systems of Type I, II, and III. Finally, in Section IV we briefly compare the three systems.

II. AMPLITUDE AND PHASE MODULATION AND DEMODULATION

In the present section, we list our basic assumptions and discuss a general modulation-demodulation scheme that includes as special cases all others treated in this paper.

A. The Signaling Alphabet and the Channel

We suppose that there is phase coherence between transmitter and the receiver. It is further assumed that the receiver knows both the time of arrival of the signal and the duration of the signal. The transmitter has at disposal M signals for transmission. These signals each be of finite duration, T seconds. We can write a set of M signals as

$$\begin{aligned} s_i(t) &= A_i \cos(\omega t - \phi_i) \\ &= C_i \cos \omega t + S_i \sin \omega t \end{aligned}$$

where $0 \leq t \leq T$ and $i = 1, 2, \dots, M$. The set of $\{s_1(t), \dots, s_M(t)\}$ is called the *signaling alphabet*. The number of signals in the alphabet is called the *size* of the alphabet. We use the familiar representation of the signals $s_i(t)$ as indicated in Fig. 1. We call the plane of Fig. 1, the *phasor plane*.

* Received December 9, 1961.

† Aerospace Communications and Controls Division, Radio Corporation of America, Camden, N. J.

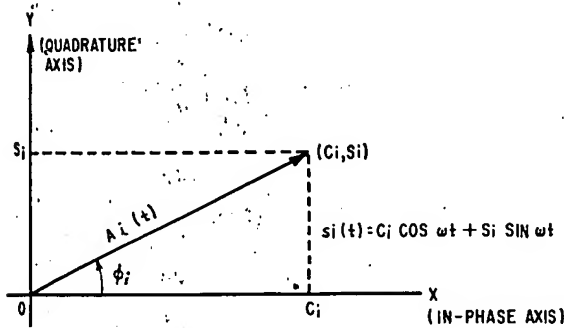


Fig. 1—Phasor representation of the signaling alphabet.

We assume that the channel is characterized by additive, zero-mean, narrow-band Gaussian noise of mean power N . The noise waveform, $n(t)$, is represented as

$$n(t) = x(t) \cos \omega t + y(t) \sin \omega t$$

where $x(t)$ and $y(t)$ are independent samples from an ensemble of functions such that the ensemble averages $\langle x^2(t) \rangle$ and $\langle y^2(t) \rangle$ are equal to N while $\langle x(t) \rangle$, $\langle y(t) \rangle$, and $\langle x(t)y(t) \rangle$ are zero. It is assumed that $x(t)$ and $y(t)$ are slowly varying in the sense that they do not change appreciably in an interval of T seconds. Ignoring propagation time, we may write the received waveform, $r(t)$, as

$$r(t) = s_i(t) + n(t) \quad (0 \leq t \leq T). \quad (2)$$

The Detection Scheme

Suppose that one of the signals in (1), say $s_i(t)$, is transmitted and that $r(t)$ in (2) is received. The received waveform is then processed as indicated in Fig. 2. The result of this process is the decision vector (u, v) with components

$$\begin{aligned} u &= C_i + \frac{1}{T} \int_0^T x(t) dt \\ v &= S_i + \frac{1}{T} \int_0^T y(t) dt. \end{aligned} \quad (3)$$

The decision scheme is conveniently described in terms of the phasor plane. Consider the vector of (3) as a point in the phasor plane. To each signal point (C_i, S_i) we associate a set of points, say D_i , called the detection region for $s_i(t)$. The vector (u, v) is decoded as $s_i(t)$, if and only if, it lies in D_i . D_1, D_2, \dots, D_M are pairwise disjoint, but their union may not exhaust the phasor plane. If (u, v) lies in none of the sets D_i , then no decision is made.

In the system of Type III the detection regions will be simple rectangular regions with edges parallel to the axes of the phasor plane so that a decision can be made directly in terms of thresholds on u and v . In the systems of Type I and II, however, the detection regions are expressible in the form $R_1 \leq R \leq R_2$, $\theta_1 \leq \theta \leq \theta_2$ where

$$\begin{aligned} R &= \sqrt{u^2 + v^2} \\ \theta &= \tan^{-1} \left(\frac{v}{u} \right). \end{aligned} \quad (4)$$

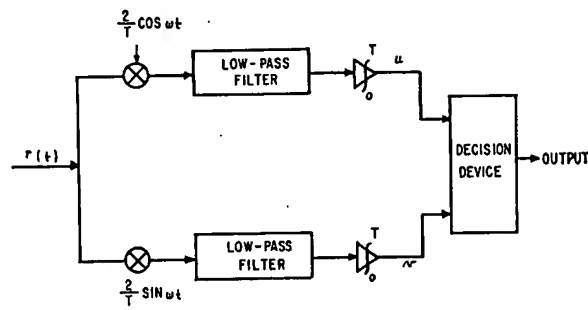


Fig. 2—Quadrature detection for AM-PM waveforms.

Hence the decision device for the latter systems will have to include or be preceded by computing elements that yield R and θ . This explains the complexity of the implementation of systems of Types I and II compared to the relative simplicity of implementation of the Type III system.

C. Probability of Error

We suppose that each of the M signals in (1) has probability $1/M$ of being selected for transmission independently of past transmissions. For $i = 1, 2, \dots, M$, $P_i(e)$ denotes the conditional probability of error when $s_i(t)$ is sent; i.e.,

$$P_i(e) = \text{Prob} \{ (u, v) \text{ is not in } D_i \mid s_i(t) \text{ is sent} \}.$$

The (average) probability of error, $P(e)$, is defined as

$$P(e) = \frac{1}{M} \sum_{i=1}^M P_i(e).$$

If P is any of the above probabilities, then \bar{P} and \tilde{P} will represent respectively a lower bound, an upper bound, and an approximation to P .

The quantities u and v in (3) are samples of random variables, say U and V respectively. From our assumptions it is readily seen that U and V are independent, normally distributed random variables with identical variance, N , and with means C_i and S_i , respectively, where (C_i, S_i) represents the transmitted signal. Then $p_i(u, v)$, the conditional probability density function of U, V is

$$p_i(u, v) = \frac{1}{2\pi N} \exp \left\{ -\frac{(u - C_i)^2 + (v - S_i)^2}{2N} \right\}. \quad (5)$$

Probabilities computed from (5) will ordinarily involve A_i, C_i and S_i . However, we shall relate probabilities to average signal power, S , where

$$S = \frac{1}{M} \sum_{i=1}^M \frac{A_i^2}{2} = \frac{1}{M} \sum_{i=1}^M \frac{(C_i^2 + S_i^2)}{2}.$$

In fact, in Section III, it is shown that for each of three separate AM-PM systems, the probability of error, $P^{(i)}(e)$, is given approximately as

$$P^{(i)}(e) \approx K_i \exp \left(-E_i \frac{S}{N} \right) = \exp \left(-E_i \frac{S}{N} + \ln K_i \right) \quad (6)$$

where K_i varies slowly with S/N relative to $\exp(-E_i [S/N])$ and both K_i and E_i depend upon the particular system discussed. E_i , on the other hand, is independent of S and N . In order to compare two systems, say system 1 and system 2, it is not uncommon to determine the ratio

$$r = \frac{(S/N)_1}{(S/N)_2} \quad (7)$$

where $(S/N)_i$ ($i = 1, 2$) is that SNR for which system i has probability of error p , where p is the same value for both systems. If (6) holds, and if K_i is a slowly varying function of $(S/N)_i$, then for sufficiently small p or sufficiently large $(S/N)_i$, the ratio r in (7) is given approximately as

$$r \approx \frac{E_2}{E_1}$$

Therefore, the quantity E_i in (6) provides a convenient measure for comparing systems for which (6) holds. From (6), we have

$$E_i = \lim_{(S/N) \rightarrow \infty} \left[\frac{-\ln P^{(i)}(e)}{S/N} \right] \quad (8)$$

We shall call E_i in (6) and (8) the *detection reliability* of system i . This concept is somewhat similar to the concept of "reliability" utilized by Peterson [6] in the theory of error-correcting codes.

III. SPECIFIC AM-PM SYSTEMS

In this section, the definitions and results of Section II are applied to three distinct AM-PM systems.

A. The Type I System

This is the system studied by Cahn [3]. In this system, the set of M signals is

$$s_{ki}(t) = A_k \cos \left(\omega t - \frac{2(i-1)\pi}{n} \right), \quad 0 \leq t \leq T;$$

$$A_k = A_1 + 2(k-1)A_1 \sin \frac{\pi}{n}, \quad A_1 > 0$$

where $k = 1, 2, \dots, m$ and $M = mn$. The optimum values of m and n for fixed peak signal power or fixed average signal power are given in Tables I and II, respectively, of [3] for the case in which M is a power of 2. Two distinct cases arise, namely, $m = 1$ and $m > 1$, which we shall consider separately.

Case 1: $m = 1$. Let the polar coordinates of points in the phasor plane be (R, θ) . Then the detection region D_{k1} of signal $s_{k1}(t)$ is defined as the set points whose polar coordinates satisfy the condition

$$\left| \theta - \frac{2(i-1)\pi}{n} \right| < \frac{\pi}{n}$$

For this case, Cahn has shown that

$$p(e) \approx 2 \left[1 - \Phi \left(\sqrt{\frac{2S}{N}} \sin \frac{\pi}{n} \right) \right] \approx \frac{\exp \left[-(S/N) \sin^2 \pi/n \right]}{\sqrt{\frac{\pi S}{N} \sin^2 \pi/n}} \quad (10)$$

where

$$\Phi(x) = \frac{1}{\sqrt{2\pi}} \int_{-\infty}^x \exp \left(-\frac{W^2}{2} \right) dW.$$

For the case $n > 2$, one can, by a slight extension of Cahn's analysis, demonstrate that the second term in (10) is in fact an upper bound for $P(e)$. For practical cases it is even a tight upper bound. In fact, following Cahn, we have

$$P(e) = 1 - \int_{-\pi/n}^{\pi/n} p(\theta) d\theta$$

where

$$p(\theta) = \frac{1}{2\pi} e^{-S/N} \left[1 + \sqrt{4\pi \frac{S}{N}} \cdot \cos \theta e^{(S/N) \cos^2 \theta} \Phi \left(\sqrt{\frac{2S}{N} \cos \theta} \right) \right]$$

Furthermore, for $x > 0$, it is known [7] that

$$1 - \frac{e^{-x^2/2}}{\sqrt{2\pi} x} \leq \Phi(x) \leq 1 - \frac{e^{-x^2/2}}{\sqrt{2\pi}} \left\{ \frac{1}{x} - \frac{1}{x^3} \right\}$$

Combining the above, we conclude that when $n \gg 2$, $P(e) \leq \bar{P}(e) \leq \tilde{P}(e)$ where

$$\bar{P}(e) = 2 \left[1 - \Phi \left(\sqrt{\frac{2S}{N}} \sin \frac{\pi}{n} \right) \right]$$

$$P(e) = \bar{P}(e) - \frac{e^{-S/N} \tan \frac{\pi}{n}}{2\pi S/N}$$

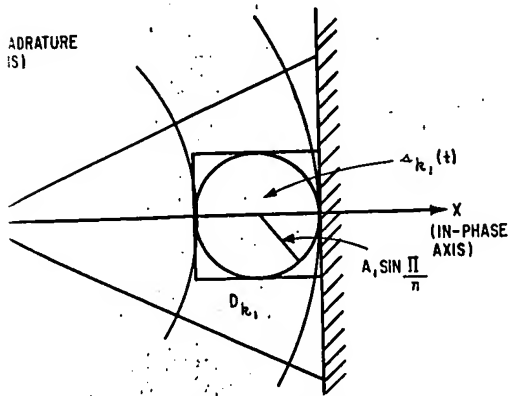
(9). Even for moderate values of S/N , $\bar{P}(e)$ and $P(e)$ are tight. For example, when $S/N = 10$, $\bar{P}(e) - P(e) < (0.012) \bar{P}(e)$.

Case 2: $m > 1$. Here D_{k1} is defined as the region in the phasor plane whose polar coordinates satisfy the condition

$$|R - A_k| < A_1 \sin \frac{\pi}{n}$$

$$\left| \theta - \frac{2\pi(i-1)}{n} \right| < \frac{\pi}{n}$$

A variety of approximations are obtainable here. Consider, for example, the detection region D_{k1} indicated in Fig. 3. By integrating $p_k(u, v)$ over the circle, the square or the shaded half plane in Fig. 3, we obtain, respectively, the distinct approximations to $P(e)$, namely

Fig. 3—The detection region D_{k1} .

$$P\left(-\frac{A_1^2}{2N} \sin^2 \frac{\pi}{n}\right) - \left[2\Phi\left(\frac{A_1 \sin \frac{\pi}{n}}{\sqrt{N}}\right) - 1\right]^2 \frac{2 \exp\left(-\frac{A_1^2}{2N} \sin^2 \frac{\pi}{n}\right)}{\sqrt{\frac{\pi A_1^2}{2N} \sin^2 \frac{\pi}{n}}} - \Phi\left(\frac{A_1 \sin \frac{\pi}{n}}{\sqrt{N}}\right) \approx \frac{1}{4} \tilde{P}(e).$$

Expression $\tilde{P}(e)$ has been given by Cahn in [3]. Results of Cases 1 and 2 can be summarized in the form:

$$P(e) \approx \frac{\exp(-E S/N)}{\sqrt{\pi E S/N}} \quad (m = 1)$$

$$\approx \frac{2 \exp(-E S/N)}{\sqrt{\pi E S/N}} \quad (m > 1)$$

$$E = \frac{A_1^2}{2S} \sin^2 \frac{\pi}{n}.$$

In Tables I and II of [3] the reliability E has been calculated and recorded in Table I.

TABLE I
RELIABILITY OF SYSTEMS OF TYPE I, II AND III

Detection Reliability, E				
Det M	Type I System		Type II System	Type III System
	Minimum Peak Power	Minimum Average Power		
1	0.50	0.50		0.500000
2	0.14645	0.14645	0.148802	0.181818
3	0.07116	0.07116	0.080056	0.100000
4	0.02595	0.02740	0.042776	0.050000
5	0.01407	0.01407	0.022008	0.023810
6	0.00557	0.00595	0.011231	0.012195
7	0.00315	0.00315	0.005712	0.005882

B. The Type II System

The Type II system was investigated by Hancock and Lucky [4]. The signaling alphabet for this system may be represented as follows:

$$s_{ki}(t) = A_k \cos\left(\omega t - \frac{(i-1)2\pi}{n_k}\right),$$

$$0 \leq t \leq T; \quad i = 1, 2, \dots, n_k;$$

$$A_k = A_1 \left[1 + 2(k-1) \sin \frac{\pi}{n_1}\right],$$

$$k = 1, 2, \dots, m; \quad (11)$$

$$n_1 = 3$$

$$n_2 = n_1 + 6$$

$$\dots$$

$$n_{m-1} = n_{m-2} + 6$$

$$n_m = M - \sum_{k=1}^{m-1} n_k.$$

In (11), m , the number of amplitude levels, is the unique positive integer such that

$$M - 9 \leq \sum_{k=1}^{m-1} [3 + 6(k-1)] \leq M - 1,$$

or equivalently,

$$\frac{M-9}{3} \leq (m-1)^2 \leq \frac{M-1}{3}.$$

n_k is the number of phase positions on the k th amplitude level. We have computed n_k according to the prescription of Hancock and Lucky for values of $M = 8, 16, 32, 64, 128$, and 256 . The results are summarized in Table II. We recall that for the Type II system the parameters n_k and m were selected so that the probability of a phase error and the probability of an amplitude error are equal and constant for all amplitude levels and so that a minimum value of average probability of error is attained.

TABLE II
AMPLITUDE LEVELS AND PHASE POSITIONS FOR THE TYPE II SYSTEM

Amplitude Level, k	Number of phase positions, n_k , on the k th amplitude level.					
	$M = 8$	$M = 16$	$M = 32$	$M = 64$	$M = 128$	$M = 256$
1	3	3	3	3	3	3
2	5	9	9	9	9	9
3		15	15	15	15	15
4			21	21	21	21
5				27	27	27
6					33	33
7					20	39
8						45
9						51
10						13

The detection region, D_{ki} , for signal $s_{ki}(t)$ is taken to be the set of all points in the phasor plane whose polar coordinates satisfy the condition

$$|R - A_k| < A_1 \sin \frac{\pi}{n_1}$$

$$\left| \theta - \frac{(i-1)2\pi}{n_k} \right| < \frac{\pi}{n_k}$$

Then, as in Section III-A, we obtain $P(e) \approx \bar{P}(e)$ where

$$\bar{P}(e) = \frac{2 \exp \left(-\frac{A_1^2 \sin^2 \frac{\pi}{n_1}}{2N} \right)}{\sqrt{\frac{\pi A_1^2 \sin^2 \frac{\pi}{n_1}}{2N}}} = \frac{2 \exp(-E S/N)}{\sqrt{\pi E S/N}}$$

From Table II we have computed the appropriate values of the detection reliability E and have recorded them in Table I.

C. The Type III System

The signaling set for the Type III system is given by (1) with

$$C_i = c_i A, \quad S_i = s_i A$$

where A is a fixed positive number while c_i and s_i are appropriately fixed integers. In this paper we consider only the cases $M = 4, 8, 16, 32, 64, 128$ and 256 . The signal points for these cases are illustrated in Fig. 4. In the case $M = 4$ it is understood that each of the four quadrants is the detection region for the signal point contained in it. In all other cases, we stipulate that the detection region for the signal point $(c_i A, s_i A)$ will be the open square, bounded by the lines $x = c_i A \pm A$, $y = s_i A \pm A$ where x and y correspond to abscissa and ordinate, respectively, in the phasor plane. We discuss $P(e)$ in two separate cases, namely, $M = 4$ and $M > 4$.

Case 1: $M = 4$. Let the signal $s_1(t)$ correspond to $C_1 = S_1 = A$ in (1). Then D_1 , the detection region for $s_1(t)$, is the region $x > 0, y > 0$ in the phasor plane.

Therefore,

$$P_1(e) = 1$$

$$- \int_0^\infty \int_0^\infty \frac{1}{2\pi N} \exp \left\{ -\frac{(x-A)^2 + (y-A)^2}{2N} \right\} dx dy.$$

Hence, by symmetry,

$$P(e) = 1 - \left[\Phi \left(\sqrt{\frac{A^2}{N}} \right) \right]^2 \approx \frac{\exp(-(1/2) S/N)}{\sqrt{(\pi/2) S/N}}$$

where $S = A^2$.

Case 2: $M = 8, 16, 32, 64, 128, 256$. In these cases we readily obtain

$$P(e) = 1 - \left[2\Phi \left(\frac{A}{\sqrt{N}} \right) - 1 \right]^2.$$

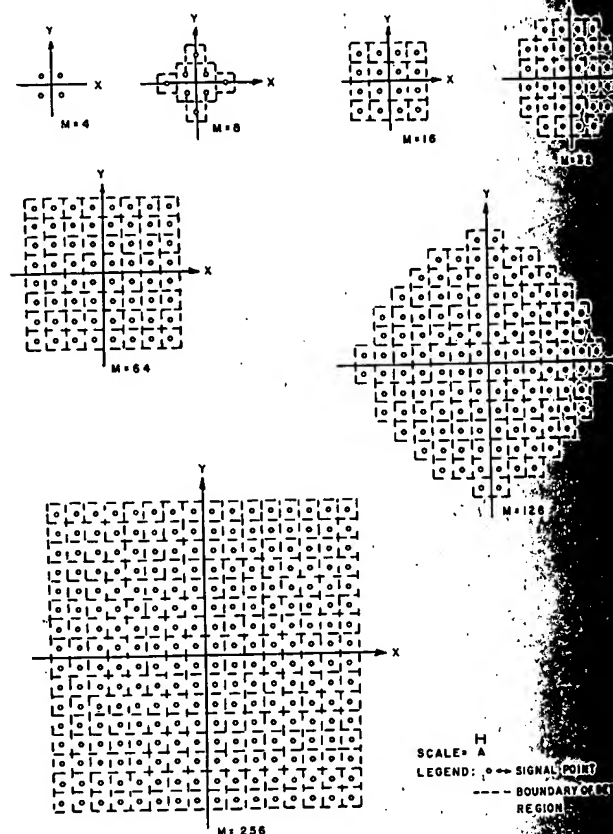


Fig. 4—Signal points and detection regions for the Type III system.

From Fig. 4 we can express $P(e)$ in terms of S/N detection reliability, E , as follows:

$$P(e) = 1 - \left[2\Phi \left(\sqrt{2E \frac{S}{N}} \right) - 1 \right]^2 \approx \frac{2 \exp \left(-\frac{E S}{N} \right)}{\sqrt{\pi E \frac{S}{N}}}$$

Values of the detection reliability are given in Table I.

Note that no serious attempt was made to distribute the signal points in an optimum way to minimize peak power or average power. Slight modifications in the distributions shown in Fig. 4 were attempted, but only to minor changes in detection reliability.

IV. COMPARISON OF TYPE I, II AND III SYSTEMS

A very convenient and common way of comparing modulation and demodulation systems is to compare SNR in decibels which the systems require in order to satisfy a specified probability of error. This comparison is readily accomplished in the present case by giving a table of values of the detection reliability E , in decibels, i.e., $10 \log_{10} E$. Table III contains values of $10 \log_{10} E$ for the three systems discussed. The Type III system enjoys an advantage of from 0 to 3.5 decibels SNR relative to the Type I system. On the other hand, the Type II and Type III systems differ by less than 1 decibel.

TABLE III

DETECTION RELIABILITY (IN DECIBELS) OF AM-PM SYSTEMS

Type I (Minimum Peak Power)	Type I (Minimum Average Power)	Type II	Type III
-3.0	-3.0	—	-3.0
-8.3	-8.3	-8.3	-7.4
-11.5	-11.5	-11.0	-10.0
-15.9	-15.6	-13.7	-13.0
-18.5	-18.5	-16.6	-16.2
-22.5	-22.3	-19.5	-19.1
-25.0	-25.0	-22.4	-22.3
$-1.7 - 10 \log_{10} M$		$1.8 - 10 \log_{10} M$	$1.8 - 10 \log_{10} M$

Although there is little advantage in terms of performance, the Type III system offers a substantial simplification of the terminal equipments relative to the Type I or Type II system. The transmitter Fig. 5 consists in effect of a language converter which translates from a source language to the sequence of (C_i, S_i) coordinates a pair of selector switches which pick off the amplitude and phase carriers appropriate to S_i and C_i . These signals are added, as in a resistive mixer, and applied to a linear power amplifier. The transmitters of Type I or Type II while roughly the same in block diagram, differ significantly from that of Type III in that they require that a large number of phases, carefully controlled, be produced rather than just the two. The receiver (Fig. 6), consists in concept of a pair of balanced modulators, low-pass filters, integrators and quantizers; one referenced to the in-phase carrier produced by the oscillator and yielding u as the output, the other referenced to the quadrature carrier and yielding v . A language converter translates (u, v) back into the source language. In practice, the quantizer remainders, (the difference between the inputs to the quantizers and the nearest quantization levels) would be used for APC and AGC purposes. It will be noted that unlike the Type I or Type II receivers, no phasemeters or arctangent computing circuits are required. Such circuits become extremely critical when the signaling alphabet, becomes large. In contrast,

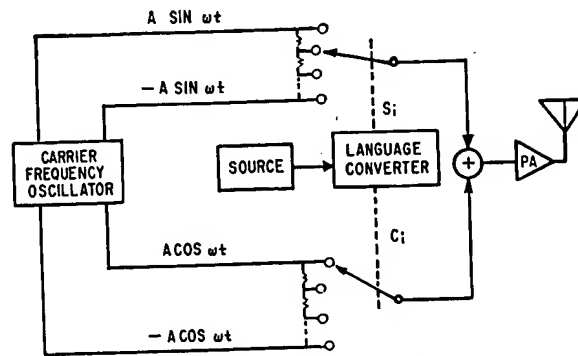


Fig. 5—Type III transmitter.

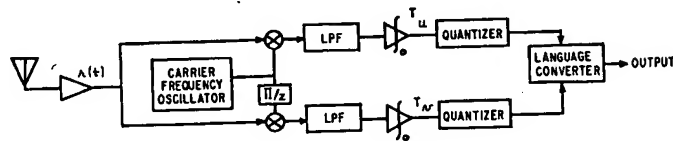


Fig. 6—Type III receiver.

even for $M = 256$, the Type III system requires only two 4-bit quantizers. It is concluded, therefore, that among the phase coherent systems considered, the Type III offers by a small margin the best performance and by a substantial margin the simplest mechanization.

REFERENCES

- [1] C. E. Shannon, "Communication in the presence of noise," *Proc. IRE*, vol. 37, pp. 10-21; January, 1949.
- [2] N. M. Blachman, "A comparison of the informational capacities of amplitude- and phase-modulation communication systems," *Proc. IRE*, vol. 41, pp. 748-759; June, 1953.
- [3] C. R. Cahn, "Combined digital phase and amplitude modulation communication systems," *IRE TRANS. ON COMMUNICATIONS SYSTEMS*, vol. CS-8, pp. 150-155; September, 1960.
- [4] J. C. Hancock and R. W. Lucky, "Performance of combined amplitude and phase-modulated communication systems," *IRE TRANS. ON COMMUNICATION SYSTEMS*, vol. CS-8, pp. 232-237; December, 1960.
- [5] C. R. Cahn, "Performance of digital phase-modulation communication systems," *IRE TRANS. ON COMMUNICATION SYSTEMS*, vol. CS-7, pp. 3-6; May, 1959.
- [6] W. W. Peterson, "Error-Correcting Codes," The M.I.T. Press, Cambridge, Mass. and John Wiley and Sons, Inc., New York, N. Y., pp. 53, 57, 58; 1961.
- [7] W. Feller, "An Introduction to Probability Theory and Its Applications," John Wiley and Sons, Inc., New York, N. Y., vol. I, p. 131; 1950.

An Efficient Power-Reduction Technique on DSL Modems

Henry K. Kwok,* Douglas L. Jones
Electrical and Computer Engineering
University of Illinois at Urbana-Champaign
1308 W. Main St., Urbana, IL 61801
email: henry@ifp.uiuc.edu, dl-jones@uiuc.edu

August 2, 2000

Abstract

Discrete multitone (DMT) has been considered for various wireline, broadband communication systems. However, it is well-known that this modulation scheme exhibits high peak-to-average power ratio (PAR). We introduce a novel approach to reduce the peak power using constellation shaping. We propose a method based on a hyper-spherical boundary, to shape ordinary DMT constellations. This method reduces the peak power by 3-6 dB with no loss of data rate and with virtually identical symbol error rate as conventional systems when no clipping is applied to the signal. When clipping is applied, it provides at least 2 dB of peak-power reduction.

1 Introduction

In a discrete multitone (DMT) system, the output time signal, $x(t)$, is generated by

$$x(t) = \sum_k \operatorname{Re}(X_k) \cdot \cos(2\pi f_k t) + \operatorname{Im}(X_k) \cdot \sin(2\pi f_k t) \quad (1)$$

for $0 \leq k < M$ where the X_k are constellation points from QAM constellations of roughly equal average energy¹ and $f_k = \frac{k}{MT}$. The sampled version of the signal can be efficiently computed by an fast Fourier transform.

However, when all the X_k take on similar values, the constellation points interfere constructively to produce a large time-sample magnitude. In fact, the time-domain peak power grows linearly as the number of frequency bands. Thus, the time samples may occasionally have very high output levels, which leads to the requirement of an expensive, highly linear, and power-inefficient analog front end (AFE) and/or a clipping mechanism to limit the time-sample magnitude, which leads to impulsive noise and performance degradation. High

peak-to-average ratio (PAR) is arguably the greatest drawback of DMT. In order to maintain an acceptable level of system reliability, the output signal is usually clipped at a high PAR which leads to higher power consumption. In fact, the AFE consumes a substantial amount of power for a typical DSL modem. This power consumption requirement may lead to various difficulties in system designs. For example, a USB DSL modem may need an extra power supply when the total power consumption of the modem exceeds the amount that the bus may supply. Also, the telephone company imposes a maximum spatial density of power consumption in the central office (CO). Lower power consumption allows more DSL modems to be more densely in the CO which leads to lower rental cost.

Several authors [1], [2] exploit some unused bandwidth in the DMT system to cancel out the large-amplitude samples generated by the other information-bearing channels. This approach requires frequency spectrum that could otherwise be used for transmission of information. One class of methods clips the transmitted signal intelligently so that the degradation due to the impulsive noise is minimized, or the receiver uses *a priori* knowledge of the clipping mechanism to decode the signal reliably [3], [1]. However, this class of methods degrades the performance of the overall system by introducing artificial noise.

Numerous methods have been proposed to reduce the PAR of another multicarrier modulation scheme - orthogonal frequency division multiplexing (OFDM). Currently, most of the existing schemes approach this problem by modifying the transmitted signal. Various block coding schemes have been used [4], [5], [6]. These schemes lower the overall data rate of the system and essentially trade bandwidth for lower peak amplitude. Others [7], [8] relax the constellation by allowing possibly more than one choice for each constellation point. The signals generated by these methods may occasionally violate the power constraint. Finally, there are methods which adjust the phase of the constellation points in order to avoid phase alignments that lead to large magnitude time samples [9], [10]. In addition, [11] points out that evaluating PAR

*This work is supported by a Tellabs fellowship at the University of Illinois.

¹Without fine power adjustment used in actual DMT systems, the average energies of these QAM constellations are exactly equal.

reduction techniques in the digital domain often leads to optimistic values. At times, over 3 dB of PAR reduction are fictitious. A phase rotation scheme with over 4 dB of PAR reduction in the discrete-time domain was shown (by [11]) to have less than 1 dB of reduction when the performance measurement is done in the continuous-time domain. We refer to this phenomenon as *peak regrowth* because the peak seems to reappear after going from the discrete-time to the continuous-time domain.

Unfortunately, most of these schemes cannot be easily apply to DMT. Most coding schemes require PSK in each tone. Phase rotation do not perform well as the per-tone constellation become large. In addition, many of these schemes assume identical and fixed constellation in each tone. DMT modem designs its constellation during the initialization according to the SNR of the subbands. Most in-band signal-modification schemes cannot be initialized in such short time.

In this paper, we propose a method for peak-power reduction in DMT systems based on constellation shaping based on the shell mapping used in the V.34 modems. It shapes the constellation into a hypersphere in order to reduces the peak, without lowering the data rate or increasing the symbol error rate. It yields up to 6 dB of peak-power reduction. We will show theoretically that the proposed scheme is immune to peak regrowth. For practical channel parameters with clipping, it yields about 2 dB of peak-power reduction.

2 Constellation Shaping

For ordinary DMT systems, we may consider the QAM constellations from all channels jointly as a real-valued $2N$ -D lattice in the frequency domain, and we choose a boundary in the $2N$ -D space such that all lattice points inside the boundary are considered to belong to the constellation. Typically, the boundary is square or rectangular in nature because the input bits can be easily divided into subgroups, each of which indexes one frequency dimension. However, when a constellation-dependent metric needs to be minimized, a rectangular constellation is often suboptimal [12].² Instead, a properly-chosen boundary may lead to better performance in terms of the particular metric without lowering the data rate or increasing the symbol error rate. In the V.34 modem standard, the purpose is to reduce the average power. In our case, the goal is to minimize the peak power, or the ∞ -norm, $\|\mathbf{x}\|_\infty$, in the time-domain. We illustrate this idea with an example.

Example 1 Suppose we use a 2-point inverse DFT to create a two-channel real-valued DMT signal. The modulation

matrix is given by:

$$\mathbf{A}_2 = \begin{pmatrix} \frac{1}{2} & \frac{1}{2} \\ \frac{1}{2} & -\frac{1}{2} \end{pmatrix} \quad (2)$$

A 16-point, square constellation (see Figure 1) is used for the unshaped baseline case. (Note that this is not a QAM constellation, but a 2-D joint real-valued cross-constellation of frequencies 1 and 2.) If $\mathbf{X} = [X_1 \ X_2]$ is a constellation point belonging to the constellation \mathcal{C} , we wish to find the quantity $\min_C \left(\max_{\mathbf{X} \in \mathcal{C}} \|\mathbf{A}_N \mathbf{X}\|_\infty \right) = \min_C \left(\max_{\mathbf{x} \in \mathbf{A}_N(\mathcal{C})} \|\mathbf{x}\|_\infty \right)$. (Note that $\mathbf{A}_N(\mathcal{C}) = \{\mathbf{x} : \mathbf{x} = \mathbf{A}_N \mathbf{X} \text{ for } \forall \mathbf{X} \in \mathcal{C}\}$.) One choice that leads to better performance is shown in Figure 2. In Figures 3 and 4, the corresponding time-domain sample vector, $\mathbf{x} = [x_1 \ x_2]$, for each constellation point is plotted. The dotted lines indicate the equi-metric line for the maximum time-sample magnitude for the unshaped and shaped case. The overall PAR reduction is 1.5 dB. As we will see later, for higher dimensions, the PAR reduction is larger.

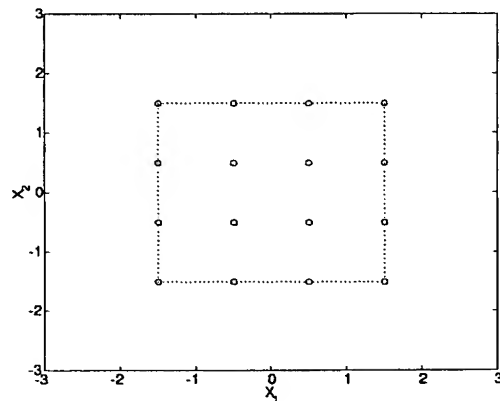


Figure 1: The unshaped, 2-D constellation.

The constellation boundary is usually determined by the metric that we want to optimize. In this paper, we propose a hyper-spherical boundary.

3 Hyper-Spherical Shaping

Spherically-shaped constellations are used in the ITU V.34 modem standard to reduce the average power of the constellation while neither lowering the data rate nor increasing the symbol error rate. For the peak-power reduction problem, a spherical constellation is also desirable because a spherical volume is invariant under rotation and reflection. Therefore, the radius of the spherical boundary is the maximum time-sample magnitude when a unitary transformation is applied to the constellation points. (Otherwise, we must scale by the

²In general, constellation shaping is a precoding technique in which a proper boundary for a multi-dimensional constellation is selected to match a certain metric of interest. See [12] for details.

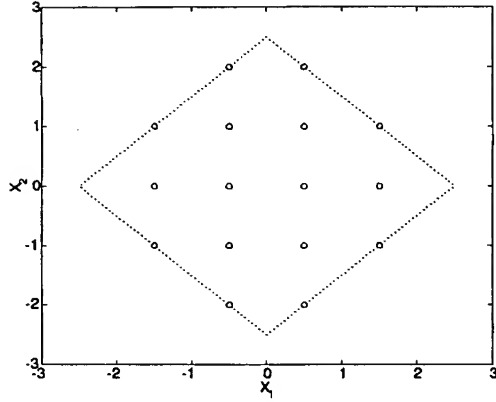


Figure 2: The shaped 2-D constellation in the 2-D real frequency domain..

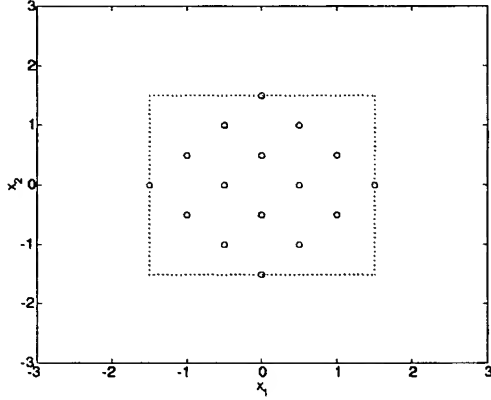


Figure 3: The time samples generated by the unshaped constellation. Note that the worst-case amplitude is 1.5.

matrix norm.) By choosing a spherical boundary, the peak time sample will be no larger than the peak magnitude of the per-channel base constellation. In other words, a hyperspherical constellation is “*amplification free*” under a unitary transformation.

In the time-domain, we may bound the magnitude of the continuous-time signal, $x(t)$, using the Cauchy-Schwartz inequality

$$|x(t)| = \left| \sum_k \text{Re}(X_k) \cdot \cos(2\pi f_k t) + \text{Im}(X_k) \cdot \sin(2\pi f_k t) \right| \quad (3)$$

$$= |\langle \mathbf{X}, \mathbf{d}_t \rangle| \leq \|\mathbf{X}\|_2 \|\mathbf{d}_t\|_2 = \sqrt{N} \|\mathbf{X}\|_2 \quad (4)$$

where $\mathbf{X} = (\dots \text{Re } X_k \dots \text{Im } X_k \dots)$, $\mathbf{d}_t = (\dots \cos(2\pi f_k t) \dots \sin(2\pi f_k t) \dots)$, and N is

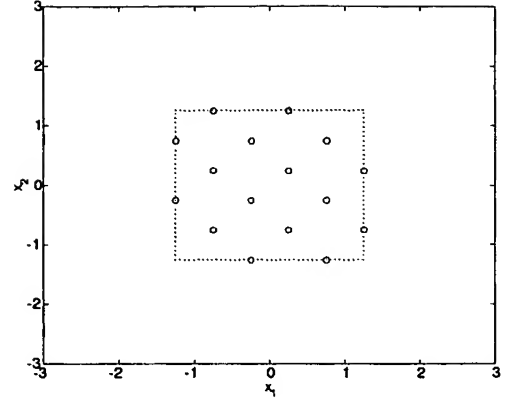


Figure 4: The time samples generated by the shaped constellation. Via shaping, the largest peak amplitude is reduced to 1.25.

the number of transmitting tones. In other words, the maximum magnitude of the complex envelope of the signal is bounded by the l_2 -norm of the constellation point. If we limit this upper-bound to a maximum value of β , we have a constellation with each point, \mathbf{X} , satisfying

$$|x(t)| \leq \sqrt{N} \|\mathbf{X}\|_2 \leq \beta \quad (5)$$

or all constellation points must be inside a $2N$ -D hypersphere of radius $\frac{\beta}{\sqrt{N}}$.

3.1 Asymptotic performance

In order to evaluate the theoretical performance of this scheme, we use the fact that the volume of an N -D hypersphere with a radius of ρ is given by [13]

$$\text{vol}(S_N) = \frac{\pi^{\frac{N}{2}}}{\Gamma(\frac{N}{2} + 1)} \rho^N \quad (6)$$

For simplicity, we ignore the fine power adjustment used to tune the bit error rate of each individual tone to the desired level. We assume that there are N square, QAM constellations each with unit variance. When the constellation size is large, we may apply the continuous approximation [12] and treat each QAM constellation as uniform random variable over a square region with an edge of $\sqrt{6}$. The maximum magnitude of the unshaped constellation is given by ³

$$M_{\text{unshaped}} = \max_t \max_{\mathbf{X}} \left| \sum_k \text{Re}(X_k) \cdot \cos(2\pi f_k t) + \text{Im}(X_k) \cdot \sin(2\pi f_k t) \right| \quad (7)$$

$$= \frac{\sqrt{6}}{2} \max_{\theta} \left| \sum_k \cos(k\theta) + \sin(k\theta) \right| \quad (8)$$

$$\approx \sqrt{3}N \quad (9)$$

³Experimentally, it can be shown that $M_{\text{unshaped}} \approx 1.6N$

Since we require that the data rate of the shaped system remains the same, the identical data-rate requirement is equivalent to requiring both the unshaped hypercube and the shaped hypersphere to have the same volume in the N -D space. Therefore, we compute the radius of a $2N$ -D sphere with the volume of U^{2N} . This yields the equation

$$6^N = \frac{\pi^N}{\Gamma(N+1)} \rho^{2N} \quad (10)$$

or the radius of the shaped constellation is given by

$$\rho = M_{\text{shaped}} = \sqrt{\frac{6}{\pi}} [\Gamma(N+1)]^{\frac{1}{2N}} \quad (11)$$

Thus, the overall peak-power reduction, $G_{\text{sphere}}(N)$, is

$$G_{\text{sphere}}(N) = \frac{M_{\text{unshaped}}}{M_{\text{shaped}}} = \frac{\sqrt{3N}}{\sqrt{\frac{6}{\pi}} [\Gamma(N+1)]^{\frac{1}{2N}} \cdot \sqrt{N}} \quad (12)$$

$$= \sqrt{\frac{\pi N}{2}} \left[\frac{1}{[\Gamma(N+1)]^{\frac{1}{2N}}} \right] \quad (13)$$

$$= \sqrt{\frac{\pi N}{2}} \left[\frac{1}{[(N+1)!]^{\frac{1}{2N}}} \right] \quad (14)$$

As N increases, we approach asymptotically

$$\lim_{N \rightarrow \infty} G_{\text{sphere}}(N) = \lim_{N \rightarrow \infty} \frac{\sqrt{\frac{\pi N}{2}}}{[(N+1)!]^{\frac{1}{2N}}} \quad (15)$$

$$= \lim_{N \rightarrow \infty} \frac{\sqrt{\frac{\pi N}{2}}}{\left[\sqrt{2\pi(N+1)} \left(\frac{N+1}{e}\right)^{(N+1)} \right]^{\frac{1}{2N}}} \quad (16)$$

$$= \lim_{N \rightarrow \infty} \sqrt{\frac{\pi e N}{2(N+1)}} = \sqrt{\frac{\pi e}{2}} \quad (17)$$

Therefore, the peak-power reduction approaches asymptotically to $\sqrt{\frac{\pi e}{2}}$, or 6.304 dB.⁴

4 Results

The peak-power reduction of the hyper-spherical shaping under various numbers of channels and constellation sizes (identical constellation for each tone) are shown in Figure 5. We can see that, for large constellations, it approaches the theoretical limit, $G_{\text{sphere}}(N)$, rather rapidly. The peak-power reduction for typical constellation sizes and numbers of channels is about 3 to 6 dB.

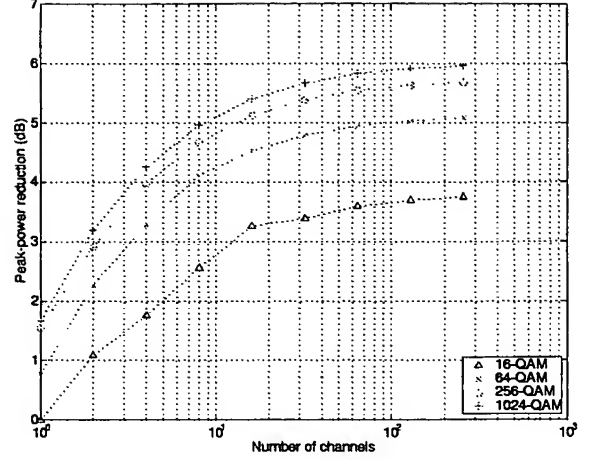


Figure 5: The peak-power reduction vs. the number of channels for several different constellation sizes.

Next, we use two channels that one may encounter in an actual ADSL. Figure 6 shows the bit allocation for the 31-channel and 215-channel cases. The amount of peak-power reduction is 4.794 dB for the 31-channel case and 5.224 dB for the 215-channel case.

In practice, we can tolerate a small amount of clipping as long as it does not increase BER significantly and the signal is compliant with the PSD mask. The ANSI ADSL standard recommends a clipping rate lower than 10^{-7} . To prevent frequent CRC frame errors, a value as small as 10^{-10} is used. This requirement allows the AFE to clip the signal at least 5.2 times of the rms value of the signal. Thus, with clipping, the PAR of a DMT system is upper bounded at 14.3 dB. With an upper limit of 6 dB of peak reduction, any systems with an unshaped PAR of over 20 dB may achieve lower PAR by clipping instead of shaping. However, we may clip the shaped system. When we apply clipping to the shaped constellation, the amount of peak-power reduction decreases. Figure 7 shows the clipping probability curve. From the curve, we see that the amount of peak-power reduction at a clipping rate of 10^{-8} is about 2.1 dB for the 31-tone case and 2.0 dB for the 215-tone case. As the clipping rate decreases asymptotically to 0, the amount of peak-power reduction approaches those without clipping (4.79 and 5.22 dB).

5 Conclusion

We have introduced the constellation shaping approach in the peak-power reduction problem for DMT systems and design a spherically shaped constellation. As the size of the constellation for each channel becomes large, the peak-power reduction achievable by these constellations is about 3-6 dB

⁴If the experimental value for M_{unshaped} is used instead, the asymptotical gain is 5.67 dB.

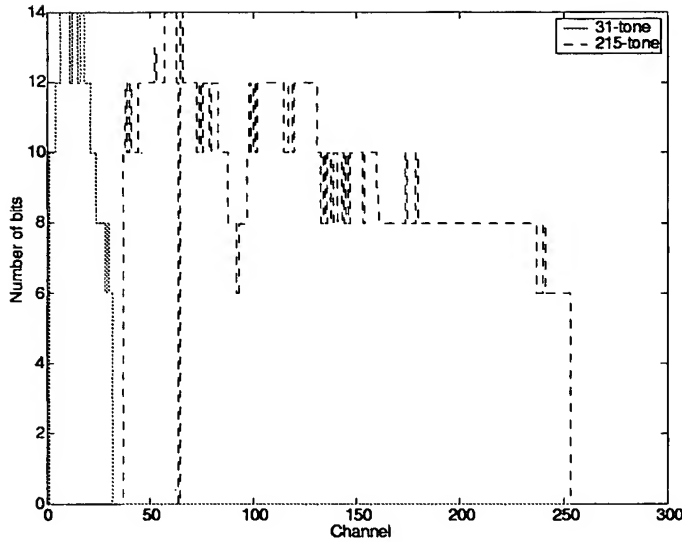


Figure 6: The bit allocation schemes used by the two simulated channels.

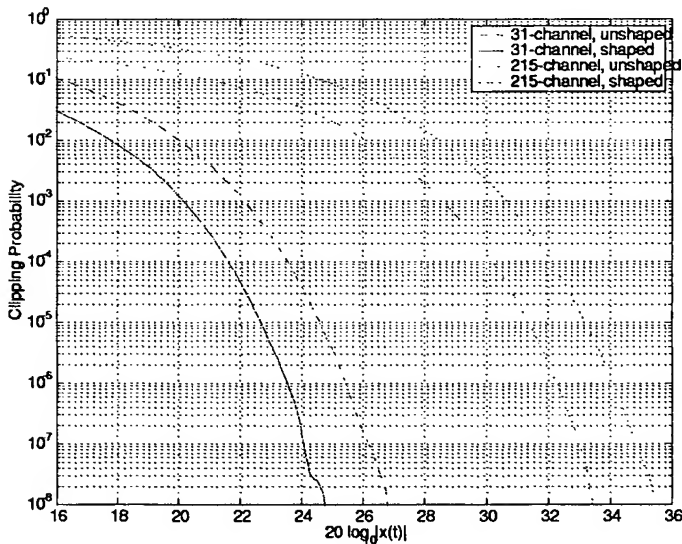


Figure 7: The clipping probability curves for the two channels. The maximum peak-power reduction for the 31-tone and 215-tone cases are 4.79 dB and 5.22 dB respectively.

without clipping. However, with clipping, the gain is reduced to about 2 dB. The hyper-spherical is one example of shaped constellations and are by no means optimal for the peak-power reduction. Recent discovery has shown that other choices of boundary may lead to even more reduction of peak power at the expense of higher computational complexity. [14], [15]

There are certain drawbacks of the shaping-based peak-power reduction methods proposed here. First, they require relatively large constellation size (and thus high data rate) to obtain significant reduction, which may limit their application to shorter loops in the DSL application. However, most DSL systems are designed with high data rate in mind. Moreover, we may use a shaped constellation with more points than required and apply coding to both reduce the data rate and increase the reliability of the system simultaneously. A second concern may be that the channels of the shaped constellation become correlated. We can apply coding on top of the shaped constellation to partially remedy this problem, as convolutional codes are applied on top of the 16-D shaped constellation in V.34 modems. Coding for DMT systems remains a topic for future research.

References

- [1] A. Gatherer and M. Polley, "Controlling clipping probability in DMT transmission," in *Proceedings of the 31st Asilomar Conference on Signals, Systems, and Computers*, pp. 578–584, 1997.
- [2] J. Tellado and J. Cioffi, "Peak power reduction for multicarrier transmission," in *Proceedings of International Symposium on Information Theory*, August 1998.
- [3] D. J. G. Mestdagh and P. M. P. Spruyt, "A method to reduce the probability of clipping in dmt-based transceiver," vol. 44, pp. 1234–1238, October 1996.
- [4] R. van Nee and A. de Wild, "Reducing the peak-to-average power ratio of OFDM," in *Proceedings of IEEE Vehicular Technology Conference*, vol. 3, pp. 2072–2076, 1998.
- [5] J. A. Davis and J. Jedwab, "Peak-to-mean power control in OFDM, Golay complementary sequences, and Reed-Muller codes," *IEEE Transactions on Information Theory*, vol. 45, pp. 2397–2417, November 1999.
- [6] K. Patterson, "Generalized Reed-Muller codes and power control in OFDM modulation," vol. 46, pp. 104–120, January 2000.
- [7] D. L. Jones, "Peak power reduction in OFDM and DMT via active channel modification," in *Proceedings of Asilomar Conference*, 1999.

- [8] J. Tellado and J. Cioffi, "Peak power reduction for multicarrier transmission," in *Proceedings CTMC, Globecom 1998*, November 1998.
- [9] S. Muller and J. Huber, "OFDM with reduced peak-to-average power ratio by optimum combination of partial transmit sequences," *Electronics Letters*, vol. 33, pp. 368–369, February 1997.
- [10] M. Friese, "Multicarrier modulation with low peak-to-average power ratio," *Electronics Letters*, vol. 32, pp. 713–714, April 1996.
- [11] C. Tellambura, "Coding technique for reducing peak-to-average power ratio in OFDM," in *Proceedings of IEEE Global Telecommunications Conference*, vol. 5, pp. 2783–2787.
- [12] G. D. Forney and L. Wei, "Multidimensional constellations - Part I: Introduction, figures of merit, and generalized cross constellation," *IEEE Journal on Selected Areas in Communications*, vol. 7, pp. 877–892, August 1989.
- [13] J. H. Conway and N. J. A. Sloane, *Sphere Packings, Lattices and Groups*. Springer, 3rd ed., 1999.
- [14] H. Kwok and D. Jones, "PAR reduction for hadamard transform-based ofdm," in *Proceedings of Computer and Information System Symposium*, 2000.
- [15] H. Kwok and D. Jones, "PAR reduction via constellation shaping," in *Proceedings of International Symposium of Information Theory*, 2000.

PAR Reduction via Constellation Shaping

Henry K. Kwok, Douglas L. Jones
Coordinated Science Laboratory
University of Illinois at Urbana-Champaign
1308 W. Main St.,
Urbana, IL 61801.

September 13, 1999

Abstract

In this paper, we introduce a novel scheme using a constellation shaping approach to reduce the peak-to-average ratio (PAR) in orthogonal frequency-division multiplexing (OFDM) systems. In time domain, the peak power bound traces out a hypercube boundary. We map this square time-domain boundary back to the frequency domain via the inverse DFT and construct a method for indexing the OFDM constellation points. The encoding and decoding of the constellation use generators and relations from group theory. The end result is a coding scheme with nearly 20 dB of PAR reduction with no reduction in data rate or performance.

1 Introduction

In an orthogonal frequency division multiplex (OFDM) system, the output time samples are generated by the inverse FFT of the constellation points. For the baseband case,

$$x_n = \sum_{k=0}^{N-1} Y_k \cdot e^{-j\frac{2\pi}{N}nk} \quad (1)$$

for $n = 0, 1, \dots, N$ and $k = 0, 1, \dots, N-1$. OFDM systems can operate either in baseband (as in the ADSL standard) or in passband; we examine only the baseband case here, although the method applies to both variations. We restrict $x = [x_0 \ \dots \ x_{N-1}]$ to be real. This allows us to define $\mathbf{X} = \begin{bmatrix} \text{Re} Y_0 & \dots & \text{Re} Y_{\frac{N}{2}} & \text{Im} Y_1 & \dots & \text{Im} Y_{\frac{N}{2}-1} \end{bmatrix}$ and \mathbf{A}_N as columns of $\sin(2\pi\frac{nk}{N})$ and $\cos(2\pi\frac{nk}{N})$, and we have:

$$\mathbf{x} = \mathbf{A}_N \mathbf{X} \quad (2)$$

In an ordinary OFDM system, $\{Y_k\}_{k=0}^{N-1}$ is a set of i.i.d. discrete random variables uniformly distributed

over a QAM constellation, \mathcal{C}_2 . By the central limit theorem, as N becomes large the set of time samples, $\{x_n\}_{n=0}^{N-1}$ becomes a set of i.i.d. Gaussian random variables with variance increasing linearly with N . Thus, the time samples may occasionally have very high output levels, which leads to the requirement of an expensive, highly linear, and power-inefficient analog front end (AFE) and/or a clipping mechanism to limit the time sample magnitude, which leads to impulsive noise and performance degradation [1]. High PAR is arguably the greatest drawback of OFDM.

Numerous methods have been proposed to reduce the PAR of OFDM. Currently, most of the existing schemes approach this problem by modifying the transmitted signal. One class of methods clips the transmitted signal intelligently so that the degradation due to the impulsive noise is minimized, or the receiver can use *a priori* knowledge of the clipping mechanism to decode the signal reliably [2], [3]. However, this class of methods degrades the performance of the overall system by introducing artificial noise into the system. Various block coding schemes have been used [4], [5], [6]. These schemes lower the overall data rate of the system and essentially trades bandwidth for lower peak amplitude. Another class of methods [7] tries to utilize some unused bandwidth in the OFDM system to cancel out the large-amplitude samples generated by the other information-bearing channels. This method requires frequency spectrum that could otherwise be used for transmission of information. Finally, there are methods which adjust the phase of the constellation points in order to avoid phase alignment that leads to large magnitude time samples [8].

In this paper, we propose a method for peak amplitude reduction in OFDM systems based on constellation shaping. The peak amplitude of the time samples are measured by the ∞ -norm in the time domain. We map this hypercube boundary back to

the frequency domain. The hypercube boundary becomes an N -D parallelogram. To encode and decode the constellation points inside this new boundary, we use group theory to compute the generators for indexing these points. This method can provide nearly 20 dB of PAR reduction in practical situations while maintaining equivalent data rate and performance. In addition, it can be combined with other existing methods to further increase the PAR reduction.

2 Constellation Shaping

For ordinary OFDM systems, we have an N -D lattice in the frequency domain, and we choose a boundary in the N -D space such that all lattice points inside the boundary are considered to belong to the constellation. Typically, the boundary is square or rectangular in nature because the input bits can be easily divided into subgroups each of which indexes one frequency dimension. However, when a constellation-dependent metric needs to be minimized, a rectangular constellation may not be the best choice [9], [10].¹ Instead, a properly-chosen boundary may lead to better performance in terms of the particular metric without lowering the data rate or increasing the symbol error rate. We illustrate this idea with an example. In our case, the goal is to minimize the peak power, or the ∞ -norm, $\|\mathbf{x}\|_\infty$, in the time-domain.

Example 1 Suppose we use a 2-point inverse DFT to create a two-channel real-valued OFDM signal. The modulation matrix is given by:

$$\mathbf{A}_2 = \begin{pmatrix} \frac{1}{2} & \frac{1}{2} \\ \frac{1}{2} & -\frac{1}{2} \end{pmatrix} \quad (3)$$

A 16-point, square constellation (see Figure 1) is used for the unshaped baseline case. (Note that this is not a QAM constellation, but a 2-D joint cross-constellation of frequency 1 and 2.) If $\mathbf{X} = [X_1 \ X_2]$ is a constellation point belonging to the constellation \mathcal{C} , we wish to find the quantity $\min_C \left(\max_{\mathbf{x} \in \mathcal{C}} \|\mathbf{A}_N \mathbf{X}\|_\infty \right) = \min_C \left(\max_{\mathbf{x} \in \mathbf{A}_N(C)} \|\mathbf{x}\|_\infty \right)$. (Note that $\mathbf{A}_N(C) = \{\mathbf{x} : \mathbf{x} = \mathbf{A}_N \mathbf{X} \text{ for } \forall \mathbf{X} \in \mathcal{C}\}$.) One choice that leads to better performance is shown in figure 2. In figure 3 and 4, the corresponding time-domain sample vector, $\mathbf{x} = [x_1 \ x_2]$, for each constellation point is plotted. The dotted lines indicate the equi-metric line for the maximum time-sample

¹In general, constellation shaping is a precoding technique in which a proper boundary for a multi-dimensional constellation is selected to match a certain metric of interest. See [9], [10] for details.

magnitude for the unshaped and shaped case. The overall PAR reduction is 1.5 dB. As we will see later, for higher dimensions, the PAR reduction is much larger.

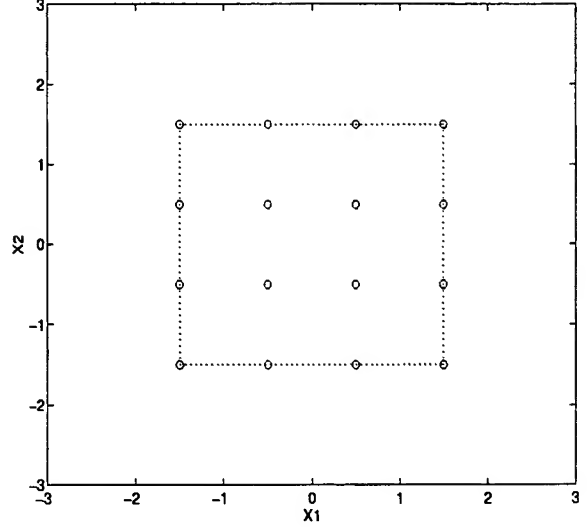


Figure 1: The unshaped, square, 2-D 16-point constellation. (4-PAM for each dimension.)

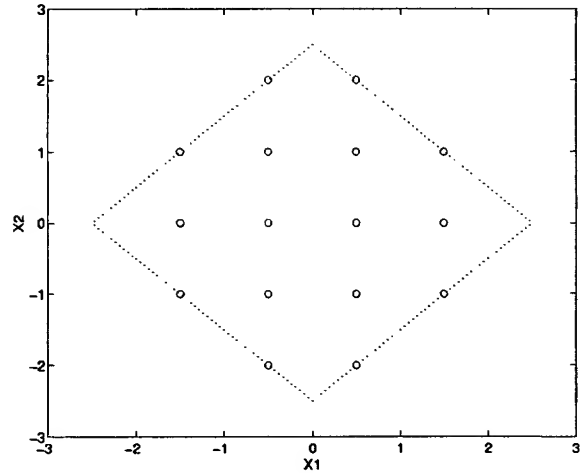


Figure 2: The shaped 2-D 16-point constellation.

The constellation boundary is usually determined by the metric that we want to optimize. In the problem of PAR reduction in OFDM systems, we use the ∞ -norm, $\|\cdot\|_\infty$, in the time domain. This metric traces out a square boundary, defined by $\|\mathbf{x}\|_\infty = \beta$, in the time domain. In the frequency domain, we get:

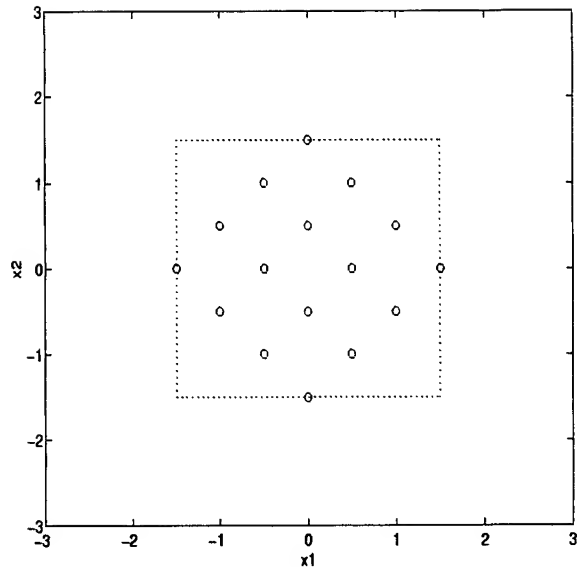


Figure 3: The time samples generated by the unshaped constellation. Note that the worst-case amplitude is 1.5.

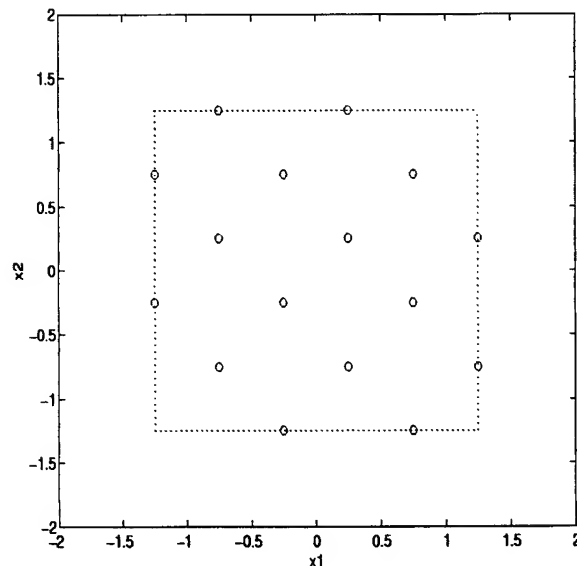


Figure 4: The time samples generated by the shaped constellation. Via shaping, the largest peak amplitude is reduced to 1.25.

$\|x\|_\infty = \|A_N X\|_\infty = \beta$. This is an N -D parallelogram in the frequency domain defined by A_N^{-1} .

3 Group Construction of the Shaped Constellation

In the previous section, we observed that for the realified, inverse DFT transformation, A_N , there exists a constellation that matches the transformation in such a way that $\max_{X \in C} \|A_N X\|_\infty$ is minimized. In this section, we introduce a systematic way to obtain these constellation points. This algorithm uses relations and generators on a free abelian group to construct a quotient group which turns out to be the constellation points we need (aside from a translation.)

First, we recall some definitions [11].

Definition 1 An abelian group F is **free abelian** if there exists a subset $X \subset F$ of elements of infinite order, called a **basis** of F , such that $F = \sum_{x \in X} \langle x \rangle$ where $\langle \delta_i \rangle$ is a cyclic group with the generator of δ_i . In other words, F is isomorphic to \mathbb{Z}^N .

Definition 2 An abelian group G has generators X and relations Δ if $G \cong F/R$, where F is the free abelian group with basis $X = \{u_1, u_2, \dots, u_N\}$, $\Delta = \{\delta_1, \delta_2, \dots, \delta_M\}$ is a set of \mathbb{Z} -linear combinations of elements of X , and R is the subgroup of F generated by Δ , or

$$R = \langle \delta_1 \rangle \oplus \langle \delta_2 \rangle \oplus \dots \oplus \langle \delta_M \rangle \quad (4)$$

where \oplus is the direct sum of two subgroups.

In our construction, given an N -D linear transformation A_N , we take F to be the integer lattice, \mathbb{Z}^N . Obviously, F is free abelian and the basis are $X = \{e_1, e_2, \dots, e_N\}$ where e_i has zero elements except for the i^{th} element which has a value of 1. These vectors are the natural basis for an N -D vector space.

Theorem 1 (Rotman, Corollary 11.2) Every group G is a quotient group of a free group.

Next, we use the relations to specify the boundary of the group. A relation, δ , is a \mathbb{Z} -linear combination of elements of X that is equal to the identity element; in other words, $\delta \in F$ and $\delta = 0$. The set of relations for a specific A_N^{-1} define the edges of the parallelogram. An N -D parallelogram is determined by N distinct edges. Recall that A_N^{-1} maps the optimal time-domain boundary to the optimal frequency-domain boundary. In the time domain, each corner

of the hypercube boundary may be represented by an N -D binary vector, \mathbf{c} . In the frequency domain, the corners become $\mathbf{A}_N^{-1}\mathbf{c}$. All 2^N corners can derive from any N corners. Thus, we may use $\mathbf{c} = \{\mathbf{e}_1, \mathbf{e}_2, \dots, \mathbf{e}_N\}$. Then, each column of \mathbf{A}_N^{-1} defines a edge of the optimal N -D parallelogram boundary and a relation in the quotient group F/R . If the columns of \mathbf{A}_N^{-1} have non-integer elements, we simply round them to the nearest integers.

It may be possible that the rounded version of \mathbf{A}_N^{-1} , denoted as $\lfloor \mathbf{A}_N^{-1} \rfloor$, may not have enough constellation points in it. To solve this, we simply scale \mathbf{A}_N^{-1} by a factor α and round it again to get $\tilde{\mathbf{A}} = \lfloor \alpha \cdot \mathbf{A}_N^{-1} \rfloor$. We choose the smallest α such that $|\det(\lfloor \alpha \cdot \mathbf{A}_N^{-1} \rfloor)|$ is greater than or equal to the number of constellation points. Note that each column of $\tilde{\mathbf{A}}$ specifies a relation in F since each corner of the parallelogram belongs to the same equivalent class, specifically, the equivalent class $[0]$. For this reason, we now refer to $\tilde{\mathbf{A}}$ as the relation matrix.

Example 2 We use the previous example. First,

$$\mathbf{A}_2^{-1} = \begin{pmatrix} \frac{1}{2} & \frac{1}{2} \\ \frac{1}{2} & -\frac{1}{2} \end{pmatrix}^{-1} = \begin{pmatrix} 1 & 1 \\ 1 & -1 \end{pmatrix} \quad (5)$$

Since $|\det(\mathbf{A}_2^{-1})| = 2 < 16$, we need to choose a bigger α . For $\alpha = 3$, $|\det(\lfloor \alpha \cdot \mathbf{A}_2^{-1} \rfloor)| = 18$. In Figure 5, we draw out the free group F , the subgroup R generated by Δ , and the quotient group (or the shaped constellation.) Note that we did not use two points in the previous example because we needed only 16 constellation points.

We now have the quotient group F/R , where R is the group generated by Δ . However, the order of this group, in general, is very large - making tabulation impossible. Instead, we should study the relation matrix $\tilde{\mathbf{A}}$ via row and column operations [12]. This procedure is very well-known and well understood in the area of abstract algebra.

Theorem 2 (Armstrong, Ch. 21-22) Any relation matrix $\tilde{\mathbf{A}}$ can be decomposed into $\tilde{\mathbf{A}} = \mathbf{UDV}$, where \mathbf{D} is diagonal with entries $\{\sigma_i\}_{i=1}^N$, where the columns of \mathbf{U} are the generators, and \mathbf{V} is the transformation between the coordinates in terms of \mathbf{X} and the canonical coordinates.²

3.1 Encoding Process

We now have a set of generators $\{\mathbf{u}_1, \mathbf{u}_2, \dots, \mathbf{u}_N\}$ and their corresponding orders $\{\sigma_1, \sigma_2, \dots, \sigma_N\}$. The encoding process involves mapping an integer I between

²For a more comprehensive treatment, please refer to [12].

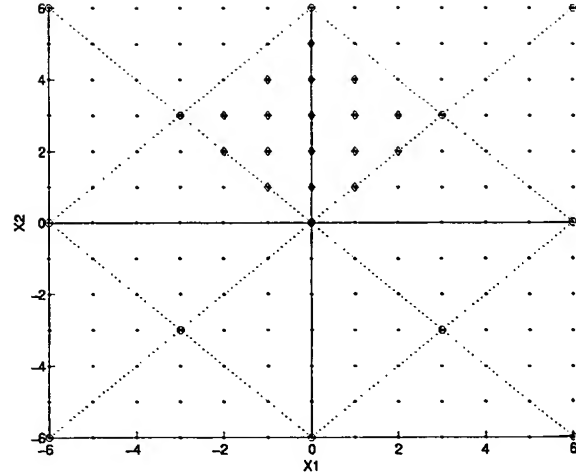


Figure 5: The free group F is the lattice depicted by the set of dots. The group R generated by the relations is the set of circles. The quotient group F/R is the set of diamonds. Note the dotted lines illustrate the cosets of F/R .

0 and $|\mathcal{C}| - 1$ to an N -D integer vector. This vector corresponds to the N -channel OFDM constellation point. First, we turn the input integer into a canonical coordinate $\Lambda = (\lambda_1, \lambda_2, \dots, \lambda_N)$ by iteratively computing

$$\begin{aligned} \lambda_i &= I \bmod \sigma_i \\ I &= \frac{I - \lambda_i}{\sigma_i} \end{aligned} \quad (6)$$

for $i = 1, 2, \dots, N$. Next, simply use the generators to compute the final constellation point:³

$$\mathbf{X} = [\lambda_1 \mathbf{u}_1] + [\lambda_2 \mathbf{u}_2] + \dots + [\lambda_N \mathbf{u}_N] \quad (7)$$

The peak-limited transmitted signal is then $\mathbf{x} = \text{DFT}^{-1}(\mathbf{X})$, exactly as in conventional OFDM.

3.2 Decoding Process

Decoding a received OFDM constellation vector \mathbf{X} is even simpler. First, compute \mathbf{X} from the received time sample vector \mathbf{x} . In the presence of noise, we simply round each elements of \mathbf{X} to the nearest integer. Then, form

$$\Lambda = \mathbf{X}^T \mathbf{V} = [\lambda_1 \quad \lambda_2 \quad \dots \quad \lambda_N] \quad (8)$$

³Note that the addition is done in the quotient group F/R . Therefore, we are actually adding equivalent classes. Following abstract algebra convention, the addition of two equivalent classes, $[a]$ and $[b]$ is defined as: $[a] + [b] = [a + b]$. See [13] for details.

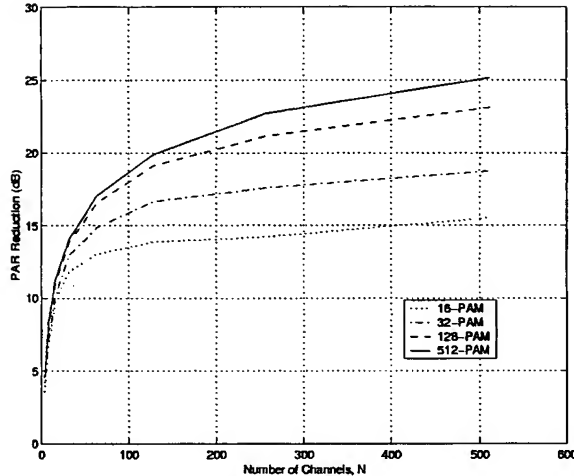


Figure 6: The PAR reduction versus the number of channels and constellation size.

Next, for $i = 1, 2, \dots, N$, compute

$$\tilde{\lambda}_i = \lambda_i \bmod \sigma_i \quad (9)$$

Finally, the original input is recovered by

$$\tilde{I} = \tilde{\lambda}_1 + \sigma_1 \left(\tilde{\lambda}_2 + \sigma_2 \left(\dots \left(\sigma_{N-1} \cdot \tilde{\lambda}_N \right) \dots \right) \right) \quad (10)$$

Due to limited space, we state without proof the following theorem.

Theorem 3 *The encoding and decoding processes can each be done in $O(N^2)$.*

To conclude this section, we present some results using this algorithm. Note that mean power of the shaped constellation is slightly larger (typically about 5%.) However, PAR reduction via increasing the average power seems to obfuscate the performance measurement; thus, we approximate the average power of the two constellations to be the same. Figure 6 shows the total amount of peak-power reduction using this constellation shaping with various numbers of channels and constellation sizes. We see that reduction of over 25 dB is possible when the constellation size is large. Even with a typical constellation size, a PAR reduction of over 15 dB is easily realized.

4 Conclusion

We have demonstrated the effectiveness of the constellation shaping approach in the PAR reduction problem for OFDM systems. As the size of the PAM constellation for each channel becomes large,

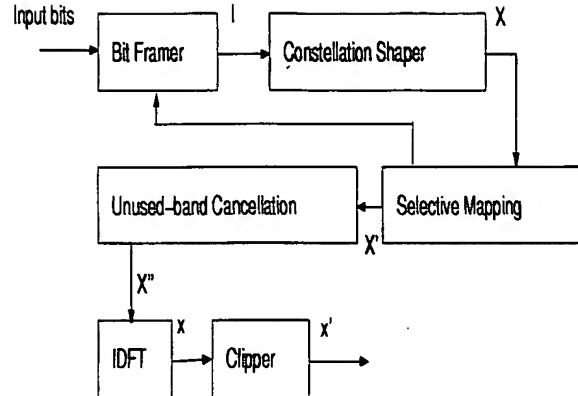


Figure 7: An OFDM modulator with various PAR reduction techniques combined.

the peak-power factor reduction is of the order of $O(N)$, where N is the number of channels. Thus, it asymptotically provides an unlimited amount of PAR reduction as the number of channels and the constellation size increase arbitrarily.

In addition, this approach can provide large PAR reduction without lowering the data rate or increasing symbol error rate. All clipping schemes introduce some artificial noise into the system; thus, they indirectly increase the signal-to-noise ratio. All coding schemes lower the overall data rate. Even the selective mapping scheme robs some of the transmission bandwidth for sending information regarding the selected phase rotation. In order for the performance to increase, the data rate must be sacrificed in these systems. The constellation shaping approach preserves the data rate and minimum distance between neighboring constellation points and yet provides a large PAR reduction. Another advantage of the shaping method is that it is complementary to existing methods. It is possible to combine this method with others to further reduce the PAR of the constellation. Figure 7 depicts one possible configuration where we use the methods of [8], [7], [3] to further reduce the PAR.

References

- [1] J. S. Chow, J. A. C. Bingham, and M. S. Flowers, "Mitigating Clipping Noise in Multicarrier System", *IEEE International Conference on Communication*, 1997.

- [2] D. J. G. Mestdagh, P. M. P. Spruyt, "A Method to Reduce the Probability of Clipping in DMT-Based Transceiver", *IEEE Trans. on Communications*, vol. 44, no. 10, Oct 1996, pp. 1234-1238.
- [3] M. Polley, and A. Gatherer, "Controlling Clipping Probability in DMT Transmission", *Proceeding of the Asilomar Conference on Signals, Systems & Computers*, v.1, pp. 578-584, 1998.
- [4] A. E. Jones, T. A. Wilkinson, S. K. Barton, "Block coding scheme for reduction of peak to mean envelope power ratio of multicarrier transmission schemes," *Electronics Letters*, December 1994, vol. 30, no. 25, pp. 2098-2099.
- [5] R. van Nee, "OFDM Codes for Peak-to-Mean Power Control and Error Correction," *Proceedings of the 1996 Global Communication Conference*, pp. 740-744, 1996.
- [6] T. A. Wilkinson, and A. E. Jones, "Minimisation of the Peak to Mean Envelope Power Ratio of Multicarrier Transmission Schemes by Block Coding," *Proceedings of the 45th Vehicular Technology Conference*, pp. 825-829, 1995.
- [7] J. Tellado, and J. M. Cioffi, "Efficient Algorithms for Reducing PAR in Multicarrier Systems", *Proceeding of ISIT*, 1998.
- [8] S. H. Müller, and J. B. Huber, "A Comparison of Peak Power Reduction Schemes for OFDM," *Proceedings of the 1997 Global Communication Conference*, pp. 1-5, 1997.
- [9] G. D. Forney, and L. Wei, "Multidimensional Constellations - Part I: Introduction, Figures of Merit, and Generalized Cross Constellations," *IEEE Journal on Selected Areas in Communications*, vol. 7, no. 6, August 1989, pp. 877-892.
- [10] G. D. Forney, and L. Wei, "Multidimensional Constellations - Part II: Voronoi Constellations," *IEEE Journal on Selected Areas in Communications*, vol. 7, no. 6, August 1989, pp. 941-958.
- [11] Rotman, J. J., "An Introduction to the Theory of Groups," 4th ed., Springer-Verlag, New York, 1995, pp. 312-317.
- [12] Armstrong, M. A., "Groups and Symmetry," Springer-Verlag, New York, chap. 21-22.
- [13] Herstein, I. N., "Abstract Algebra," 3rd ed., Prentice Hall, New Jersey, 1996, pp. 77-82.

High-Order Optimum Hexagonal Constellations

Charles D. Murphy

Laboratory of Signal Processing
Helsinki University of Technology
P.O. Box 3000
FIN-02015 HUT
FINLAND
cmurphy@wooster.hut.fi

ABSTRACT

Bandwidth-limited high-rate digital communications systems use large constellations such as M -ary QAM, $M \in \{64, 128, 256, 512, 1024\}$. These square or cross-shaped constellations, though easy to implement, do not pack the symbols together as efficiently as possible, and besides are symmetric when the symbols are equiprobable and independent, so that no channel information is available from blind third-order statistics of the channel outputs. We develop high-order "optimum" [1] hexagonal constellations, some of which are naturally asymmetric, and all of which can be modified to be asymmetric without exceeding the peak and average power levels of the corresponding M -ary QAM constellations.

INTRODUCTION

When bandwidth is limited and data rates are high, digital communications systems employ large constellations of closely-packed symbols. M -ary QAM constellations with $M = 64, 128, 256, 512$, and 1024 satisfy the requirement of sending 6, 7, 8, 9, or 10 bits per symbol, assuming that the transmitted symbols are equiprobable and independent. M -ary QAM constellations are simple to construct using a pair of identical in-phase and quadrature modulators, and the symbol decision map is readily defined by a small set of comparators. On the other hand, QAM-type constellations are known to be suboptimum in terms of symbol separation for a given average transmitted symbol power [2], and they are symmetric.

A constellation is *symmetric* if one or more complex rotations by $\theta_r \in (0, 2\pi)$ result in a constellation with identical symbol values and probabilities. Assuming equiprobable i.i.d. generation of symbols from a QAM constellation, there are three such rotation angles. When the receiver is blind, it is not possible to generate an absolute phase reference, necessitating differential encoding for proper recovery of the data. Also, the third-order statistics of symmetric constellations contain no information about the channel. When there is inter-symbol interference (ISI) that is potentially mixed-phase in nature, statistics of at least fourth order are necessary to guarantee optimum channel identification or equalizer tap settings [3].

An *asymmetric* constellation allows a blind absolute phase estimate at the receiver and enables blind equalization of mixed-phase channels using third-order statistics. Third-

order statistical estimates may converge more quickly than their fourth-order kin, and lower-order blind equalization algorithms can be much simpler than higher-order algorithms.

Here we investigate high-order constellations whose symbols are on hexagonal lattices. These constellations have been proposed in the past as "minimum error" alphabets, having an asymptotic advantage over QAM-type constellations of 0.8 dB in the average power needed to assure a particular symbol separation [1], [2], [4]. From our perspective, these constellations are interesting as alternatives that are either naturally asymmetric or that have some leeway - i.e. 0.8 dB - for introduction of a controlled amount of asymmetry. We find the "optimum" M -ary hexagonal constellations for $M = 128, 256, 512$, and 1024 and comment on methods for enhancing their level of asymmetry.

SYSTEM MODEL

The transmitted symbol sequence $\{x[n]\}$ consists of i.i.d. symbols from the constellation \mathcal{S} . The receiver knows the values of the symbols and their probabilities. There are no pilot tones or pilot symbols, so the receiver must process the channel output sequence $\{y[n]\}$ using only the knowledge of the constellation statistics.

$$y[n] = \sum_{k=k_1}^{k_2} h_k x[n-k] + w[n] \quad (1)$$

The channel output in (1) contains both linear ISI - represented by the channel coefficients $h_{k_1}, \dots, h_{-1}, h_{+1}, \dots, h_{k_2}$ - and additive noise. The noise sequence $\{w[n]\}$ is often treated as being white and Gaussian. Even when it is not Gaussian, it may be symmetric, so that third-order statistics of the noise may fall out of the equalization equations.

The receiver produces an estimate $\hat{x}[n]$ of the symbol $x[n]$. The final decision as to the transmitted symbol is that $x \in \mathcal{S}$ nearest to $\hat{x}[n]$. If the channel coefficients are known, $\hat{x}[n]$ can be the output of a feed-forward linear filter or of a decision-feedback structure [5]. When the channel coefficients are not known, they may be estimated, subsequent to which filter taps are derived, or the tap values may be generated directly.

A measure of asymmetry is

$$\gamma = E\{|x[n]|^2 x[n]\}, \quad (2)$$

which is a third-order statistic. If we apply a similar statistic to (1),

$$F_{t,m} = E\{y[n]y^*[n+t]y[n+m]\} \quad (3)$$

we find that

$$F_{t,m} = \gamma \sum_{k=k_1}^{k_2} h_k h_{k+t}^* h_{k+m} \quad (4)$$

with symmetric white noise. Information about the amplitude and the phase of the channel can be obtained from a suitable set of $F_{t,m}$ statistics.

When undertaking blind equalization, each $F_{t,m}$ will be estimated using a sequence of channel outputs. A larger value of $F_{t,m}$ is preferable to a smaller one, as an error in the estimate is then relatively smaller. The constellation design may help or hinder timely convergence of the statistical estimates via the direct scaling of the $F_{t,m}$ statistics by γ .

HEXAGONAL CONSTELLATIONS

Hexagonal constellations appear in [1] and [2] as potential solutions to the problem of finding the constellation that minimizes the average transmitted power given a required minimum symbol separation. The hexagonal constellations considered had 8, 16, 32, and 64 symbols, and analysis of hexagonal and square-lattice (e.g. QAM) constellations showed that hexagonal constellations have a 0.8 dB advantage over QAM constellations with identical minimum symbol separation.

"Optimum" hexagonal constellations with 128, 256, 512, or 1024 symbols have been of little interest even though QAM constellations of these sizes have been used in high-rate bandwidth-limited communications systems. A principal reason for this is the simplicity of symbol generation and decision-making with QAM constellations. However, analogous structures for hexagonal constellations are no longer much of a problem due to advances in digital and mixed signal processing technologies. A main reason for renewed interest in hexagonal constellations is the potential for asymmetry at no cost in average transmitted power beyond that of QAM constellations currently in use. Indeed, depending on the amount of desired asymmetry, up to 0.8 dB of power can be saved.

A. Construction Method

For purposes of comparison, all of the constellation measurements will assume a unit minimum symbol separation. The symbols of the constructed constellations occupy points of a hexagonal lattice, while those of the QAM constellations occupy points of a square lattice.

We will require that the hexagonal constellations have no DC component. This is a common feature that aids in spectral shaping [5]. Were there a DC component, it would act as a sequence of pilot symbols added to the transmitted data symbols and could be used by the receiver accordingly.

The first step in the construction process is to list the points on a unit-spaced hexagonal lattice within a cer-

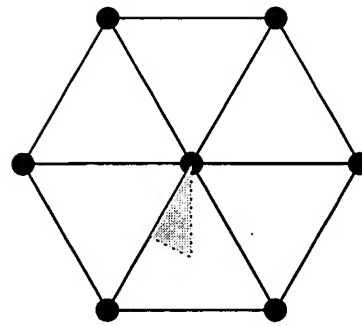


Fig. 1. Points on a Hexagonal Grid

tain radius of some central point. Figure 1 shows several points on such a lattice. The gray triangle shown in the figure depicts a region of space in which the center of the constellation may be located relative to the lattice points. All locations outside the gray triangle are equivalent to locations within it due to the symmetric nature of the lattice. Note that there are three points that will possibly result in a symmetric constellation. These are the three vertices of the triangle. A hexagonal constellation centered on the upper vertex may exhibit 2-fold, 3-fold, or 6-fold symmetry. A constellation centered on the left vertex may exhibit 2-fold symmetry, and on the right vertex 3-fold symmetry.

From a given starting point, we take the M lowest-power symbols in the list as potential members - less their mean - of the M -ary "optimum" hexagonal constellation. The mean provides a new starting point. Using this point, we select the M lowest-power symbols and form a zero-mean constellation. If the minimum distance between each point in one constellation and the points in the other is zero (or close enough to zero, since we carry out the computations on a computer), the process ends. Otherwise, it repeats until such time as successive potential constellations match. We begin the search for the constellations on each of the vertices, and choose the lowest-average-power results as the "optimum" constellations.

As a test, we used this procedure to find the "optimum" M -ary hexagonal constellations for $M = 4, 7, 8, 11, 16, 19$, and 32 and found that the constructed constellations agreed with those of the literature [1], [2].

B. 64-Point Constellations

The first high-order hexagonal constellation we examined is an "optimum" 64-HEX, shown in Fig. 2 [1]. This constellation is symmetric, since a rotation by π preserves the symbol values. The starting point for construction of this algorithm was the upper vertex of the gray triangle in Fig. 1. The average power of this constellation is $P_{avg} = 8.8125$ and the peak power is $P_{peak} = 16.125$.

When the starting point is instead the left vertex, the suboptimal 64-HEX-SO constellation of Fig. 3 is generated. The average power of this constellation is $P_{avg} = 8.8254$ - slightly greater than that of the 64-HEX - but $\gamma = -0.1424 + 0.0237j$.

A 64-QAM constellation has $P_{avg} = 10.5$, $P_{peak} = 24.5$, and $\gamma = 0$. In terms of average power, hexagonal constel-

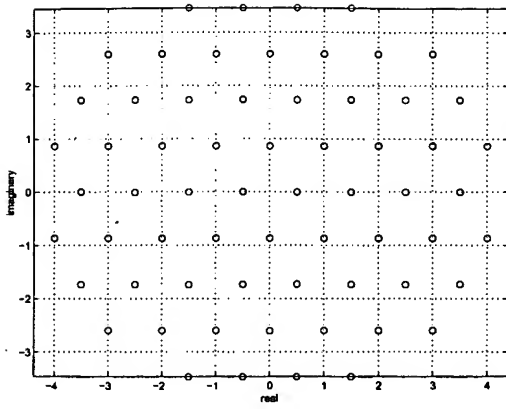


Fig. 2. Symmetric "Optimum" 64-HEX Constellation

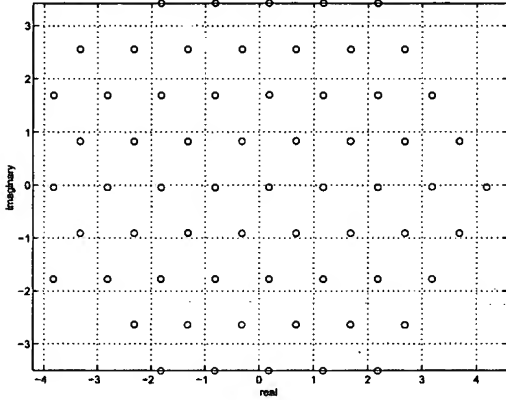


Fig. 3. Asymmetric Suboptimal 64-HEX-SO Constellation

lations have a 0.75 dB advantage. In terms of peak power, the 64-HEX advantage is 1.65 dB while the 64-HEX-SO advantage is 1.4 dB.

C. 128-Point Constellation

The "optimum" 128-point constellation appears in Fig. 4. For this constellation, $\gamma = -0.2044$, $P_{avg} = 17.6366$, and $P_{peak} = 34.519$. The corresponding statistical quantities of the cross-shaped 128-QAM constellation are $\gamma = 0$, $P_{avg} = 20.5$, and $P_{peak} = 42.5$. In dB, the average and peak power of 128-HEX show improvements of 0.65 and 0.9 compared with the power measurements of 128-QAM.

D. 256-Point Constellation

Figure 5 shows the "optimum" 256-HEX constellation with $\gamma = -0.1662 + 0.0569j$, $P_{avg} = 35.2536$, and $P_{peak} = 71.77$. For 256-QAM $P_{avg} = 42.5$, $P_{peak} = 112.5$, and of course $\gamma = 0$. The average and peak power advantages of 256-HEX are 0.81 dB and 1.95 dB.

The 256-HEX constellation is beginning to look somewhat circular in shape, as opposed to the hexagonal constellations with fewer symbols, which were distinctly hexagonal. The 256-QAM constellation is simply a large square of 16 symbols by 16 symbols.

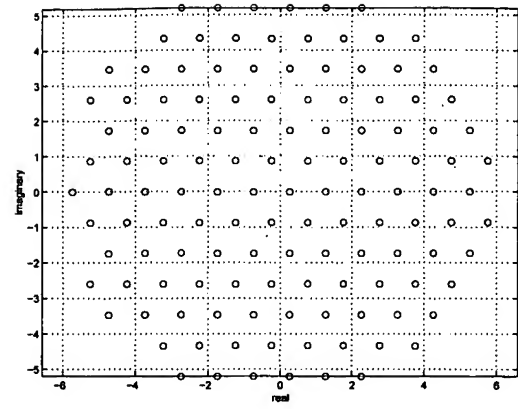


Fig. 4. "Optimum" 128-HEX Constellation

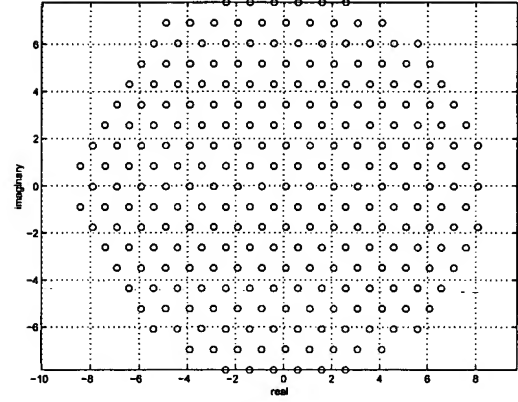


Fig. 5. "Optimum" 256-HEX Constellation

E. 512-Point Constellation

Figure 6 depicts an "optimum" 512-HEX constellation. The geometry of the constellation is quite circular - a "best" packing of the symbols into the smallest possible area. The statistics for 512-HEX are $\gamma = -0.06209$, $P_{avg} = 70.53$, and $P_{peak} = 143.43$. For 512-QAM, another cross-shaped constellation, the statistics are $\gamma = 0$, $P_{avg} = 82.5$, and $P_{peak} = 188.5$.

Though 512-HEX shows 0.68 dB and 1.19 dB P_{avg} and P_{peak} improvement compared to 512-QAM, and has a non-zero γ , it is clear numerically and to the naked eye that 512-HEX is only weakly asymmetric. In order to enable blind equalization in a reasonable amount of time, some of the power improvement should be traded off during constellation design for an increased γ .

F. 1024-Point Constellation

The final "optimum" hexagonal constellation is the 1024-HEX constellation of Fig. 7. 1024-HEX has $\gamma = 0.12146$, $P_{avg} = 141.13$, and $P_{peak} = 279.9$. 1024-QAM has $\gamma = 0$, $P_{avg} = 170.5$, and $P_{peak} = 480.5$. By switching from 1024-QAM to 1024-HEX, it is possible to reduce the P_{avg} by 0.82 dB and P_{peak} by 2.35 dB.

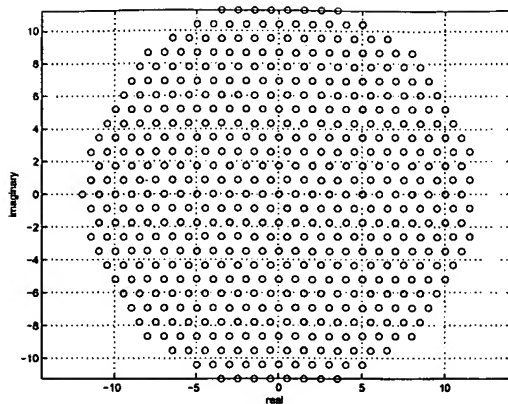


Fig. 6. "Optimum" 512-HEX Constellation

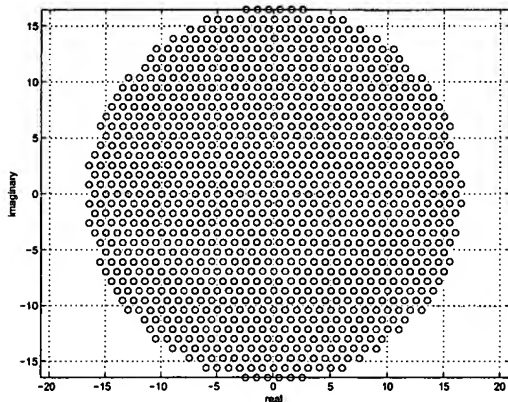


Fig. 7. "Optimum" 1024-HEX Constellation

G. Practical Issues

We have proposed M -ary hexagonal constellations as replacements for M -ary QAM constellations. The transition entails use of transmitters and receivers with modestly higher complexity. Benefits include power savings and asymmetry. If desired, some of the power savings can be spent on improving the asymmetry properties of the constellation, again with only a minor increase in symbol generation and decision-making complexity.

One issue we have not discussed is phase jitter [6]. A small phase error moves low-power symbols a small distance in the complex plane, and high-power symbols a large distance. The symbol decision regions are effectively the same size for most of the symbols in the high order hexagonal constellations, which may bar their use in a jitter-susceptible channel. If this is the case, a system design should include a power-dependent angular phase separation, which would make the decision regions much less uniform in shape and the design process less simple than that presented here.

Another difficulty is that the symbols are quite closely packed in the hexagonal constellations (also in the high order QAM constellations), so that there is little room for error in equalization. A small amount of residual ISI can lead to an exorbitantly-high symbol error rate. We hope that the low-complexity third-order blind algorithms whose use is enabled by constellation asymmetry will al-

TABLE I
CONSTELLATION COMPARISONS GIVEN UNIT MINIMUM SYMBOL SEPARATION

Constellation	γ_3	$P_{average}$	P_{peak}
64-QAM	0	10.5	24.5
64-HEX	0	8.8125	16.75
64-HEX-SO	0.14439	8.8254	17.737
128-QAM	0	20.5	42.5
128-HEX	0.2044	17.6366	34.519
256-QAM	0	42.5	112.5
256-HEX	0.17606	35.254	71.77
512-QAM	0	82.5	188.5
512-HEX	0.06209	70.53	143.43
1024-QAM	0	170.5	480.5
1024-HEX	0.12146	141.13	279.9

low hexagonal constellations to be used in some channels where QAM counterparts are considered impractical.

CONCLUSION

High-order hexagonal constellations having $M = 64, 128, 256, 512$, or 1024 symbols meet a minimum symbol separation requirement using 0.8 dB less average transmitted power than M -ary QAM constellations. So-called "optimum" hexagonal constellations [2] for these large values of M were found and their second- and third-order statistical properties tabulated. The average and/or peak transmitted power advantages of these constellations over QAM constellations can be traded off for enhanced asymmetry. This allows blind equalization of ISI-corrupted symbol sequences using third-order statistics rather than statistics of higher order.

REFERENCES

- [1] G.D. Forney Jr., R.G. Gallager, G.R. Lang, F.M. Longstaff, and S.U. Qureshi, "Efficient Modulation for Bandlimited Channels", *IEEE Journal on Selected Areas in Communications*, Vol. SAC-2, No. 5, pp. 632-647, September 1984.
- [2] R.D. Gitlin, J.F. Hayes, and S.B. Weinstein, *Data Communications Principles*, New York: Plenum Press 1992.
- [3] D. Hatzinakos and C.L. Nikias, "Blind Equalization Based on Higher-Order Statistics (H.O.S.)", *Blind Deconvolution*, S. Haykin (ed.), PTR Prentice Hall, Englewood Cliffs, 1994.
- [4] G. Foschini, R.D. Gitlin, and S.B. Weinstein, "Optimization of Two-Dimensional Signal Constellations in the Presence of Gaussian Noise," *IEEE Transactions on Communications*, Vol. COM-21, No. 13, pp. 28-38, January 1974.
- [5] J.G. Proakis, *Digital Communications*, New York: McGraw-Hill 1995.
- [6] N.K. Jablon, "Joint Blind Equalization, Carrier Recovery, and Timing Recovery for High-Order QAM Signal Constellations," *IEEE Trans. on Signal Processing*, Vol. 40, No. 6, pp. 1383-1398, June 1992.

**This Page is Inserted by IFW Indexing and Scanning
Operations and is not part of the Official Record**

BEST AVAILABLE IMAGES

Defective images within this document are accurate representations of the original documents submitted by the applicant.

Defects in the images include but are not limited to the items checked:

☒ **BLACK BORDERS**

☒ **IMAGE CUT OFF AT TOP, BOTTOM OR SIDES**

☐ **FADED TEXT OR DRAWING**

☒ **BLURRED OR ILLEGIBLE TEXT OR DRAWING**

☐ **SKEWED/SLANTED IMAGES**

☐ **COLOR OR BLACK AND WHITE PHOTOGRAPHS**

☐ **GRAY SCALE DOCUMENTS**

☐ **LINES OR MARKS ON ORIGINAL DOCUMENT**

☐ **REFERENCE(S) OR EXHIBIT(S) SUBMITTED ARE POOR QUALITY**

☐ **OTHER:** _____

IMAGES ARE BEST AVAILABLE COPY.

As rescanning these documents will not correct the image problems checked, please do not report these problems to the IFW Image Problem Mailbox.